University of Florida
Civil and Coastal Engineering

UF

University of Florida
Civil and Coastal Engineering

Final Report **July 2018**

Use of Small Unmanned Aerial Vehicles (sUAV) for Structural Inspection

Principal investigator:
Jennifer A. Bridge, Ph.D.

Co-Principal investigator:
Peter G. Ifju, Ph.D.

Department of Civil and Coastal Engineering
University of Florida
P.O. Box 116580
Gainesville, Florida 32611

Sponsor:
Florida Department of Transportation (FDOT)
Office of Maintenance
Richard I. Kerr, P.E. – Project Manager

Contract:
FDOT Contract No. BDV31-977-55

Disclaimer

The opinions, findings, and conclusions expressed in this publication are those of the authors and not necessarily those of the State of Florida Department of Transportation.

SI* (Modern Metric) Conversion Factors

*APPROXIMATE CONVERSIONS **TO** SI UNITS*

SYMBOL	WHEN YOU KNOW	MULTIPLY BY	TO FIND	SYMBOL
LENGTH				
in	inches	25.4	millimeters	mm
ft	feet	0.305	meters	m
yd	yards	0.914	meters	m
mi	miles	1.61	kilometers	km
AREA				
in^2	square inches	645.2	square millimeters	mm^2
ft^2	square feet	0.093	square meters	m^2
yd^2	square yard	0.836	square meters	m^2
ac	acres	0.405	hectares	ha
mi^2	square miles	2.59	square kilometers	km^2
VOLUME				
fl oz	fluid ounces	29.57	milliliters	mL
gal	gallons	3.785	liters	L
ft^3	cubic feet	0.028	cubic meters	m^3
yd^3	cubic yards	0.765	cubic meters	m^3
NOTE: volumes greater than 1000 L shall be shown in m^3				
MASS				
oz	ounces	28.35	grams	g
lb	pounds	0.454	kilograms	kg
T	short tons (2000 lb)	0.907	megagrams	Mg (or "t")
TEMPERATURE (exact degrees)				
ºF	Fahrenheit	5(F-32)/9 or (F-32)/1.8	Celsius	ºC
ILLUMINATION				
fc	foot-candles	10.76	lux	lx
fl	foot-Lamberts	3.426	$candela/m^2$	cd/m^2
FORCE and PRESSURE or STRESS				
kip	1000 pound force	4.45	kilonewtons	kN
lbf	pound force	4.45	newtons	N
lbf/in^2	pound force per square	6.89	kilopascals	kPa

*SI is the symbol for the International System of Units. Appropriate rounding should be made to comply with Section 4 of ASTM E380.

SI* (Modern Metric) Conversion Factors

*APPROXIMATE CONVERSIONS **FROM** SI UNITS*

SYMBOL	WHEN YOU KNOW	MULTIPLY BY	TO FIND	SYMBOL
LENGTH				
mm	millimeters	0.039	inches	in
m	meters	3.28	feet	ft
m	meters	1.09	yards	yd
km	kilometers	0.621	miles	mi
AREA				
mm^2	square millimeters	0.0016	square inches	in^2
m^2	square meters	10.764	square feet	ft^2
m^2	square meters	1.195	square yards	yd^2
ha	hectares	2.47	acres	ac
km^2	square kilometers	0.386	square miles	mi^2
VOLUME				
mL	milliliters	0.034	fluid ounces	fl oz
L	liters	0.264	gallons	gal
m^3	cubic meters	35.314	cubic feet	ft^3
m^3	cubic meters	1.307	cubic yards	yd^3
MASS				
g	grams	0.035	ounces	oz
kg	kilograms	2.202	pounds	lb
Mg (or "t")	megagrams (or "metric	1.103	short tons (2000 lb)	T
TEMPERATURE (exact degrees)				
ºC	Celsius	1.8C+32	Fahrenheit	ºF
ILLUMINATION				
lx	lux	0.0929	foot-candles	fc
cd/m^2	candela/m^2	0.2919	foot-Lamberts	fl
FORCE and PRESSURE or STRESS				
kN	kilonewtons	0.225	1000 pound force	kip
N	newtons	0.225	pound force	lbf
kPa	kilopascals	0.145	pound force per square inch	lbf/in^2

*SI is the symbol for the International System of Units. Appropriate rounding should be made to comply with Section 4 of ASTM E380.

Technical Report Documentation Page

1. Report No.	2. Government Accession No.	3. Recipient's Catalog No.

4. Title and Subtitle	5. Report Date
Use of Small Unmanned Aerial Vehicles for Structural Inspection	July 2018
	6. Performing Organization Code
7. Author(s)	8. Performing Organization Report No.
Jennifer A. Bridge, Ph.D., Peter G. Ifju, Ph.D., Travis J. Whitley, Andrew P. Tomiczek	
9. Performing Organization Name and Address	10. Work Unit No. (TRAIS)
University of Florida Engineering School of Sustainable Infrastructure & Environment University of Florida 365 Weil Hall / PO Box 116550 Gainesville, FL 32611	11. Contract or Grant No. BDV31-977-55
12. Sponsoring Agency Name and Address	13. Type of Report and Period Covered
Florida Department of Transportation 605 Suwannee Street, MS 30 Tallahassee, FL 32399-0450	Draft Final Report 5/15/2016 – 7/31/2018
	14. Sponsoring Agency Code

15. Supplementary Notes

16. Abstract

The objective of this research project was to develop and demonstrate a small unmanned aerial vehicle system (sUAV) that can be used to perform structural inspections currently requiring under-bridge inspection vehicles (UBIV). One goal was to create an sUAV with the ability to provide data and deficiency identification with the same or better accuracy than that acquired by current visual methods. This project included the optimization of University of Florida sUAVs equipped with optical sensors, an assessment of available image processing software, and an assessment of current data storage. Six high mast light poles (HMLP) and eight bridges were inspected as part of this project; approximately half of the inspections were performed alongside traditional inspections, and the remainder were performed with no prior knowledge of the structure to compare findings with the results of recently performed inspections. Cost and data storage requirements were compared between current inspection procedures and sUAV inspections to quantify potential changes resulting from utilizing sUAV for structural inspections.

G17. Key Word	18. Distribution Statement
Small Unmanned Aerial Vehicle, sUAV, Bridge Inspection, High Mast Light Pole Inspection.	No restrictions.

19. Security Classif. (of this report)	20. Security Classif. (of this page)	21. No. of Pages	22. Price
Unclassified	Unclassified	150	

Acknowledgments

The authors thankfully acknowledge the support of this research by the Florida Department of Transportation (FDOT).

Executive Summary

Structural inspections are required on traffic structures throughout the state of Florida. Routine inspections of bridges are required at least once every twenty-four months, and inspections of galvanized high mast light-poles (HMLPs) are required every sixty months. Current inspection practices for bridges with difficult access (e.g., high level bridges over water) often require mobilization of under-bridge inspection vehicles (UBIVs) and maintenance of traffic (MOT) due to lane closures. Visual inspections of HMLPs are conducted by an inspector on the ground with a pair of binoculars.

The goal of this project is to demonstrate the feasibility of using small unmanned aerial vehicles (sUAV) for structural inspections. sUAVs could potentially enhance current inspection practices. For visual inspection of bridges, sUAVs would eliminate the need for MOT, and they could be used for structures with load restrictions. For visual inspection of HMLPs, sUAVs could provide views of the structure that would be impossible to see from the ground, for example, the top of the luminaire.

The first step in completing this project was to modify an sUAV for use in structural inspections. The vehicle needed to be maneuverable enough to provide adequate views of the structure and avoid obstructions, while also having a large enough payload to carry sensors for flight and high quality imaging. The optimization of the sUAV for structural inspection was a process that continued throughout the duration of the project. To demonstrate the feasibility of using sUAVs for structural inspections, six HMLPs and eight bridges were inspected throughout this project. Additionally, practical considerations, such as cost and increased data storage, were investigated, and image processing tools for deficiency tracking and quantification were evaluated.

Based on the outcomes from the inspections conducted throughout this project and feedback from Certified Bridge Inspectors (CBIs), a realistic assessment of the feasibility, including both advantages and disadvantages of using sUAVs for inspections is also given. Recommended best practices for sUAV structural inspections are provided. Preliminary recommendations include periodically replacing the use of UBIVs on bridges in good condition (e.g., every other inspection cycle). The most immediate and significant impact an sUAVs could make on current inspection practices would likely be for special and damage inspections. If a single specific deficiency must be monitored, mobilizing an sUAV could be more efficient than mobilizing a UBIV, and no MOT would be required. For a damage inspection, the use of UBIVs may be impossible, making an sUAV a realistic alternative.

Table of Contents

List of Figures

List of Tables

List of Abbreviations

AHM	Altitude Hold Mode
ATC	Air Traffic Control
CBI	Certified Bridge Inspector
CFR	Code of Federal Regulations
COA	Certificate of Authorization
FAA	Federal Aviation Administration
FDOT	Florida Department of Transportation
FPV	First-Person View
GPS	Global Positioning Satellites
GPSM	GPS Mode
HMLP	High Mast Light Pole
MOT	Maintenance of Traffic
OFM	Optical Flow Mode
RPIC	Remote Pilot in Command
SD	Secure Digital
sUAV	Small Unmanned Aerial Vehicle
UBIV	Under-Bridge Inspection Vehicle
UF	University of Florida
VLOS	Visual Line of Sight
VO	Visual Observer

1. Introduction

1.1 Project Overview

The objective of this research project was to develop and demonstrate a small unmanned aerial vehicle system (sUAV) that can be used to perform structural inspections currently requiring under-bridge inspection vehicles (UBIV). One goal was to create an sUAV with the ability to provide data and deficiency identification with the same or better accuracy than that acquired by current visual methods. This project included the optimization of University of Florida (UF) sUAVs equipped with optical sensors, an assessment of available image processing software, and an assessment of current data storage and reporting methods. Six galvanized high mast light poles (HMLP) and eight bridges were inspected as part of this project; approximately half of the inspections were performed alongside traditional inspections and the remainder were performed independently with a certified bridge inspector. A cost comparison with current inspection procedures was also performed to quantify the potential financial benefit of utilizing sUAV for structural inspections.

The following tasks were carried out to achieve the project research objective:

- **Task 1A – Literature Review**: Compile and review literature related to sUAV for structural inspection.
- **Task 1B – Site Selection and COA Application**: Select appropriate sites for the inspections to be carried out and compile and submit necessary information required to secure COAs for the selected sites.
- **Task 2A – Aerial Vehicle Evaluation**: Assess critical operational parameters to achieve project objectives and perform practice flights with surrogate structures.
- **Task 2B – Sensor Evaluation, Selection and Mounting**: Determine image quality and resolution requirements and select sensors to meet inspection and control requirements.
- **Task 3 – Image Processing for Deficiency Assessment**: Identify deficiencies of interest and investigate the use and performance of image processing software.
- **Task 4 – High Mast Light Pole (HMLP) Inspections**: Perform six HMLP inspections.
- **Task 5 – Bridge Inspections**: Perform eight bridge inspections, four alongside ongoing traditional inspections.
- **Task 6 – Cost Analysis**: Compare current FDOT inspection costs to cost of conducting inspections with the use of sUAV.
- **Task 7 – Electronic Video Storage**: Evaluate image and video storage requirements and make recommendations on storage and archiving methods.
- **Task 8 –Draft of Final Report and Closeout Teleconference**
- **Task 9 – Final Report**

This final report is a compilation of the findings reported in previous task reports.

1.2 Current HMLP Inspection Practices

The primary purpose of inspections is to protect the safety of the public by identifying structural and material deficiencies that may lead to failure and by taking action. Two separate inspections are required on HMLPs: a structural inspection of the pole and a mechanical and electrical inspection of the lighting fixture. In the state of Florida, the structural inspections must be performed every sixty months (FDOT, 2018).

Current structural inspection practices for HMLPs include a visual inspection of the pole by a qualified technician. Additionally, the pole is physically inspected for tight bolts and a sound foundation. Inspectors perform the visual portion of the inspection by walking around the pole and carefully looking over its surface through a pair of binoculars. Inspectors focus on the structure's slip joints, connections of segments of HMLPs, as deficiencies tend to appear at these locations. The most common deficiency found during inspections is corrosion; however, cracks are occasionally found at the slip joints. Images are taken of deficiencies for record-keeping and for maintenance requests. Images of the rest of the inspection are not required. During this project, the feasibility of an alternative visual inspection method of HMLPs using an sUAV was investigated.

1.3 Current Bridge Inspection Practices

Bridge deficiencies are typically identified through visual inspection, although non-destructive testing and material sampling may be used in specific cases. Three basic types of bridge inspections will be considered for this study: routine inspections, special inspections, and damage inspections. According to the National Bridge Inspection Standards (2004) provided in Title 23 of the Code of Federal Regulations (CFR) Part 650, routine inspections are required at least every 24 months; however, depending on the bridge posting rating and the component condition rating, inspections may be required more frequently. A routine inspection includes looking at all elements of the bridge superstructure, deck underside, and substructure that are accessible from the ground. For prestressed concrete girder spans, this method would entail inspecting the bearings and the pier cap at the start and end of each span, as well as looking down the bay between each beam from each end. This method is typically sufficient, as notable deficiencies (i.e., Condition State 3 and above) according to the Bridge and Other Structures Inspection and Reporting Manual (FDOT, 2016) are noticeable from a distance in prestressed concrete spans. Condition State 3 represents a poor condition of a bridge element. An example of a Condition State 3 in a prestressed concrete element would be a spall greater than one-inch deep or six-inches in diameter. For steel girder spans, the inspection crew would typically make a pass down the length of the span underneath the bay between each beam, as deficiencies such as corrosion and missing bolts in lateral bracing typically require a closer view of the structure.

Special inspections are used to monitor particular known or suspected deficiencies, and damage inspections are unscheduled inspections used to assess structural damage resulting from environmental factors or human actions. These inspection types are defined in the National Bridge Inspection Standards. Special inspections are usually not comprehensive enough to meet the requirements of routine inspections. Damage inspections must be sufficient to determine if a bridge requires load restrictions or closures or the extent of repair required.

Bridges with superstructures that are hard to reach, such as bridges spanning a river, may require the use of UBIVs to complete a visual inspection (Figure 1-1). UBIVs allow inspectors to view portions of bridge superstructures, substructures, and deck undersides from arm's length that would otherwise be impossible to view. Although UBIVs provide inspectors with a close and hands-on view of the structure, they have disadvantages. UBIVs are expensive to rent, and they require maintenance of traffic (MOT) due to lane closures. In the case of special inspections, use of UBIVs may be impractical, and for damage inspections, use of UBIVs may not be possible. Additionally, though rare, UBIV instability has led to injury, and even death, of inspectors.

(a) (b)

Figure 1-1. UBIV overturning: (a) West Hartford Connecticut, August 2015. (b) Portsmouth, Rhode Island, August 2016.

1.4 Previous Studies on the Use of sUAVs for Structural Inspection

Due to rapid advancements in sUAV technology in recent years, research interest in the use of sUAVs for structural inspections has grown significantly. In this section, several relevant studies conducted in the past few years will be summarized.

In 2008, the California Department of Transportation sponsored a project resulting in the development of a tethered aerial vehicle with a range of 200 feet intended for bridge inspections (Moller, 2008). The system consisted of two propellers with rotation in opposite directions to prevent the craft from rotating. The sUAV was controlled and powered using an umbilical cord system that physically connected it to the pilot, limiting its range of motion, but giving it an essentially unlimited flight time. The system did not have any sensors, aside from those used for piloting purposes.

The Georgia Institute of Technology then assessed the usability of sUAVs in construction jobsite safety inspections (Irizarry et al., 2012). For this study, recommendations for an ideal sUAV for jobsite inspections were made, and laboratory testing to determine the accuracy of using an sUAV for jobsite inspections was conducted. The researchers selected an inexpensive commercial quadcopter, a Parrot AR.Drone, for the study. This sUAV has a 720p camera and a flight time of about 12 minutes. Based on their results, the authors recommended sUAVs for jobsite inspections have autonomous navigation, sufficient battery life, high-resolution cameras, and a compact device, such as a tablet, to view video streaming from the sUAV. Although this

application does not require as detailed views as would be required for structural inspections, these recommendations are applicable for structural inspections as well.

Hallermann and Morgenthal (2014) proposed sUAV inspection strategies for large bridges. The sUAV used in this study was an AscTec Falcon, which is a custom sUAV from Germany. The cameras used for the project had a resolution of 14 Megapixels. In this study, the authors proposed using GPS based autonomous flight paths. The authors also quantified the drift of the sUAV used. Over one minute at an altitude of 80 m, their sUAV drifted about 2.25 m horizontally and 1 m vertically. During this study, a test inspection was performed of a large scale retaining wall. This demonstration was not like a routine bridge inspection. Instead, the sUAV was flown 30 m above the retaining wall, and high-resolution images were captured. With the images of the wall, a 3D reconstructed model was created using Agisoft PhotoScan, a proprietary 3D reconstruction software.

In 2015, the Florida Institute of Technology provided a proof of concept for the use of sUAVs for bridge inspections (Otero et al., 2015). The research team used an Arducopter Mega V2.5 Hexacopter and a smaller DJI Phantom Vision 2+ quadcopter. The Arducopter was able to operate in constant winds of up to 17 mph and for as long as 20 minutes. The team utilized a GoPro Hero 3 Black edition camera, capable of taking high-definition video and still photography, mounted on a gimbal as their primary data collection sensor on the Arducopter. The camera was also capable of streaming live video, a feature which was used to assist the inspectors and pilot in directing the sUAV.

The research team at FIT performed inspections on four HMLPs as part of their project. They experimented with different flight patterns to find the approach which would provide the most thorough and efficient inspection. The flight patterns investigated included circling around the HMLP in 5-foot increments, spiraling up around the HMLP, and flying directly up and down the side of the HMLP from four different angles. The last approach was determined to be the most effective, as it was the fastest and it produced sequences of images that were easier to analyze. The team stated that a distance of five feet from the HMLP during flight was easy to maintain and provided adequate picture quality for inspection purposes. Two of the inspections were performed alongside traditional FDOT inspections, and the team was asked to focus primarily on the more difficult to reach locations, such as the slip joints and luminaires. The sUAV was able to identify a missing screw on the top of one HMLP.

The research team also performed five bridge inspections, three of which were done alongside FDOT inspectors. The three tests performed with the FDOT inspectors included a concrete highway bridge, a steel drawbridge, and a concrete with steel mid-span bridge. The inspections initially utilized the larger Arducopter equipped with the GoPro camera to record video of the bridges, as well as to provide a live stream to the inspector and to help guide the pilot. The team was instructed by the FDOT inspectors to focus primarily on difficult to reach areas of the bridges, such as gusset plates and between girders, and they were able to capture images of cracks, rust penetration through the concrete, bolts in various stages of decay, including several that were missing entirely, and concrete spalling. Flying in the confined space between the girders of the bridge proved difficult because of the turbulence produced by the

sUAV itself, so the team continued that inspection with the smaller DJI Phantom quadcopter. The sUAVs were piloted manually.

Khan et al. (2015) used an sUAV carrying a multi-spectral imaging system to inspect the top of a bridge deck. The primary focus of this study was detecting delaminations in concrete bridge decks. Throughout this study, the research team used three different aerial vehicles: a DJI F550, a Skyjib X4, and a manned helicopter. The two sUAVs were used in an experimental test of a model concrete bridge deck measuring 31 ft x 13 ft x 8 in. The sUAVs were equipped with a GoPro Hero 3 and with a FLIR TAU2 infrared camera for thermal imaging. The helicopter was used for an in-field inspection of a bridge. Because the focus of this study was on delaminations in concrete bridge decks, the aerial vehicles were only flown above the structures, so GPS was not a limitation. Additionally, during routine bridge inspections, delamination is only one of many deficiencies inspectors must check.

Brooks et al. (2015) focused on using sUAVs to inspect the tops of bridge decks, as well as confined spaces, in a report produced by the Michigan Tech Research. The research team used a Bergen Hexacopter to investigate whether an adequate inspection could be performed using an sUAV while decreasing costs and increasing safety over traditional inspection approaches. The hexacopter was capable of flying for a maximum of 18 minutes. Using information from its onboard GPS, the sUAV could compensate for wind to autonomously maintain its position. The sUAV was equipped with a Nikon D800 camera which was used to capture two pictures per second while on a preset flight pattern. Using Agisoft Photoscan, the research team produced a 3D model of the bridge using the georeferenced still images, which required at least 60% overlap between sequential photos. The sUAV also had an onboard LiDAR system which was used to produce a point cloud of the bridge; however, the model obtained from the LiDAR and GPS data together did not have a high level of accuracy. The point cloud model was improved when the LiDAR data was aligned using a feature that ran straight along the entire length of the bridge, such as a gutter; however, on a bridge with no such feature, the model would be inaccurate. The sUAV was also equipped with a thermal camera to enable the detection of any delamination in the concrete of a bridge.

Throughout the course of the project, two concrete highway bridges, which were closed to traffic for repair, were inspected to assess the capabilities of the sUAV. The images taken were used to produce a 3D model with a resolution of 0.1 inch. A spall detection algorithm was used on the model to accurately quantify the amount of spall on the bridge by detecting differences in surface elevation. The thermal camera was used to spot areas which may have contained a delamination, and then those areas were tested in the field by traditional methods to verify its presence. The thermal camera was able to detect the difference in heat caused by the delamination; however, it also picked up patchy heat variations caused by the repairs that had been done to the surface of the bridge over the course of its life. This false positive delamination detection limited the detection accuracy to approximately 58.8%. The LiDAR sensor was only flown over one of the structures and produced useful data once the point cloud was aligned using a feature that ran straight across the entire length of the bridge. The authors concluded that the results showed significant promise due to the ability of the sUAV to obtain quality data which could be used to assess the condition of the bridge, and that the use of this system seems to provide significant cost savings when compared to current inspection practices.

In a study for the Minnesota Department of Transportation, Zink and Lovelace (2015) attempted to inspect three bridge structures using an sUAV. The research team utilized an Aeryon Skyranger Quadcopter, which cost approximately $140,000, to investigate the effectiveness of utilizing sUAV technology for the purposes of performing inspections. The prefabricated sUAV had a 50-minute fly time, which is relatively long for one battery charge. Using its built-in GPS, the sUAV was able to follow a preprogrammed flight pattern. The sUAV had high definition still and video capture capabilities, as well as a zoom lens and live video streaming, which the team used to locate cracks and other forms of deterioration that an inspector in the field would typically investigate. The sUAV was also equipped with a thermal imaging camera to detect the presence of any deck delamination.

The Minnesota team performed inspections on four bridges of varying size and condition; two were concrete highway bridges and the other two were steel bridges. All of the bridges required different approaches to obtain access, including launching from a boat and from above the bridge. The team compared the data and images collected with notes from previous inspections and found that they were able to detect essentially the same issues as the inspectors, as long as the sUAV could access the part of the bridge in question. The authors concluded that the sUAV was useful for providing access to areas of bridges that are difficult to inspect using traditional under bridge inspection vehicles; however, the system was limited by poor GPS reception under the bridges, and by areas with little clearance in which the sUAV was unable to maneuver.

Chan et al. (2015) summarized obstacles sUAV inspections face and potential solutions to many of these obstacles. Although no experimental testing was performed during this study, the authors raise many valid points. The authors suggest that the two main factors for sUAV inspection platforms to be successful are cost effectiveness and platform flexibility. By platform flexibility, the authors mean the different sensors must be able to be integrated into the sUAV. Limitations to sUAV inspections pointed out by the authors include regulatory requirements, such as the fact that an sUAV may not be operated above moving vehicles. This would prohibit the use of sUAVs for inspections of overpasses. Additionally, the authors recommended including obstacle avoidance systems, informed by laser range finders and optical flow sensors. Because GPS is often used for programming flight paths for sUAVs, and GPS is often not reliable underneath bridges, the authors recommend using an alternative method to locate the sUAV. In their paper, the researchers suggest the use of simultaneous localization and mapping in GPS denied areas.

Gillins et al. (2016) conducted an sUAV inspection of a bridge superstructure. In their inspections, the research team used a DJI Phantom 3 Pro quadcopter. The pilot flew the sUAV manually, keeping a stand-off of about 2 or 3 meters from the structure. High quality images of the structure were taken during the inspection, but there were several limitations. The camera used during their inspection did not have a zoom lens. Additionally, because the sUAV used in the project had the camera mounted to the bottom, the researchers were not able to take images of elements on the bridge underside. The researchers also faced problems with the lack of GPS due to the proximity of the bridge. No other sensors were used to assist with flight for their inspection.

Irizarry et al. (2017) also identified potential benefits and limitations of sUAV bridge inspections. The information in this paper is based on focus groups with Georgia Department of Transportation Bridge Management Group officials. Limitations specified by the authors include lack of GPS signal and potential interference with the sUAV from nearby powerlines. The authors recommended using a camera that can be pointed directly upward. Also, the authors suggested using images from sUAVs to create 3D models of bridges.

In the above studies, flight underneath the bridge proved to be a severe limitation of the sUAV inspection systems. In some of the studies, researchers did not attempt to fly underneath a bridge, due to lack of GPS signal, while others attempted to fly manually, relying heavily on the skill of the pilot. Still others only suggested approaches for sensor-aided under-bridge flight. In this study, a method for flight underneath a bridge using additional sensors to assist the pilot in operation of the sUAV is both proposed and demonstrated.

1.5 Report Overview

Subsequent sections of this report are organized as follows: Section 2 provides an overview of sUAV inspection operations. This section will describe the Federal Aviation Administration (FAA) regulations for sUAVs, the recommended crew for inspections, the vehicle airframe, sensors, and flight modes used for inspections, and the ground station. Section 3 summarizes the six HMLP inspections performed during the project. Section 4 summarizes the eight bridge inspections conducted throughout the project. These sections will describe both a timeline of events during the inspections, as well as lessons learned. Following the inspection summaries, since many images were gathered during inspections, a discussion of existing image processing technology will be provided in Section 5. Practical considerations, including cost and data storage requirements for sUAV inspections, will be discussed in Section 6. Finally, based on the results of the inspections performed and the practical and logistical considerations surrounding sUAV inspections, conclusions and recommendations are given in Section 7.

2 Overview of sUAV Inspection Operations

This section provides a description of the overall sUAV inspection system, the recommended crew for inspection, as well as relevant FAA regulations used in this project. A significant portion of this project was spent selecting and creating an ideal sUAV for inspections. As a result, the sUAV changed dynamically throughout the project. The main requirements for an ideal platform is one that can support the optical payload, have sufficient flight time, great modularity (ability to have its components replaced), stable flying characteristics, compact size, and low cost. In this section, the sUAV used for initial HMLP inspections will be discussed, followed by the sUAV used for bridge inspections. These two platforms will be compared to highlight important changes from the initial design to the final sUAV used for inspections.

2.1 Current sUAV Flight Regulations

Currently, to operate any aircraft in the national airspace system the FAA has specific certifications, regulations, and required approvals for particular types of aircraft (Small Unmanned Aircraft Systems 2016). Regulations for sUAVs, defined as an unmanned aircraft weighing less than 55 pounds, including the airframe and the payload, will be discussed in this section.

An sUAV may only be controlled by a person with a remote pilot certificate, or by someone under the direct supervision of a remote pilot in command (RPIC). The RPIC must also be able to directly take control of the sUAV if required. Requirements for a remote pilot certificate include being at least 16 years of age, being able to speak, write, and understand the English language, not having a physical or mental condition that would interfere with safe operation of an sUAV, and passing an aeronautical knowledge test. The aeronautical knowledge test includes applicable regulations, airspace classification, emergency procedures, communication procedures, and other information needed for safe operation of an sUAV. Additionally, a recurrent aeronautical test is required every 24 months.

A remote pilot certificate does not give an RPIC unrestricted operation of an sUAV, however. Other regulations apply. For example, an sUAV may not be operated from a moving car or boat, unless it is flown over an area that is sparsely populated, and it is not transporting another person's property for money. Also, operation of an sUAV is not permitted during the night. The RPIC, a visual observer (VO), and the person controlling the sUAV (if not the RPIC), must all have a visual line of sight (VLOS) on the sUAV that is not aided by any cameras for the duration of the flight. The FAA does not require a VO, but VOs can provide additional awareness of the sUAV and potential obstacles during the flight. Another important restriction specified in this section is that an sUAV may not be operated over a person unless that person is (1) directly participating in the sUAV operations, or (2) under a covered structure or inside a stationary vehicle. This restriction prevents sUAV inspections of highway bridges passing over other roadways. In addition, operation of sUAVs is not permitted in certain airspaces unless authorized by air traffic control (ATC). An RPIC must request authorization at least 72 hours in advance from ATC.

Many of the restrictions described in this section may be allowed if a Certificate of Waiver or Authorization (COA) is granted. With a COA, sUAV operations may deviate from

some regulations, including VLOS operation, operation at night, and operation in certain airspaces. A request for a COA must contain a description of the proposed sUAV operations and a valid reason as to why the sUAV can safely be operated under the COA. The FAA may grant a COA if it determines that the sUAV can be safely operated under those terms.

2.2 Recommended Crew for Inspections

The minimum crew recommended for the structural inspections consists of three members: an RPIC, a certified inspector and a VO. The RPIC is responsible for the overall safety of the flight and with complying with FAA regulations. The inspector operates the camera and looks for structural deficiencies. The inspector would be responsible for collecting all necessary images. The VO, although not required by the FAA, would provide additional situational awareness to the crew by monitoring potential hazards in the flight path and monitoring battery levels. All three members of the crew must communicate effectively to increase the safety of operations and to make sure the inspection is thorough.

2.3 sUAV Used for HMLP Inspections

The primary focus for the HMLP inspections conducted during this project was the collection of high-resolution video of portions of the structure that would otherwise be impossible to view from the ground. With this goal, the airframe, sensors, and flight modes used for HMLP inspections will be described in this section.

2.3.1 Description of Airframe and Sensors for Flight Control and Image Collection

At the beginning of the project, three sUAV airframes were considered: an eight rotor DJI S1000+ and a custom built carbon fiber hexacopter and a custom built carbon fiber quadcopter. The quadcopter was rejected because its original design did not have the payload capacity to lift the camera. For the HMLP inspections, a hexacopter was chosen over the S1000+ because it more modular and less expensive. The sUAV used for HMLP inspections is shown in Figure 2-1. The landing gear changed for multiple times, as will be discussed at the end of this chapter. For the second set of HMLP inspections, a propeller guard was added.

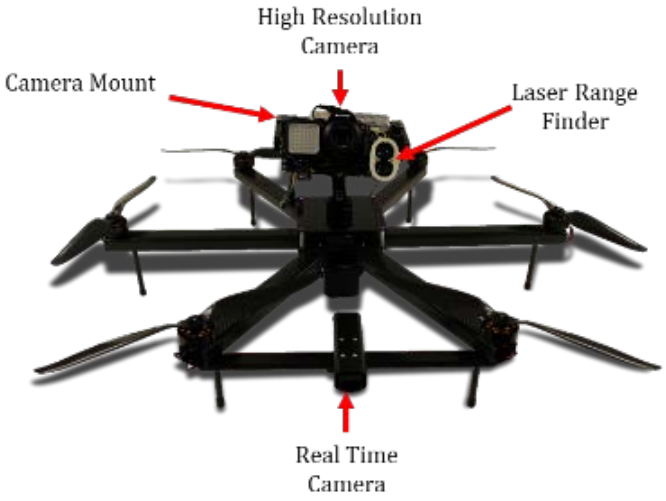

Figure 2-1. Concept of sUAV used for first HMLP inspections

Because the primary goal of the HMLP inspections was to safely collect high quality video of areas of HMLPs that would be difficult to view from the ground, the camera payload was very important. The high-resolution camera selected for HMLP inspections was a Sony α7R, equipped with a 35-mm lens. The camera takes 36 Megapixel still images and 1080p video. Video is streamed to the inspector's monitor at the ground and saved to an SD card in the camera. Brushless gimbal motors on the camera mount allow the inspector to direct the camera independently of the vehicle. The brushless motors also stabilize the camera, so the video is not shaky.

The rest of the sensors are primarily for flight control. A CONNEX ProSight real time camera is mounted to the front of the sUAV, providing a first-person-view (FPV) from the vehicle to the RPIC. The video from the real time camera is streamed with low latency. A laser range finder mounted to the camera was used to maintain an offset distance from the center of the HMLP. A laser range finder has two main components: a laser and a collector. The laser range finder emits a laser pulse and measures the time it takes for the laser pulse to return to the collector to determine distance. In addition, a GPS receiver, not shown in Figure 2-1, was used to determine, and later control, the position of the sUAV during flight.

2.3.2 HMLP Inspection Flight Modes

HMLPs do not obstruct GPS, so GPS controlled flight modes could be used. With GPS, automated flight paths could be used as a safe and efficient method of inspecting HMLPs with sUAVs. The flight mode used for the first set of inspections consisted of a GPS latitude and longitude hold with a controlled ascent and descent rate. For this method, the sUAV was flown up and down two opposite faces of the HMLP, pausing at slip joints. Although this flight method was simple, it required relocation of the ground station between the two flights. The ascent and descent rate could be set to a constant velocity. This controlled change in altitude was called Stabilize Mode.

A new flight mode, Circle Mode, was introduced for the second set of inspections. Circle Mode is a flight algorithm developed at UF that allows the sUAV to maintain a constant radius from the HMLP. Using its onboard GPS and compass, the elevation and radial position of the sUAV can be easily adjusted while in Circle Mode. The method used to inspect the HMLPs consisted of an ascent to the top of the HMLP, a 90˚ counterclockwise rotation about the pole, a descent to approximately twenty feet above the base of the pole, another 90˚ rotation and ascent, and one final rotation and descent (see Figure 2-2). This method eliminated the need for more than one flight, meaning the ground station no longer needed to be relocated, and it made flying the sUAV easier to control for the RPIC. The RPIC moved with the sUAV to keep a direct line of sight on the vehicle. As the height of the sUAV relative to the HMLP is difficult to judge from the ground, the RPIC relied on the inspector and the VO to determine when the sUAV reached the top of the light pole.

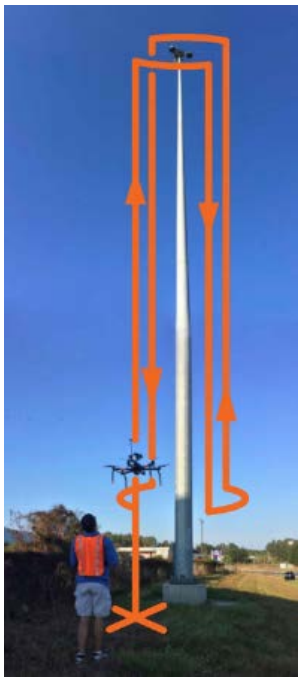

Figure 2-2. Schematic of Circle Mode flight path

In the time since the last HMLP inspection, a new, automatic flight path has been developed. With Spiral Mode, the sUAV maintains a constant radius from the HMLP, flies to the top of the HMLP while panning side to side using the rangefinder to determine when it has surpassed the top of the light pole. Once at the top, it flies back down in a spiral so that all sides of the light pole can be seen. This flight method does not depend on any piloting skill. One limitation to this flight method is that it can be difficult to determine which side of the HMLP the sUAV is on when a picture is taken, but all the pictures are tagged with positional and attitude information of the aircraft so one can go back and determine exactly where the photo was taken.

2.4 sUAV Used for Bridge Inspections

Bridge inspections present a number of significant challenges for sUAV operations. Operating underneath a bridge can render GPS, used for flight control, ineffective. Thus, to maneuver the sUAV to guide the airframe and obtain images of the bridge elements underneath the bridge, position control technology other than GPS must be used. Sensors and materials on the sUAV were used to improve flight control, image collection, and landing safety as detailed below.

2.4.1 Description of Airframe and Sensors for Flight Control and Image Collection

Achieving a balance between payload features and vehicle maneuverability proved to be a constant challenge when optimizing the sUAV for bridge inspection. Adding additional sensors may improve data collection, but the additional weight reduces flight time and makes flight control more difficult for the RPIC. With this in mind, the final vehicle used for bridge inspections is shown in Figure 2-3. A quadcopter was selected because it provided greater maneuverability than a hexacopter. This quadcopter is larger than the quadcopter originally considered in Section 2.3.1, giving it a sufficiently large payload for the imaging and flight

sensors. It should be noted that no off-the-shelf sUAS is purpose-built for under bridge inspections.

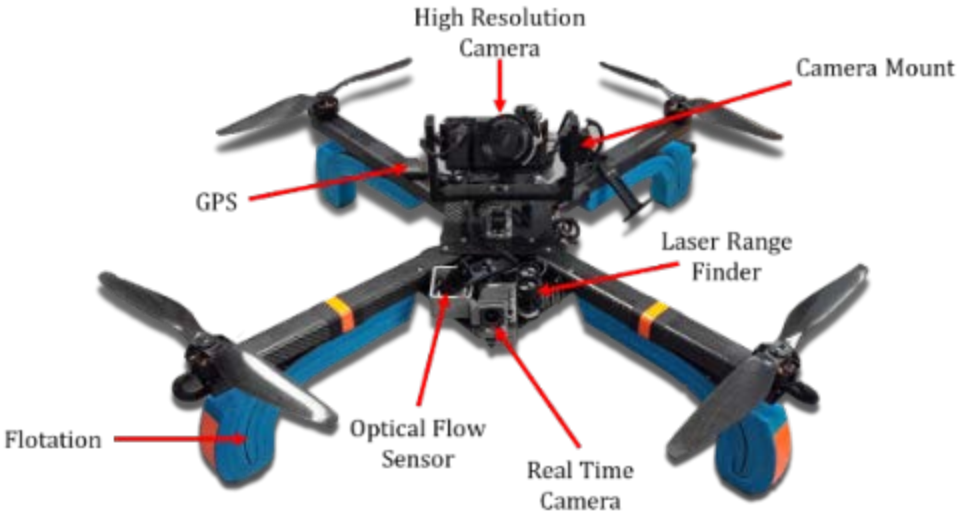

Figure 2-3. sUAV used for bridge inspections

The high-resolution camera is the primary sensor for data collection. Instead of the Sony α7R, a Sony α6000, equipped with a 16-50 mm zoom lens, was used for the bridge inspections. The camera takes 24 Megapixel still images and 1080p video. A GoPro was considered for the vehicle due to its lightweight and compact design, but the selected camera offers higher resolution, zoom capabilities, and better sensor performance. Video and images from the camera are both streamed to the inspector's monitor at the ground and saved to an SD card in the camera. The inspector can zoom in and out and switch between recording video and taking still images while the sUAV is still in the air. The camera was changed because the α6000 body and zoom lens were less expensive and lighter than the α7R, and the pixel density of the α6000 sensor is higher.

Servo motors were used for the camera mount to reduce weight from the brushless motors. The camera could be directed independently of the sUAV, and the camera mount pitch motor is stabilized, but the video is still slightly shaky. Use of brushless motors could have improved video stabilization but would have added weight, resulting in a decreased flight time. Although the video is not stabilized, it is still clear enough for an inspector to spot a deficiency. Clarity of still images is not affected by the lack of stabilization, as the shutter speed is fast enough to eliminate camera shake.

The majority of the remaining sensors and features on the vehicle are present to assist the RPIC with flight. The CONNEX ProSight real time camera is still used to provide an FPV from the vehicle to the RPIC. The laser range finder measures the vertical distance from the sUAV to the bottom of the bridge, which will be referred to as the stand-off distance. This stand-off distance is automatically maintained by the autopilot, the system that enables the sUAV to fly and keeps the aircraft stable. The autopilot used by the sUAV is a 3DRobitic's Pixhawk.

An optical flow sensor is essentially a small video camera that can detect motion of pixels between video frames. It can be used to measure the motion of the sensor relative to the object being filmed. By attaching an optical flow sensor to the sUAV, the relative motion of the sUAV to the bridge can be determined. When the sensor is provided a vertical distance from the bridge, d, it can determine the horizontal velocity, V, from the angular rate of change of pixels across video frames, ω (see Figure 2-4). For example, one application for optical flow sensors is in optical computer mice, which track the offset of pixels of the surface below the mouse to determine the distance and the direction the mouse has moved.

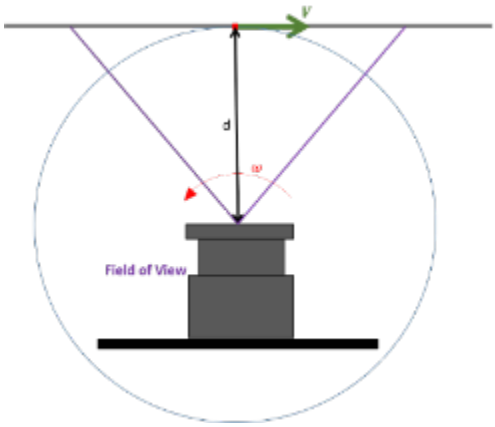

Figure 2-4. Optical flow sensor using angular velocity of pixels, ω, between frames to determine horizontal velocity, V

For application on an sUAV underneath a bridge, an optical flow sensor can be used to hold position and determine location by integrating the velocities of the pixels between frames. The optical flow sensor is programmed to look up at the bridge underside instead of the ground. This orientation is preferable to downward facing optical sensor because if the sUAV is above water, the optical flow sensor may try to follow the movement of the water and ripples on the surface of the water. The optical flow sensor must be informed by the vertical distance from the bottom of the bridge obtained from the laser-range finder and the orientation of the sUAV from an onboard compass. This navigation information is then used by the autopilot to maintain a position and velocity commanded by the RPIC. The optical flow sensor also has a gyroscope to account for rotation of the camera relative to the bridge. Measurements from the optical flow sensor, the laser range finder, the barometer, and the inertial measurement unit (IMU) are fed into a Kalman filter, which combines the data from these sensors into one source of position data, to allow for greater control and obstacle avoidance of the sUAV without GPS. These sensors allow the sUAV to be flown underneath a bridge where GPS is denied without having to rely entirely on manual piloting.

Because the bridge inspections in this project are above bodies of water, the sUAV landing gear was retrofitted with polyethylene foam to increase the buoyancy of the vehicle. With the added flotation system, if an emergency landing were required, the vehicle and payload would be recoverable from the water and may be protected from extensive water damage. The addition of polyethylene foam to the vehicle had the further benefit of dampening the impact of the sUAV landing on the ground.

2.4.2 Bridge Inspection Flight Modes

The sUAV has three primary modes of flight for bridge inspections: Optical Flow Mode (OFM), Altitude Hold Mode (AHM), and GPS Mode (GPSM). For a flight underneath a bridge, where GPS may not be sufficient, the sUAV would typically initially be piloted to the bridge underside in AHM. When sufficiently underneath the bridge deck, OFM will be engaged. In this mode, the aircraft will continue to operate in AHM with the addition of incorporating a laser rangefinder which automatically maintains a minimum standoff distance from the bottom of the bridge deck. Within the flight mode, when the aircraft is close enough for the optical flow sensor to find enough feature points to provide accurate position data, the sUAV would automatically switch to using the optical flow sensor to hold position similar to that of using GPSM, greatly reducing the effort by the pilot to maintain positioning of the aircraft in the presence of wind. For flights outside of the bridge, the sUAV would be operated in GPSM. These flight modes were under development during the initial bridge inspections and were refined throughout the project.

2.5 Description of Ground Station

The ground station (see Figure 2-5) has two monitors. 720p video from the FPV camera is streamed with no apparent lag to the RPIC's monitor, and the view from the high-resolution camera is streamed to the inspector's monitor at 1080p. There are also two transmitters at the ground station: the RPIC's transmitter, which controls the sUAV, and the inspector's transmitter, which controls the direction of the camera independently of the sUAV, and allows the inspector to take videos or images. Additionally, the ground station has a laptop running Mission Planner, a free, open-source ground station application.

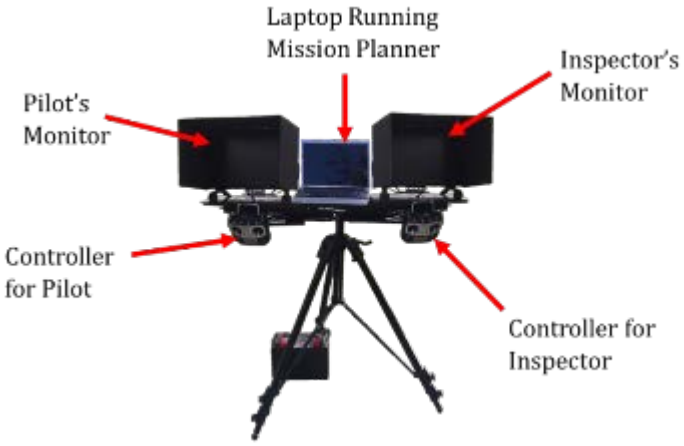

Figure 2-5. Ground station used during inspections

2.6 Changes to sUAV throughout Project

The sUAV changed significantly throughout the project. At the beginning of the HMLP inspections, a hexacopter was used. As the project progressed, a quadcopter was found to be preferable, as it is more maneuverable. The landing gear was adjusted several times, as can be seen in Figure 2-6. The final landing gear had a sufficient shear strength for landings with velocity parallel to the ground, it dampened the impact of the sUAV landing on the ground, and it provided buoyancy in case an emergency water landing was required.

As bridge inspections are a more difficult application for sUAV operations than HMLP inspections, the likelihood of losing the sUAV is higher. This is the primary reason the high-resolution camera was changed from a Sony α7R to a less expensive α6000 that still had high enough resolution and low light imaging quality. The α6000 camera had a lower overall resolution, but a higher pixel density and a less expensive optical zoom lens. As a result, the new camera payload was also able to pick up smaller deficiencies than the camera payload used for HMLP inspections. In addition, the α6000 weighs less than the α7R. The imaging controls were improved throughout the project, as well. Initially, an inspector could only direct the camera and collect video. For the last few inspections, the inspector had the ability to switch between video and image collection while the sUAV was still in the air.

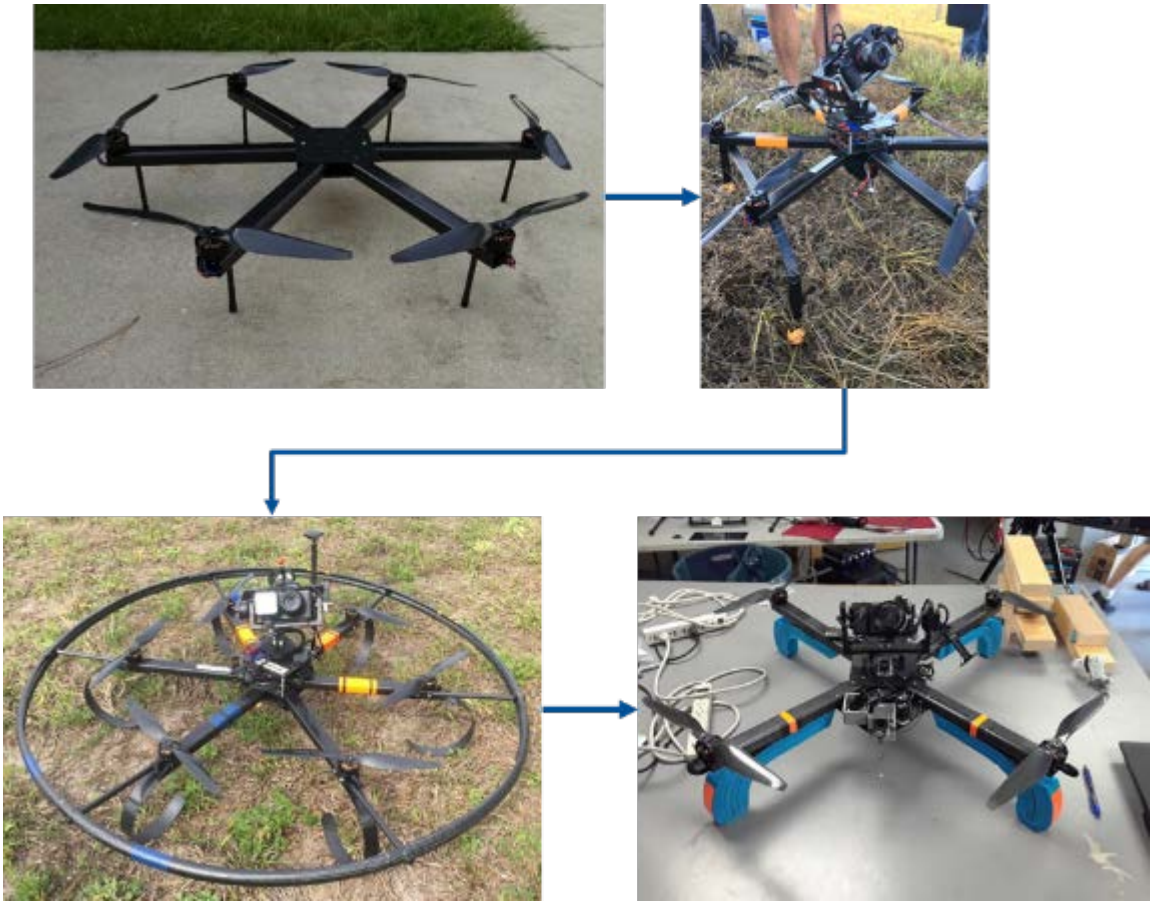

Figure 2-6. Changes to sUAV landing gear

3 Summary of HMLP Inspections

With an understanding of the crew, the vehicle, and the flight modes used for HMLP inspections, the six HMLP inspections conducted during this project will be discussed in this section. The UF team inspected HMLPs at two separate locations. The first three HMLPs were inspected during a regularly scheduled inspection with an inspection crew at the intersection of State Road 6 and I-75. The last three HMLPs were inspected at the intersection of I-295 and Town Center Parkway (see Figure 3-1).

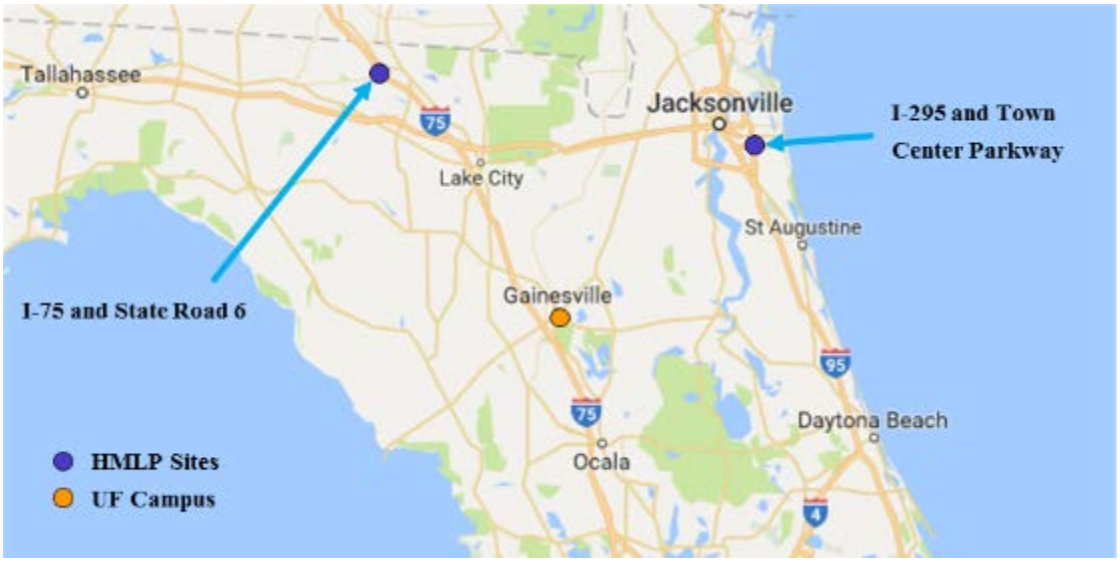

Figure 3-1. Locations of HMLP inspections

3.1 State Road 6 and I-75

The inspection at State Road 6 and I-75 was conducted on Tuesday, November 1, 2016 with inspectors from a consulting firm. Three HMLPs were inspected: 32P049, 32P050, and 32P054 (see Figure 3-2). For these three inspections, video was streamed from the sUAV to a monitor during the inspection, and high-resolution video 1080p was saved to an SD card to be reviewed later. A 35-mm lens was mounted on the camera.

After the in-field portion of the inspection, an inspection report was created using still frames pulled from the video. VLC media player was used to obtain the full-resolution still images from the video, by pausing the video at the desired moment and extracting the frame. For each HMLP, the process of obtaining the images used in the inspection image report took less than ten minutes.

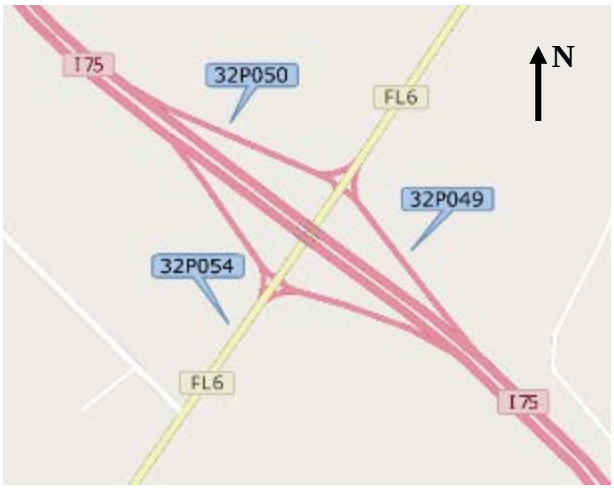

Figure 3-2. Locations of HMLPs at State Road 6 and I-75

The crew overseeing the flight of the sUAV consisted of more than the minimum number of recommended crew members described in Section 2.2. For this inspection, in addition to the three recommended crew members, two additional crew members were involved. One inspector, unaffiliated with the research at UF, controlled data acquisition by maneuvering the camera gimbal and monitoring the streaming video. The final crew member provided additional awareness of the systems on the ground as well as the flight operation. The crew monitoring the ground station is shown in Figure 3-3. Note that the fifth crew member, the RPIC, is not shown.


Figure 3-3. Crew monitoring ground station during inspections at State Road 6 and I-75

For these inspections, two flight methods were investigated. The first two HMLPs were inspected using the first method described in the HMLP Inspection Flight Modes section; the GPS position was held, while the altitude of the sUAV was adjusted. The third pole, 32P054, was inspected by manually flying the sUAV up one side of the pole and encircling the slip joints.

This method eliminated the need for more than one flight but relied more heavily on the skill of the pilot.

Conditions for the inspection were calm. Wind speed remained under 4 mph for the duration of the inspections. The sky was clear, which caused the exposure of the pole in the video to be dark when the sun was directly behind the pole.

3.1.1 32P049

The first HMLP inspected for this research project was 32P049. The inspector controlled the camera gimbal. The other crew members, the RPIC and the VO, were from UF. A timeline of events for this inspection is provided in Table 3-1.

Setup time took about twelve minutes. The flight up and down the southeast side of the pole was conducted first, which took about three minutes. Temporary streaming video pixilation was experienced when the sUAV reached the top of the HMLP. The video saved to the SD card did not pixelate. After the antenna on the sUAV was rotated from the top to the bottom of the sUAV, the problem of streaming video pixilation was resolved. Between the inspection of the southeast face and the northeast face, the battery for the sUAV was replaced, and the ground station was relocated. The northeast face of 32P049 was inspected next. The sUAV initially had trouble stabilizing and was forced to make an emergency landing. This was likely caused by not being connected to enough GPS satellites. The minimum number of GPS satellites for stable operation of the sUAV is eight, however the ideal number is twelve. After some troubleshooting, the sUAV was able to inspect the northeast face of the HMLP. No additional unplanned landings occurred during the remaining HMLP inspections. A typical image pulled from the video inspection of this structure is shown in Figure 3-4. The image is of the southeast face of the first slip joint of 32P049.

Figure 3-4. View of southeast face of first slip joint of 32P049

During this inspection, the sun was behind the HMLP. The brightness of the background caused portions of the video to be underexposed, so the HMLP was too dark. Later, it was determined that by pointing the camera downward, this effect is reduced. Tear down time was about five minutes. No deficiencies were detected on this HMLP.

Table 3-1. HMLP 32P049 inspection timeline

Time	Description	Duration
	Pre-Flight Setup	12 min
9:14	Began Flying on Southeast Face of Pole	3 min
9:17	Returned to Ground	
9:17	Relocating Ground Station	7 min
9:24	Began Flying on Northwest Face of Pole	1 min
9:24	Returned to Ground Unexpectedly	
9:25	Troubleshooting Stabilization Issues	7 min
9:32	Began Flying on Northwest Face of Pole	3 min
9:35	Returned to Ground	
9:35	Tear Down and Packing up	5 min
9:40	Inspection Finished, Discussion of Impressions	
	Total Inspection Time	38 min

3.1.2 32P050

The second HMLP inspected at this site was 32P050. The inspector controlled the camera gimbal. The other crew members, the RPIC and the VO, were from UF. A timeline of events for this inspection is provided in Table 3-2.

Setup took about ten minutes, and the southeast side of the pole was inspected first. The flight up and down the southeast side of the pole was conducted first, and this took about three minutes. No streaming video pixilation was experienced during this flight. Between inspections of the southeast and northwest faces of the HMLP, the ground station was relocated. The northwest face of the pole was then inspected. This face also took about three minutes. During this inspection, the benefit of pointing the camera at a downward angle, as to reduce the effect of a bright background was realized. Tear down of the ground station took about four minutes. No deficiencies were detected on this HMLP.

The inspector suggested performing one flight, circling around the slip joints, instead of relocating the ground station multiple times for the inspection of one HMLP. Following his recommendation, the inspection of the next pole, 32P054, was conducted in one flight.

Table 3-2. HMLP 32P050 inspection timeline

Time	Description	Duration
9:52	Pre-Flight Setup	12 min
10:04	Began Flying on Southeast Face of Pole	3 min
10:07	Returned to Ground	
10:07	Relocating Ground Station	4 min
10:11	Began Flying on Northwest Face of Pole	3 min
10:14	Returned to Ground	
10:14	Tear Down and Packing up	7 min
10:15	Inspector Finished Standard Inspection	
10:21	sUAV Inspection Finished	
	Total Inspection Time	29 min

3.1.3 32P054

The third HMLP inspected at this site was 32P054. The inspector controlled the camera gimbal. The other crew members, the RPIC and the VO, were from UF. A timeline of events for this inspection is provided in Table 3-3.

Unloading the truck and setting up the ground station took about ten minutes. This inspection began at the northeast face of the pole. The sUAV ascended to the first seam, at which point it encircled the HMLP. Flying the sUAV in a circle proved to be difficult and was achieved cumbersomely. The second seam was not encircled. The duration of this flight was about five minutes. This method reduced time in the air by about one minute compared to the other two poles and eliminated the need to move the ground station. However, only one seam was encircled. Encircling both seams would have added time to the flight. After the flight, it took about four minutes to tear down the ground station.

This HMLP was the third pole to be inspected. The HMLP that was originally selected was changed to avoid nearby power lines. During this inspection, corrosion, which had been detected in previous inspections, was found above the first slip joint on the northeast face of the pole. An image of the corrosion, pulled from a frame of the video, is shown in Figure 3-5.

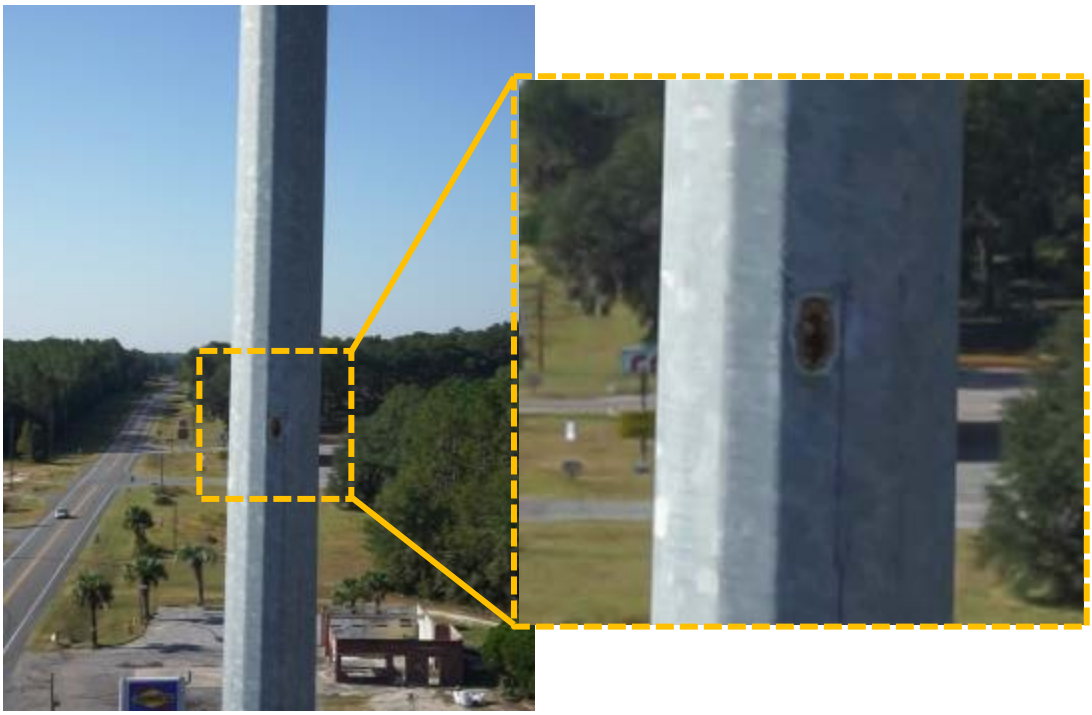

Figure 3-5. Corrosion above first slip joint on northeast face of 32P054

Table 3-3. HMLP 32P054 inspection timeline

Time	Description	Duration
10:29	Pre-Flight Setup	10 min
10:39	Began Flying on Northeast Face of Pole	5 min
10:42	Completed Circle around First Slip Joint	
10:44	Returned to Ground	
10:44	Tear Down and Packing up	7 min
10:51	sUAV Inspection Finished	
	Total Inspection Time	22 min

3.2 I-295 and Town Center Parkway

This inspection was conducted on February 14, 2017 at the intersection of I-295 and Town Center Parkway. Three HMLPs were inspected: 72P740, 72P741, and 72P743 (see Figure 3-6). As with the previous set of inspections, video was streamed from the sUAV to a monitor during the inspection, high-resolution video was saved to an SD card to be reviewed later, and frames were pulled from the video to create a report containing still images from the inspection using the same method described in Section 3.1. As with the first inspection, streaming video experienced minor pixilation as the sUAV approached the top of the HMLP as a result of the distance between the sUAV and the receiver; however, the video saved to the SD card was not affected.

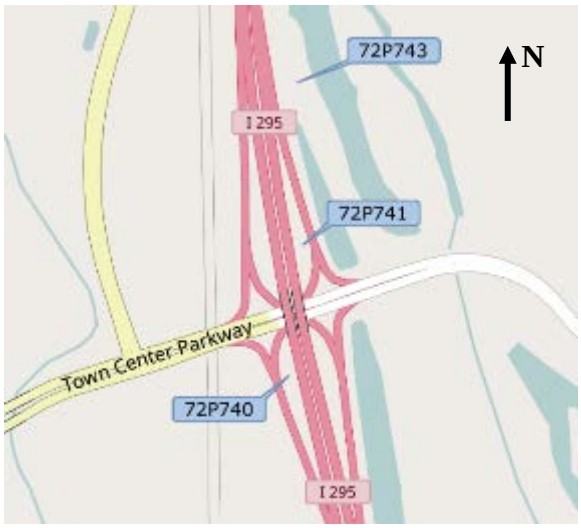

Figure 3-6. Locations of HMLPs at Town Center Parkway and I-295

The crew overseeing the flight of the sUAV consisted of the minimum recommended crew. The RPIC controlled the sUAV, the inspector controlled data acquisition by maneuvering the camera gimbal and monitoring the streaming video, and the VO provided additional awareness of the systems on the ground as well as the flight operation. All members of the crew were affiliated with UF.

For these inspections, the HMLPs were inspected in Circle Mode. After each HMLP inspection, the battery was replaced, although its charge was typically at about sixty or seventy percent at the end of each flight. Conditions for the inspection were calm. Wind speed remained between four and 10 mph for the duration of the inspections. The sky was mostly cloudy, resulting in well-lit conditions for video.

3.2.1 72P740

The first pole inspected at Town Center Parkway and I-295 was 72P740. A timeline of events for this inspection is provided in Table 3-4.

Unloading the truck and setting up the ground station took about fourteen minutes. The setup time was longer than any previous inspection because the ground around the HMLP was sloped. Taking off from a non-level surface results in an initial difficulty stabilizing the sUAV, so a piece of plywood was used to make a level platform (see Figure 3-7). Figure 3-7 also shows the propeller guard added to the sUAV. Additionally, to use Circle Mode, the distance from the pole and the direction of a line from the sUAV to the HMLP must be known. Therefore, steel tape was used to set the HMLP to a five-meter radius from the center of the HMLP, and the front of the sUAV was carefully aligned to point towards the pole.

Figure 3-7. Plywood launch pad

This inspection began at the west face of the pole. The inspection then proceeded according to the method described in Section 2.3.2. The duration of this flight was about four minutes. This method significantly reduced time in the air from previous inspections, and did not require relocation of the ground station. No deficiencies were detected on this HMLP.

Table 3-4. HMLP 72P740 inspection timeline

Time	Description	Duration
10:32	Pre-Flight Setup	14 min
10:48	Began Flight	4 min
10:52	Returned to Ground	
11:02	Tear Down and Packing up	6 min
11:08	sUAV Inspection Finished	
	Total Inspection Time	24 min

3.2.2 72P741

The second pole inspected at Town Center Parkway and I-295 was 72P741. A timeline of events for this inspection is provided in Table 3-5.

Unloading the truck and setting up the ground station took approximately nine minutes. The ground around the HMLP was sloped again, but the setup time was reduced due to increased experience and, thus, increased efficiency of the crew. The setup process was the same as for the previous pole.

This inspection began at the east face of the pole. The inspection then proceeded according to the method described in Section 2.3.2. The duration of this flight was just over three minutes, and tear down of the ground station took about six minutes. No deficiencies were detected on this HMLP, which is consistent with the inspection report provided by the FDOT. A typical image pulled from the video inspection of this structure is shown in Figure 3-8. This image shows a view of the luminaire from the north.

Figure 3-8. View of luminaire of 72P741 from north

Table 3-5. HMLP 72P741 inspection timeline

Time	Description	Duration
11:22	Pre-Flight Setup	9 min
11:31	Began Flight	3 min
11:34	Returned to Ground	
11:34	Tear Down and Packing up	6 min
11:40	sUAV Inspection Finished	
	Total Inspection Time	18 min

3.2.3 72P743

The final HMLP inspected by UF was 72P743. A timeline of events for this inspection is provided in Table 3-6.

This inspection shows the consistency of the approach used to inspect HMLPs. The setup time, the inspection time in the air, and the pack-up time were nearly identical to those of the 72P741. 72P743 was located on level ground, so the plywood launch pad was not needed. This inspection began at the north face of the pole. The inspection then proceeded according to the method described in Section 3.2, except that this flight included an additional revolution around lighting fixture. No deficiencies were detected on this HMLP.

Table 3-6. HMLP 72P743 inspection timeline

Time	Description	Duration
11:43	Pre-Flight Setup	8 min
11:51	Began Flight	4 min
11:55	Returned to Ground	
11:55	Tear Down and Packing up	6 min
12:01	sUAV Inspection Finished	
	Total Inspection Time	18 min

3.3 Summary and Comparison of Inspections

The results from the inspections at Town Center Parkway and I-295 showed the significant improvements made to the sUAV system since the first inspections at State Road 6 and I-75. The development of a new flight pattern made the largest impact on the inspection procedure. By adding Circle Mode, flights were faster and easier to control than the previous inspections, and the entire pole could be inspected in a single flight. Circle Mode simplified the controls and did not rely as heavily on the skill of the pilot.

Other improvements to the system include the addition of a propeller guard around the vehicle and improved landing gear. The landing gear provided greater stability for the sUAV when landing with velocity parallel to the ground. Figure 3-9 shows the RPIC landing the sUAV on the plywood platform during the second set of inspections. In this image, the propeller guard and the landing gear can be seen.

Figure 3-9. RPIC landing sUAV on plywood launch pad after inspection of 72P741 during Town Center Parkway and I-295 inspections

The system requires more equipment than conventional inspections, and it is still constrained by wind, tree branches, power lines, and other similar obstructions. Although the

setup and breakdown times are greater for the sUAV inspection than traditional inspections, the brevity of the flight mitigates these problems. The cost of the sUAV is also higher than conventional inspections, as will be discussed in Section 6.2. In both inspections, the sUAV was able to provide views of the HMLP that would not be feasible from current HMLP inspection practices.

Table 3-7. Comparison of sUAV HMLP inspections

Inspection	Light-pole	Setup Time	Pack-up Time	Time in Air	Total sUAV Inspection Time
SR-6 and I-75	32P049	12 min	5 min	7 min	38 min
	32P050	12 min	7 min	5 min	29 min
	32P054	10 min	7 min	5 min	22 min
Town Center Parkway and I-295	72P740	14 min	6 min	4 min	24 min
	72P741	9 min	6 min	3 min	18 min
	72P743	8 min	6 min	4 min	18 min

3.4 Inspector Feedback

After the HMLP inspections at State Road 6 and I-75, a set of post-inspection questions was distributed to the inspectors and FDOT employees in attendance at the demonstration. In this section, the responses to these questions are discussed. Overall, the responses indicated an openness to the use of new technology, but offered suggestions for improvement to the system and expressed concern about the benefits of using an sUAV for HMLP inspections compared to the limitations. The most common comments brought up by the inspectors are discussed below. Inspectors were pleased with the ability of the sUAV to get closer to the HMLP than an inspector could. The main limitations brought up in the responses included setup time, extra equipment required, camera zoom capabilities, and the negative video exposure effects when facing the sun.

The sUAV has the ability to view areas of an HMLP that inspectors are unable to view or require binoculars to view. Since the sUAV can remain a constant distance from the HMLP, it has an advantage over an inspector standing on the ground, who must view the second slip joint from nearly eighty feet below. This is an advantage for the sUAV as compared to current inspections because the entire HMLP can be viewed from a consistent and close distance. Additionally, the sUAV can view the top of the light fixture, which is not possible for an inspector on the ground. This view, however, is not required for the structural inspection.

Setup time for the sUAV inspection is significantly more than that for the current inspection practices. Compared to walking up to the HMLP with a pair of binoculars and a chipping hammer, which takes almost no time, setting up the ground station for the sUAV took nearly ten minutes from when the equipment was taken out of the vehicle to when the sUAV was ready for the inspection. Since the current inspection only takes about twenty minutes, this setup time is significant. It should be noted that the sUAV inspections took about the same time for an inspection of a single HMLP as current inspection practices. Video was collected during these inspections, and as a result, the video had to be reviewed at a later time. This would cause a larger increase in time and effort for each inspection. As will be discussed later, it may be more efficient to only collect high-resolution still images needed for inspection reports.

Current inspection practices require qualified inspectors, a pair of binoculars and a chipping hammer. With the sUAV, more equipment and personnel are required. This would increase both initial cost of purchasing the sUAV and the in-field inspection cost to pay for the extra personnel required in the inspection. Also adding to the cost would be a qualified RPIC for the sUAV. Additionally, in response to the post-inspection interviews, inspectors expressed concern that the system was cumbersome.

On several occasions, inspectors asked whether the camera mounted on the drone had zoom capabilities. In response to the many people who suggested a zoom lens would improve the quality of inspections, the lens was changed for bridge inspections.

One issue that came to light during the inspections was that when the sUAV was inspecting the HMLP from the side opposite from the sun, the shadow side of the HMLP appeared very dark in contrast to the bright background. It became apparent that in these situations, angling the camera either up or down, so that the sun was not directly in the field of view, was enough to improve the image exposure and provide an image of quality sufficient to perform the inspection.

The HMLPs were inspected by flying up and down the side of the pole from different angles, as to visually inspect the entire structure. This was done because flying in this pattern makes locating a deficiency noticed in the footage easier. However, if only images are collected during the inspection, an inspector could note the location of the deficiency in the field during the inspection. During the first set of inspections, the sUAV was flown up and down, and then picked up by hand and moved to other angles around the HMLP, as to avoid having the pilot perform a complex flight maneuver to change the viewing angle. For the second set of inspections, Circle Mode was implemented, which greatly reduced the amount of work on the pilot and allowed for the inspection of the entire HMLP to be done in a single flight. With the new proposed flight mode, Spiral Mode, the amount of work for sUAV inspections could be further reduced.

4 Summary of Bridge Inspections

After the six HMLP inspections were completed and the sUAV was redesigned for operation underneath a bridge, eight bridge inspections throughout north Florida were conducted. Three inspections were conducted alongside regularly scheduled inspections that required UBIVs, and the other five were conducted independently, with a CBI present. The structures offered a variety of structural elements and materials to inspect. Table 4-1 provides a summary of the inspection sites, and Figure 4-1 shows the locations of the inspections.

Table 4-1. Overview of bridge inspection sites

Date	Location	Length (ft)	Clearance (ft)	Materials
Jun. 28, 2017	Atlantic Boulevard	2,350	74	Steel and prestressed concrete
		2,955	65	Steel and prestressed concrete
Jul. 18, 2017	William V. Chappell Jr.	2,002	65	Steel and prestressed concrete
Jul. 19, 2017	Harris Saxon	2,447	65	Prestressed concrete
Aug. 1, 2017	Fanning Springs	815	26	Prestressed concrete
		806	26	Prestressed concrete
Oct. 10, 2017	SR-6 over Withlacoochee	505	29	Steel
Oct. 12, 2017	SR-40 over Ocklawaha	2,734	49	Steel and prestressed concrete
Oct. 25, 2017	US-41 over CSXRR	521	21	Steel
Dec. 14, 2017	SR-228 over Washington St.	7,163	30	Steel and prestressed concrete

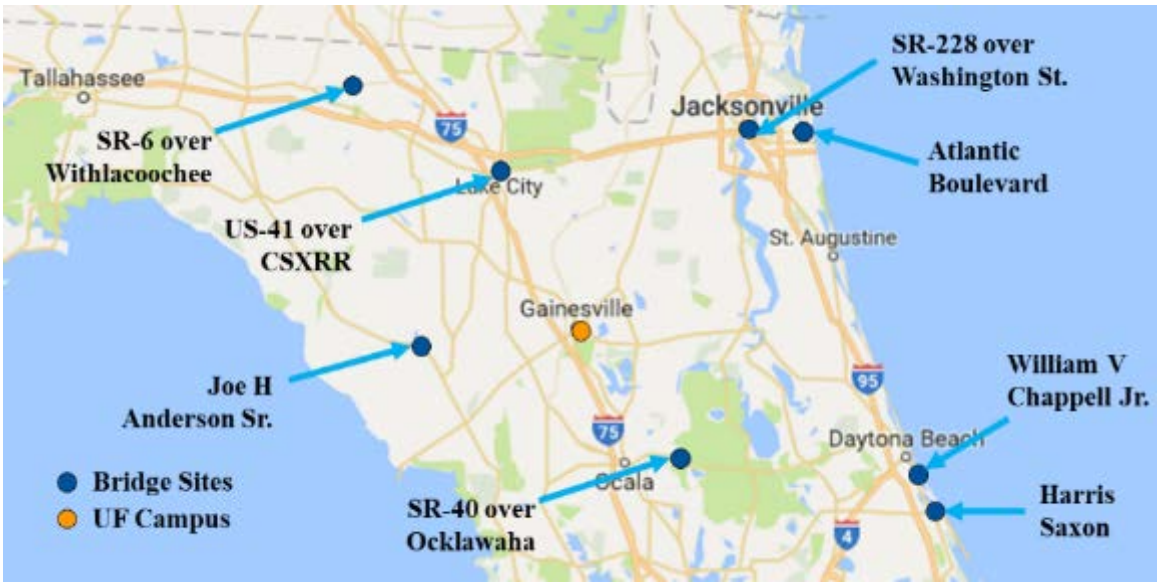

Figure 4-1. Locations of bridge inspections

Inspections were conducted alongside CBIs from FDOT. After each inspection, these inspectors provided feedback about the effectiveness of the sUAV for bridge inspection, including what worked and what needed to be improved. The following sections provide details on each of the bridge inspections, including the inspection setup, flight times, and outcomes. The inspections are presented in chronological order and highlight changes or improvements that were made to the system and the methods as more experience was gained by the research team.

During the inspections, saving still images proved to be more advantageous than saving videos and pulling frames of the videos for inspection reports. Still images are much higher resolution than videos, post-processing a video to save a frame from a video requires additional time and effort, and the still images take up less storage than videos. Also, a certified inspector in the field can determine if a still image is adequate, so saving videos of the structure should not be required.

Two general approaches to sUAV bridge inspections were considered for this study. The first approach involved inspection of only previously known deficiencies, so it would be similar to a special inspection or a damage inspection. The second approach would be a complete sUAV routine bridge inspection to have similar outcomes as current routine bridge inspections.

4.1 Atlantic Boulevard over the San Pablo River – 720044 and 720690

The inspection at Atlantic Boulevard over San Pablo River was conducted on Wednesday, June 28, 2017 with inspectors from FDOT (see Figure 4-2). Portions of two structures were inspected: 720044 and 720690. The weather was dry, but wind gusts reached up to 15 mph during the inspection, creating difficult conditions for the RPIC. A total of ten flights were conducted, with a CBI controlling the camera for the fifth through tenth flights. This inspection was largely a learning experience for UF team.

Figure 4-2. Aerial view of 720044 and 7206690

The inspections began underneath Span 9 of 720044 on a dive boat with a landing platform assembled on the front (see Figure 4-3). Span 9 is the first steel span of 720044. Two flights were attempted at this location. The sUAV had difficulty stabilizing due to wind gusts and an optical flow lens with a high focal length, resulting in a too narrow field of view. Because the optical flow lens had a narrow field of view, the optical flow sensor was unable to pick up enough reference points underneath the bridge to accurately determine the velocity and position of the sUAV.

Figure 4-3. Crew, ground station, and sUAV set up on dive boat

After the first two flights from the boat, the vehicle and the ground station were relocated to the land underneath Span 9 of 720690. Span 9 is the first steel span of 720690. Three flights were conducted at this location. The first two flights were primarily for troubleshooting the systems involved in flight control. The optical flow lens was changed, and the sUAV control gains were increased, making the controls more sensitive, to account for the wind gusts. After these two test flights, the team became more confident in the vehicle and began a third flight. The vehicle was able to hold position better than before, but still drifted a significant amount. For the last five minutes of this nine-minute flight, the vehicle began traversing the beams in Span 9 of 720690, inspecting the bearings over Pier 10 and the connections of the lateral bracing between the beams in Span 9 (See Figure 4-4.a). While still set up at this location, the sUAV was used to inspect Bearing 9-1 over Pier 9, which is cracked and torn, as well as the outside face of Beam 8-1, which is a prestressed concrete girder.

After inspecting portions of Spans 8 and 9 of 720690, the ground station was relocated to the land beside Span 6 of 720044. Span 6 of 720044 is a prestressed concrete stringer-girder span. At this location, a spall on the North bottom flange of Beam 6-6 (See Figure 4-4.b) and a spall on Pier Cap 6 under Beam 6-7 were inspected. During the first flight, the camera on the sUAV would not switch from video to imaging mode, so a second flight was required at this location.

(a) (b)

Figure 4-4. Sample images from inspection at 720044 and 720690: (a) connection of lateral bracing between beams in Span 9, 720690, and (b) spall on Beam 6-6, 720044

The crew, along with the ground station and the sUAV, returned to Span 9 of 720044 in the dive boat. During the first flight at this location the sUAV was not able to engage the optical flow sensor and was brought back to the boat. The final flight of the day started well. The sUAV recorded video of the bearings in Span 9 over Pier 10, as well as the connections of the lateral bracing between the beams and the splice plate connections on the beams of Span 9. After obtaining a satisfactory amount of video, the team began to bring the sUAV back to the boat.

However, the UF team changed its mind and decided to fly up to the bridge to capture images in this span. When ascending, the sUAV was accidentally switched into Stabilize Mode, rather than OFM. In this situation, because the sUAV was ascending toward the bridge when Stabilize Mode was engaged, the vehicle continued to ascend into the bottom of the structure, resulting in a failure of the system. To address this accident for future flights, the sUAV was reconfigured to automatically switch into OFM when it is close to the bottom of the bridge or other obstacles.

Table 4-2. Atlantic Boulevard over San Pablo River inspection timeline

Flight	Time	Duration	Location	Description
1	10:45	2 min	720044 Span 9 deck underside	Problem stabilizing. sUAV returns to the ground. Troubleshooting with optical flow.
2	10:51	3 min		Optical flow locks in, but sUAV is blown around by wind. Move to land for troubleshooting.
3	11:13	4 min	720690 Span 9	Optical flow locks in, but sUAV is blown around by wind. Optical flow lens changed and gains adjusted.
4	11:34	1 min		With new optical flow lens. Troubleshooting instability.
5	11:44	9 min		RPIC becomes confident in controls. sUAV traverses span, inspecting bearings and connections.
6	12:07	8 min	720690 Pier 9	Certified inspector controls camera, inspects Bearing 9-1 over Pier 9, as well as North face of Beam 8-1.
7	12:44	3 min	720044 Span 6	Inspecting spall on North bottom flange of Beam 6-6. Camera would not come out of record to take images of deficiency.
8	12:51	6 min		Inspecting spall on Beam 6-6 and spall on Pier Cap 6 under Beam 6-7.
9	13:26	1 min	720044 Span 9	Return to boat to inspect deck underside. Experienced problem with flight and returned to boat.
10	13:30	6 min		Inspecting bearings in Span 9 over Pier 10 and connections throughout Span 9.

4.2 SR-A1A over the Halifax River – 790148

The inspection at SR-A1A over the Halifax River, structure 790148, was conducted on Tuesday, July 18, 2017 with inspectors from FDOT (see Figure 4-5). Weather conditions were calm throughout the duration of the inspection, with wind gusts less than 5 mph. A team member from UF operated the camera, since he had practice with the controller, and the CBI told the camera operator where to look.

Figure 4-5. Aerial view of 790148

The first flight was meant to be a test flight to see if the vehicle would be able to hold position. The sUAV was able to hold position well, so the team proceeded to inspect the face of Beam 5-4, the conduit attached to Pier Cap 5A, and a pipe fixture in Bay 1 of Span 5 over Pier 5A. After a successful first flight, the sUAV was used to inspect cracking with efflorescence in Pier Cap 4B (see Figure 4-6.a) and in the deck underside in portions of Span 4. Finally, the team moved to Span 7, the first steel span in 790148, to inspect bearings over Pier 7 (see Figure 4-6.b), splice plates in the beams, and corrosion and paint failures throughout the span. For this final flight, the sUAV was launched from the concrete footer at the base of Pier 7 (see Figure 4-7).

(a) (b)

Figure 4-6. Sample images from inspection at 790148: (a) cracking with efflorescence in Pier Cap 4B, 790148, and (b) interior bearings in Span 7 over Pier 7

Figure 4-7. sUAV set up on footer at the base of Pier 7

Although the wind was calm during this demonstration inspection, the UF team faced a different potential problem. The reflection of the sun in the Halifax River caused a shimmering effect on the underside of the bridge. This reflection posed a potential problem because the optical flow sensor uses the change of position of reference points to hold its position, and the reflection of the sun was not stationary due to waves on the surface of the water. However, the reflection did not affect the optical flow.

Table 4-3. SR-A1A over Halifax River inspection timeline

Flight	Time	Duration	Location	Description
1	9:24	9 min	Span 5, Pier 5	Inspecting Beam 5-4 South face, as well as conduit box and staining on Pier 5A.
2	9:46	9 min	Span 4, Pier 4	Inspecting cracking with efflorescence on Pier Cap 4B, as well as the deck underside in Span 4.
3	10:23	9 min	Span 7	Inspecting bearings 7-3 through 7-6 over Pier 7, splice plates, and corrosion and paint failures throughout span.

4.3 SR-44 over the Indian River – 790152

The inspection at SR-44 over the Indian River, structure 790152, was conducted on Wednesday, July 19, 2017 with inspectors from FDOT during a regularly scheduled inspection of the structure (see Figure 4-8). Weather conditions were initially calm, but wind gust speeds increased to about 8 mph for the latter portion of the inspection. A team member from UF operated the camera, since he had practice with the controller, and the CBI told the camera operator where to look.

Figure 4-8. Aerial view of 790152

The first flight began at Span 4, looking at the bearings over Pier 5. The flight was cut short because the stand-off distance was overly conservative; the sUAV could safely fly closer to the bottom of the bridge. After reducing the stand-off distance by about three feet, the second flight began in the same location. The view of the bearings was better than from the ground, but worse than an inspector would see in a UBIV. The third flight was similar to a routine inspection. The inspection began looking at bearings over Pier 5, traversing beams and inspecting the deck underside, and looking at specific details and deficiencies in this span. The setup for sUAV operations for these flights is shown in Figure 4-9.


Figure 4-9. Crew, ground station, and sUAV in parking lot underneath 790152

After inspecting Span 4, the crew relocated to Span 6 and conducted a special inspection of two specific deficiencies: debris in Bay 7 on Pier Cap 6 and missing anchor bolts on the outside of Beam 6-1. The sUAV was not programmed to transition from OFM flight underneath the bridge to GPSM flight outside the bridge. As a result, the sUAV was not flown outside the bridge, so the missing anchor bolts were not seen. Finally, the inspection crew moved to Span 9 to take an image of a large spall in the deck underside of Bay 9 over Pier Cap 9. Because the sUAV was in the outermost bay of the bridge, the optical flow camera only had a partial view of the bridge, which resulted in a smaller estimate of displacement than the sUAV was experiencing. Because of this, along with wind gusts, the sUAV had difficulty stabilizing and took three attempts to take an image of the deficiency. This spall and the debris on Pier Cap 6 were photographed both by the inspection crew in the UBIV and by the sUAV. Figure 4-10 shows a comparison of these images. As can be seen, the quality is comparable.

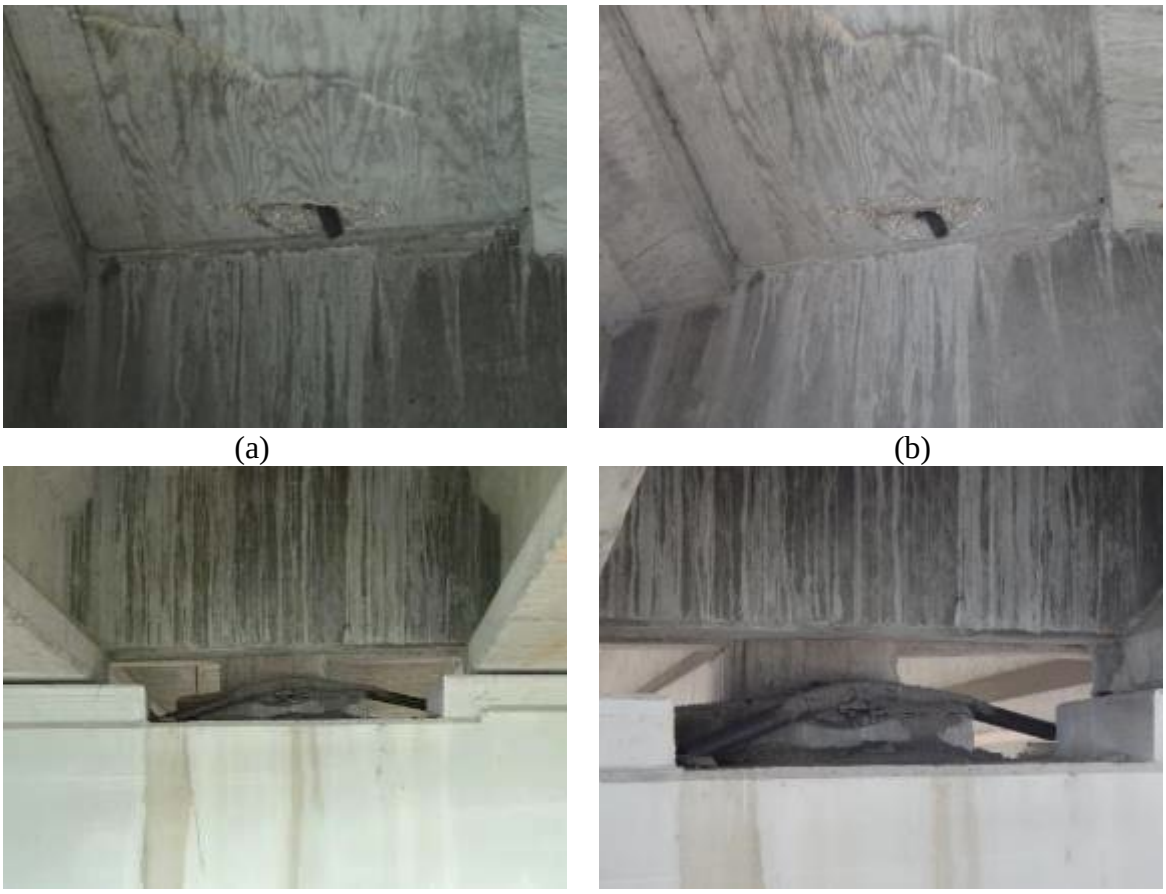

(a) (b)

(c) (d)

Figure 4-10. Comparison of images taken from sUAV (a and c) and images taken from UBIV (b and d). (a - b) spall in deck underside of Bay 9 over Pier Cap 9; (c - d) debris in Bay 7 on Pier Cap 6

Inspectors present at the demonstration inspection of SR-44 over the Indian River provided the highest quantitative feedback of the sUAV system out of all eight inspections. Overall, the sUAV performed well. The images taken from the sUAV were comparable to images taken from the UBIV, but the sUAV could not inspect the bearings as thoroughly as inspectors in the UBIV could. Also, the sUAV had some difficulty stabilizing towards the end of

the inspection, and three attempts were needed to take the image of the spall in the deck underside in Span 9.

Table 4-4. SR-44 over Indian River inspection timeline

Flight	Time	Duration	Location	Description
1	10:26	2 min	Span 4, Pier 5	Inspecting bearings over Pier 5. sUAV brought down to reduce stand-off distance from bottom of bridge.
2	10:30	4 min		Inspecting bearings and beam ends over Pier 5
3	10:45	8 min	Span 4, Pier Cap 4	Inspecting bearings and beam ends over Pier 4, deck underside in Span 4, cracking in Pier Cap 4, a pipe fixture in bay 11 over Pier 4, and traversing beams in Span 4.
4	11:14	5 min	Span 6, Pier Cap 6	Inspecting debris in bay 7 over Pier 6, anchor bolts inside of Beam 6-1 over Pier 6, and looking down beams in Span 6 from Pier 6.
5	11:34	1 min	Pier Cap 9, Bay 9	Inspecting spall in deck underside in bay 9 over Pier 9. Trouble stabilizing, returned to ground.
6	11:36	1 min		Inspecting spall in deck underside in bay 9 over Pier 9. Needed to increase stand-off distance because beams in this span were deeper, returned to ground.
7	11:39	2 min		Inspecting spall in deck underside in bay 9 over Pier 9. Successfully obtained image.

4.4 US-19 over the Suwanee River – 300031 and 300061

The inspection at US-19 over the Suwannee River in Fanning Springs, structures 300031 and 300061, was conducted on Tuesday, August 1, 2017, with an inspector from FDOT (see Figure 4-11). The wind was calm, with gusts up to about 7 mph. A team member from UF operated the camera, since he had practice with the controller, and the CBI told the camera operator where to look. Due to a low clearance and tight girder spacing, the undersides of the structures were too dark for the optical flow sensor to pick up enough feature points to accurately determine velocity and position of the sUAV. As a result, flying underneath the bridges presented a large challenge, and the sUAV required manual flight operation.

Figure 4-11. Aerial view of 300031 and 300061

Operating from a boat (see Figure 4-12), the first flight began underneath Span 12 of 300031. Debris build-up (see Figure 4-13), bearings, and insignificant cracking were the focus of this flight. However, due to insufficient light underneath the bridge, the optical flow could not pick enough feature points underneath the bridge, causing the sUAV to be unstable in the air. This bridge was darker than the previous structures because of its low clearance and close girder spacing.


Figure 4-12. Crew, ground station, and sUAV on boat during inspection of 300031 and 300061

The next two flights were performed outside of the structure, north of 300031. Spans 11, 12, and 13 were inspected. The team was looking at vegetation on the fascia beams, cracking in the beam ends, and Post 5 in the bridge railing along Span 11, which was spalled through. From this location outside of the bridge, the interior bearings were also inspected with the sUAV. The sUAV was able to get a good view of the bearings, although images were not lit well enough to

adequately inspect the interior bearings from the individual still images. However, 3D reconstruction using multiple images at this site offers improvement in deficiency detection over individual images. 3D reconstruction is discussed in Section 5.3. Finally, the sUAV was moved to the land underneath Span 5 of 300061. Although it was still dark, taking off from and landing on the ground was easier than from a boat. However, the sUAV still had trouble stabilizing when using optical flow.

Figure 4-13. View of debris build-up on Bent Cap 12 of 300031

The inspection at the bridges over the Suwannee River revealed the need to focus on effective GPS-free flight in low light areas. A variety of options were considered, including sonar or an external light. Focus was instead placed on improving the performance of the optical flow sensor in low light situations. This was done by quadrupling the resolution of the optical flow sensor and widening its field of view, which allows the sensor to detect more feature points. Additionally, a "low light" mode was enabled on the sensor, making the sensor more sensitive to light.

Table 4-5. US-19 over Suwannee River inspection timeline

Flight	Time	Duration	Location	Description
1	10:27	3 min	300031, Span 12	Inspecting Pier Cap 12 for debris build-up, bearings, and cracking. Too dark to fly underneath bridge.
2	10:44	5 min	300031, Fascia	Inspecting North exterior beams in Spans 11 to 13.
3	11:01	7 min		Attempting to inspect interior bearings from outside of structure. Bearings over Pier 11 and Pier 12.
4	11:45	6 min	300061, Span 5	Launch from boat, inspecting Pier Cap 5, looking at bearings and debris. Move to Span 10 of 300031, but did not see much.

4.5 SR-6 over the Withlacoochee River – 320016

The inspection at State Road 6 over the Withlacoochee River, structure 320016, was conducted on Tuesday, October 10, 2017 during a scheduled routine inspection (see Figure

4-14). Weather conditions were calm throughout the duration of the inspection, with wind gusts less than 5 mph. A team member from UF operated the camera, since he had experience with the controller, and the CBI told the camera operator where to look. The three main spans of the structure consist of two main steel girders and transverse steel floor beams. The bridge is fracture critical.

Figure 4-14. Aerial view of 320061

All flights during this inspection were conducted from the ground underneath Span 4 of the structure (see Figure 4-15). The first two flights conducted were underneath Span 4, within the first floor beam bay. The flight plan for this area involved flying up in the middle of the floor beam bay, then flying in a circle within the bay inspecting at the web stiffeners in the girders, the splices (see Figure 4-16.a) and connections, and the bearings over Pier 5 (see Figure 4-16.b). The first flight was cut short because the stand-off distance was too large. By reducing the stand-off distance, the sUAV was able to obtain a closer look at the bridge elements during the second flight. Flight six was also conducted in the second floor beam bay underneath Span 4. The inspectors focused on stiffeners, floor beams, splice plates, and the diaphragm over Pier 5. This diaphragm is reported to exhibit pumping under live loads, but this was not seen from the sUAV.

(a) (b)

Figure 4-15. View underneath Span 4 of 320061: (a) UBIV routine inspection of Span 4, and (b) sUAV demonstration routine inspection of Span 4 conducted shortly after.

The third flight was an FPV inspection of Span 5, meaning there was not a VLOS on the sUAV during the inspection. The sUAV was navigated to Span 5 in AHM, and the RPIC had a

VLOS on the vehicle. The sUAV entered underneath the structure at about mid-span, at which point the RPIC operated the sUAV in OFM through the FPV camera. If the FPV camera were to lose video feed, the backup plan was to continue to fly using the high-resolution camera for navigation, although this did not happen. Although this flight demonstrated the ability to conduct an FPV inspection, it was difficult to know where the sUAV was without a VLOS. For the seventh flight, the sUAV returned to Span 5, and a more methodical approach was used. The sUAV entered Span 5 at mid-span, and then moved to the first floor beam bay of the span. Then, the sUAV was flown down the length of the span, and the inspectors looked at the inside face of Beam 5-4. This flight provided a realistic method of conducting an FPV inspection, while still knowing the location of the sUAV.

The fourth and fifth flights were conducted in GPSM on the outside of the structure. The plan was to inspect the outside faces of girders 4-1, 5-3, and 6-5. However, the sUAV was unable to maintain its position due to a magnetometer anomaly. A magnetometer measures magnetic fields, so it can be used as a compass. The magnetometer anomaly occurred because the magnetometer and the GPS disagreed on the direction that the sUAV was traveling. If the GPS thinks the sUAV is traveling north and the magnetometer thinks the sUAV is traveling east, the system will realize one of these is incorrect. As a result, these flights were cut short. The eighth and final flight was also at this location, and the sUAV looked more stable. For this flight, both video and images were taken of the exterior of the bridge.

(a) (b)

Figure 4-16. Sample images taken during inspection of 320016: (a) splices in the girders, and (b) bearing over Pier Cap 5.

This inspection demonstrated the ability to conduct an FPV inspection of a span without a VLOS on the sUAV. The sUAV cannot be within an arm's reach of all parts of the structure and cannot conduct a hands-on inspection, so it may not be used for fracture critical inspections. Still, the sUAV inspection system was able to capture high quality images of the structure. It should be noted that the focal length on the sUAV's camera may be adjusted to provide images equivalent to an inspector's view at arm's reach of the structure. The haunched girders allowed the sUAV to access better views of the bearings than it typically could for girders with constant depth.

Table 4-6. SR-6 over Withlacoochee River inspection timeline

Flight	Time	Duration	Location	Description
1	10:00	1 min	Span 4, first floorbeam bay	Inspecting web stiffeners, splices, and bearings over Pier 5, flight shortened because stand-off was too far (3 m)
2	10:02	6 min		Inspecting web stiffeners, splices, and bearings over Pier 5
3	10:30	6 min	Span 5	FPV inspection of Span 5
4	11:35	2 min	North fascia	Outside faces of Girders 4-1, 5-3, and 6-5. Flight shortened due to magnetometer anomaly.
5	11:39	1 min		Outside faces of Girders 4-1, 5-3, and 6-5. Flight shortened due to magnetometer anomaly.
6	11:49	8 min	Span 4, Girder 4-2	Span 4, Girder 4-2, inspecting stiffeners, floorbeams, splice plates, and diaphragm over Pier 5.
7	12:22	10 min	Span 5	FPV inspection of Span 5
8	12:40	5 min	North fascia	Outside faces of Girders 4-1, 5-3, and 6-5. Took video and images of deficiencies.

4.6 SR-40 over the Ocklawaha River – 360055

The inspection at SR-40 over the Ocklawaha River, structure 360055, was conducted on Thursday, October 12, 2017, with inspectors from FDOT (see Figure 4-17). A UF team member operated the camera, since he had practice with the controller, and the CBI told the camera operator where to look. Wind conditions started out calm, but increased up to 11 mph by the end of the inspection. This bridge had a service road underneath, so the ground station was set up in a truck, allowing for rapid relocation of the system. Additionally, the trees on either side of the bridge offered some protection from the wind. Routine inspections on this structure are conducted at night to reduce impact on traffic, so an sUAV inspection could be beneficial because maintenance of traffic would not be required.

Figure 4-17. Aerial view of 360055

This inspection was primarily a demonstration of the potential use of sUAVs for routine bridge inspections. The first three flights were under prestressed concrete girder spans. The inspection method used was to start at the beginning of the span, looking at bearings and the pier cap, rotating the sUAV to look down the bays between the beams, moving to the end of the span, and repeating looking down the bays and inspecting the bearings, similar to the method described in Section 2.4.2. The sUAV was not able provide as high quality views of the bearings as inspectors in a UBIV can, although a smaller airframe may have been able to access better views of the bearings.

The fourth flight took place underneath steel girder spans. The inspection method used for the steel span was more thorough than the method used for the prestressed concrete spans. The process involved looking at bearings 1 and 2 at the beginning of the span, flying down the bay between Beam 1 and Beam 2 while focusing on connections and diaphragms, looking at bearings 1 and 2 at the end of the span, flying back down the same bay, and then moving to the next bay and repeating. The fifth and final flight was a special inspection of bearing 17-5 over Pier 18, which had nearly reached its maximum range of movement (see Figure 4-18).

Figure 4-18. Bearing 17-5 over Pier 18

The SR-40 bridge over the Ocklawaha River was an ideal location for attempting an sUAV routine bridge inspection. The access road underneath the structure allowed the ground station to be set up in a truck, so nothing had to be carried. In addition, the sUAV took off from and landed on the truck, making the system compact and easy to move. The sUAV was able to quickly inspect the prestressed concrete spans, but it could not access a view of the bearings comparable to an inspector in a UBIV. The sUAV was not flown outside the bridge, because the tree line was close to the bridge exterior.

Table 4-7. SR-40 over Ocklawaha River inspection timeline

Flight	Time	Duration	Location	Description
1	9:42	7 min	Span 9	Proposed routine inspection method for prestressed span. Stand-off too large to see bearings (2.5 m)
2	10:08	8 min	Span 10	Proposed routine inspection method for prestressed span. Decreased stand-off (2.0 m) provided better view of bearings, but not good enough
3	10:31	7 min	Span 11	Proposed routine inspection method for prestressed span.
4	10:59	5 min	Span 15	Proposed routine inspection method for steel girder span. Video unstable
5	11:26	3 min	Span 17	Special inspection of bearing 17-5 over Pier 18

4.7 US-41 over CSXRR – 290032

The inspection at US-41 over CSXRR, structure 290032, was conducted in Lake City on October 25, 2018 with an official from FDOT (see Figure 4-19). A UF team member operated the camera, since he had practice with the controller, and the CBI told the camera operator where to look. The weather was clear, with wind gusts up to 8 mph. The bridge superstructure is made up of ten spans each with ten steel girders.

Figure 4-19. Aerial view of 290032

The first two flights were conducted underneath Span 8. The first flight was a trial, to determine an appropriate stand-off distance. After this flight, the sUAV was set to have a stand-off distance of 1.5 meters, and was used to inspect bearings and beam ends in Span 8 over Bent 9.

The next two flights were conducted at Span 7. The first flight in this location was set to a lower stand-off distance (1.35 meters), but due to the breeze, the flight was shortened, and the

stand-off was set back to 1.5 meters to be safe. The second flight under Span 7 was an inspection of the bearings and beam ends in Span 7 over Bent 7 (see Figure 4-20.a).

After these flights, the system was moved to Span 6, where the fifth and sixth flights were performed. The plan for the fifth flight was to start at Beam 6-1 near Bent 7 to look for minor pitting on Bearing 6-1. However, likely due to either wind gusts measured on the barometer or lag from the laser range finder, the sUAV hit the superstructure. Neither the bridge nor the sUAV was damaged, so another flight was attempted in this location. The stand-off distance was increased to 1.75 meters, and the barometer was covered with foam to try to block wind gusts. This flight was successful, and Bearing 6-1 over Bent 6 and the cover plate ends were inspected.

The final flight was an inspection of the mid-span diaphragms and the cover plate ends (see Figure 4-20.b) in Span 5. Initially, the sUAV had trouble stabilizing, but its stability improved later on. The sUAV was not flown in the bays next to the exterior beams.

(a) (b)

Figure 4-20. Sample images from inspection of 290032: (a) bearings and beam ends in Span 7 over Pier Cap 7, and (b) cover plate end in Span 5.

Because the structure had ten girders per span, the girder spacing was relatively tight. The girders were not as deep as most of the other structures inspected, so the sUAV was able to fly closer to the bridge deck underside. However, due to an unconservative stand-off and breezy conditions, the sUAV made contact with the structure during the fifth flight. The sUAV was able to take good images of the cover plate ends, but these images could likely have been taken from the ground with a lens with a higher focal length.

Table 4-8. US-41 over CSXRR inspection timeline

Flight	Time	Duration	Location	Description
1	10:03	2 min	Span 8	Trial flight
2	10:07	8 min		Inspecting bearings and beam ends in Span 8 over Pier 9
3	10:24	1 min	Span 7	Flight shortened due to too low stand-off
4	10:26	10 min		Inspecting bearings and beam ends in Span 7 over Pier 7
5	10:52	3 min	Span 6	Bearing 6-1 over Pier 7
6	11:17	10 min		Bearing 6-1 over Pier 6 and terminal of cover plates
7	11:41	8 min	Span 5	Inspecting diaphragms mid-span and terminal of cover plates

4.8 SR-228 over Washington Street – 720114

The eighth and final inspection for this project took place at SR-228 over Washington Street, structure 720114, an approach structure to the Hart Bridge in Jacksonville, FL (see Figure 4-21). This inspection was conducted on December 14, 2017 during a regularly scheduled routine inspection. A team member from UF operated the camera, since he had practice with the controller, and the CBI told the camera operator where to look. The weather was clear, and wind gusts reached up to about 12 mph. The portion of the structure inspected was primarily over parking lots, so the ground station was set up in a truck for ease of transportation.

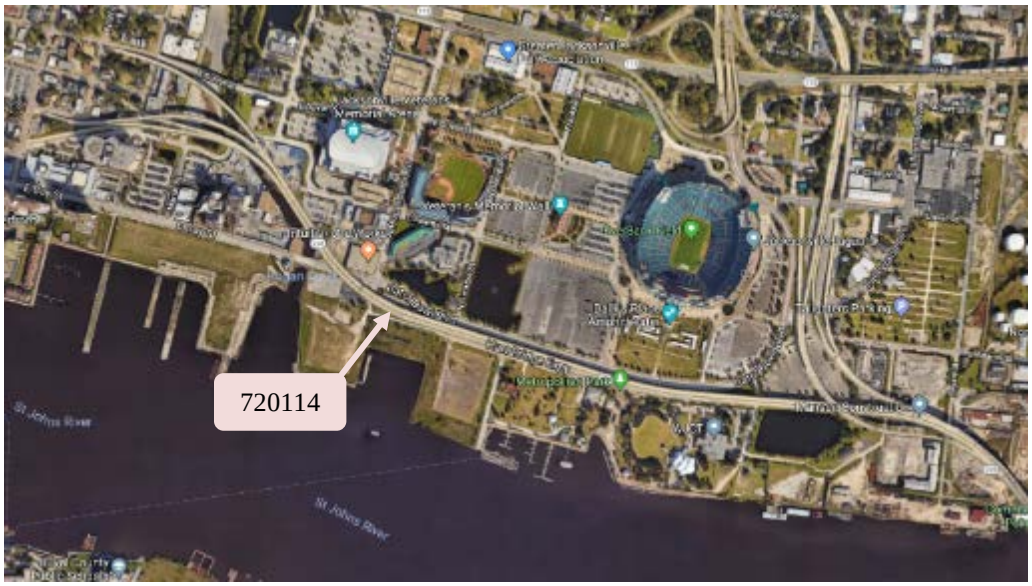

Figure 4-21. Aerial view of 720114

The inspection began with a demonstration routine inspection of Span 33, which has a prestressed concrete girder superstructure. The stand-off was set to 2.5 meters, and no notable deficiencies were found in this span during this inspection or in the inspection report.

After this initial flight, the battery was changed, and the system was relocated to Span 32, which is a steel girder span. The first flight in this location was cut short because video signal

was lost, due to a faulty HDMI cable. After this problem was fixed, the next flight was also shortened due to trouble stabilizing. The sUAV also had difficulty stabilizing during the third flight underneath this span, but images of peeling paint and spalled lugs were captured. The sUAV may have had difficulty stabilizing due to the increased stand-off distance for the steel girders, or due to the lack of texture underneath the bridge, which could make it difficult for the optical flow camera to find feature points. Because of the poor stability in optical flow mode, for the fourth flight in this area, the sUAV was flown manually with altitude assistance. Some images of a spall over Bent 32 underneath Beam 32-7 were taken (see Figure 4-22.a), but the sUAV was unable to hold its position well. This may have been due to wind gusts measured on the barometer, so the autopilot was covered with foam, as it was in the previous inspection.

After inspecting Span 32, Spans 34, 35, 36, and 37 were inspected with the suggested routine bridge inspection method for prestressed concrete girder spans. Figure 4-22.b shows a typical image of a bearing under a prestressed concrete girder taken from the sUAV. These four spans were inspected in five flights over the course of about fifty minutes. These flights went well. Flight 9, the first flight underneath Span 37, was cut short because the FPV camera mount came off, so it needed to be glued together. After the last flight underneath Span 37, there were no fully charged batteries remaining, so the inspection team had to wait for the batteries to finish charging.

The final four flights at this structure were all underneath Span 34 at Pier Cap 34. The purpose of these four flights was to take still images of the Pier Cap for the purpose of creating a 3D reconstruction, which is shown in Section 5.3.

(a) (b)

Figure 4-22. Sample images from 720114: (a) spall in Pier Cap 32 under Beam 32-7, and (b) bearing under a typical prestressed concrete girder.

This structure spanned over parking lots, so there was access for a car underneath much of the bridge. Because of this, the ground station was set up in the truck. Unlike the inspection of the Ocklawaha Bridge, 360055, the sUAV took off from and landed on the ground instead of the truck (see Figure 4-23). This inspection demonstrated the speed with which the sUAV is able to inspect prestressed concrete spans. However, the sUAV still could not access an adequate view of the bearings. Additionally, the inspection flights were limited by the number of charged batteries, and the inspection had to stop for about an hour to wait for the batteries to charge.

Figure 4-23. sUAV and ground station set up on truck underneath 720114

The sUAV had a lot of difficulty stabilizing underneath the steel span, and for the last flight under the steel span, the sUAV was operated only with altitude assistance (without the optical flow sensor). This flight, although it resulted in some usable images, was very unstable.

Table 4-9. SR-228 over Washington Street inspection timeline

Flight	Time	Duration	Location	Description
1	9:40	6 min	Span 33	Routine inspection of prestressed span
2	10:00	1 min	Span 32	No video signal (HDMI cable)
3	10:06	1 min		Routine inspection of steel girder span
4	10:09	5 min		Routine inspection of steel girder span
5	10:32	6 min		Bearings over Pier 32
6	10:52	5 min	Span 34	Routine inspection of prestressed span
7	11:03	5 min	Span 35	Routine inspection of prestressed span
8	11:14	6 min	Span 36	Routine inspection of prestressed span
9	11:26	0 min	Span 37	Routine inspection of prestressed span
10	11:34	7 min		Routine inspection of prestressed span
11	12:36	4 min	Span 34	Taking images for 3D reconstruction of Pier cap 34
12	12:40	1 min		Taking images for 3D reconstruction of Pier cap 34
13	12:43	2 min		Taking images for 3D reconstruction of Pier cap 34
14	12:46	5 min		Taking images for 3D reconstruction of Pier cap 34

4.9 Inspector Feedback and Summary

After each bridge inspection, a survey was sent to all inspectors and FDOT employee bystanders present. The number of completed surveys per inspection ranged from one to five, and the total number of completed surveys is 16. With these numbers, one should be cautious drawing conclusions from the qualitative feedback. Feedback for two specific questions are discussed in this section, and the rest of the quantitative feedback is summarized in Appendix A.1.2. For each quantitative question, one is defined as the lowest, or worst, rating, and five is the highest, or best, rating.

The first metric discussed is the overall rating of the sUAV system used for bridge inspections compared to current inspection methods (See Figure 4-24). This is the cumulative data from all inspections. As can be seen, the responses are mostly average to slightly above average.

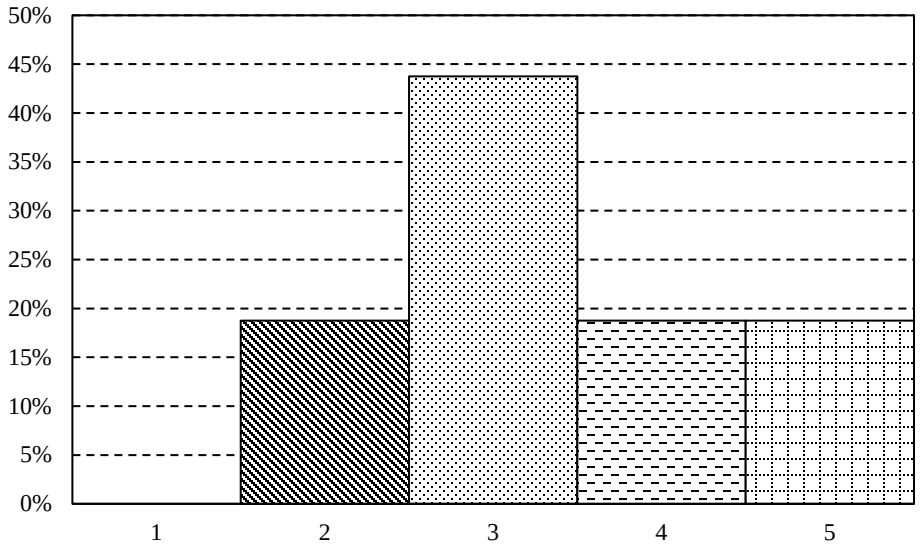

Figure 4-24. Overall rating of the sUAV inspections

Additionally, the respondents were asked whether or not sUAV bridge inspections should be adopted. The majority of responses agreed that the use of sUAVs for bridge inspections should be adopted (See Figure 4-25).

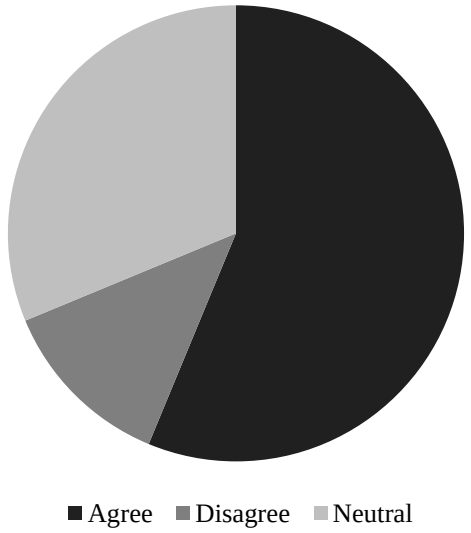

Figure 4-25. Response data on whether sUAV inspections should be adopted

Some of the qualitative feedback received from these surveys is also very helpful. For example, when asked to describe the most effective use of an sUAV for bridge inspections, respondents suggested use for structures that cannot be accessed by UBIVs due to strength

concerns. Respondents also provided constructive criticism. Among the most common suggestions to improve the system included quantifying the size of deficiencies, which will be discussed in the next section, longer flight times, and increased flight stability underneath the bridge. Limitations also included poor optical flow performance underneath steel spans and in low light.

From the eight bridge inspections, it was determined that high-resolution still images were more beneficial than video, as images are much higher resolution (24 Megapixels compared to 2 Megapixels), they require less storage than video, and they can be selected in the field by an inspector, rather than requiring post-inspection time watching video. The most beneficial applications for sUAV bridge inspections would be with special or damage inspections and potentially with occasional routine inspections of prestressed concrete bridges. The following image processing, data storage, and cost comparison discussions in Sections 5 and 6 will be based on these findings.

5 Image Processing

As discussed at the end of Section 4, the primary form of data generated during sUAV inspections will be images. Because sUAV inspections have the potential to generate a significant number of images, an investigation into software for image processing was conducted. Three primary types of post-processing software will be discussed: automated deficiency detection, deficiency tracking and quantification, and digital image 3D reconstruction.

5.1 Automatic Deficiency Detection

Advancements in the field of image processing for deficiency detection are being made. Some studies have focused on making improvement in the detection of individual deficiencies, some developed ways to quantify the deficiencies, and others worked on reducing computation time. All of these studies have solved some of the issues that are still preventing fully autonomous deficiency detection; however, there are still missing pieces that need to be addressed to make this type of image processing software widely available. At the current time, no commercially available software for deficiency detection that fulfills the needs of this project has been developed. However, the research discussed in the following sections shows promise for the development of commercial programs in the near future.

5.1.1 Deficiency Detection and Quantification Algorithms Developed in Research

Fujita et al. (2006) conducted an early study to detect cracks in concrete automatically from noisy images. To achieve this goal, this study detailed a method utilizing two pre-processing techniques to remove noise, such as shadows, blemishes, and divots from images taken of concrete. As can be seen in Figure 5-1, the method described in this research was successful in eliminating much of the noise in the image. This research shows the importance of pre-processing techniques required for development of crack detection software.

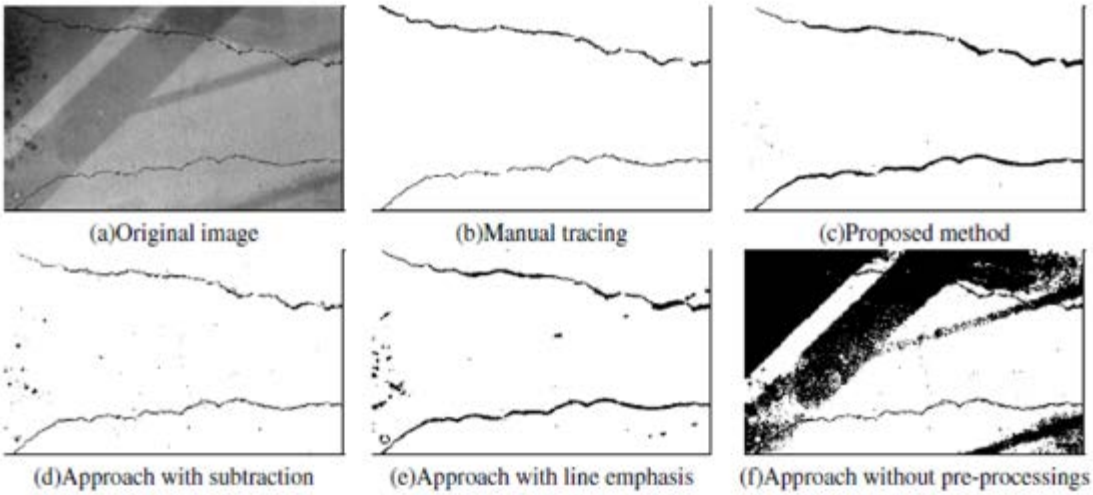

Figure 5-1. Comparison of results of different noise removal techniques (Fujita et al., 2006)

Yamaguchi and Hashimoto (2010) developed an algorithm for computationally efficient detection of cracks in large images (larger than 10 megapixels). Taking into consideration the thin, linear nature of cracks, this study classifies dark regions as cracks. The process described in this paper was able to detect cracks with the same accuracy as previous methods while reducing

the computation time. With this approach, approximately 20 to 25% of the pixels identified as cracks in an image were false positives, and about 20 to 25% of true crack pixels were not identified. Computation time will be an important consideration for the development of future commercial software. In Figure 5-2, (a) is the original image, (b), (c), (d), and (e) show the a comparison of different crack detection methods, and (f) shows the true cracks in the images as determined by a human.

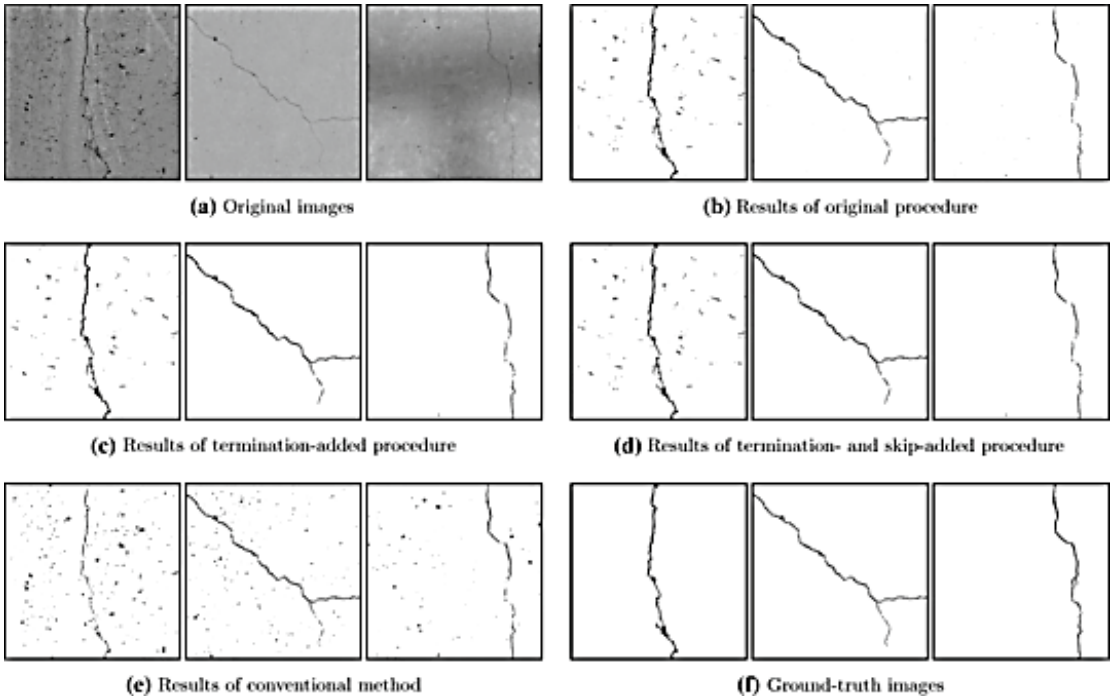

Figure 5-2. Comparison of percolation, conventional, and human crack detection methods (Yamaguchi and Hashimoto, 2010)

The purpose of the study by Zhu et al. (2011) was to evaluate structural safety after earthquake events. Its two primary goals were to develop a method for producing a crack map for each image and to retrieve crack properties, such as length, orientation, and width. The cracks were detected using a similar method to the one used by Yamaguchi and Hashimoto (2010). An algorithm to locate the centerline of the crack and break the crack into straight segments was developed to determine the dimensions of the crack. The length of a crack was estimated as the height of a box encompassing the crack in the direction of a crack segment. The maximum width was calculated by finding the largest distance from a point on the crack centerline to the crack boundary and doubling it. Figure 5-3 shows an output from the crack quantification algorithm. The algorithm was developed in Microsoft Visual Studio, and the average error in crack properties when compared to the actual measurement was 2.21% for crack length and 0.35% for crack width.

In the paper, Zhu et al. (2011) state, “the test results have shown that no matter how accurate existing crack detection methods are, there are always some cracks that are not visible in images, but are visible to human eyes. This limitation cannot be simply overcome by the improvement of crack detection methods or with higher resolution image capturing cameras.” This research shows that a program to detect crack properties is potentially feasible, but requires improvement before commercially available software can be developed.

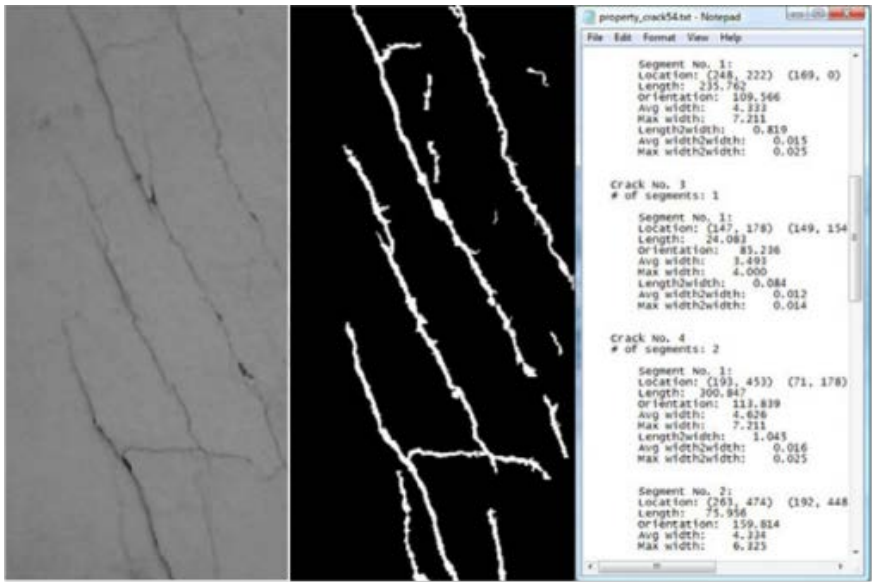

Figure 5-3. Sample photo with output of crack properties (Zhu et al., 2011)

Jahanshahi et al. (2013) and Jahanshahi and Masri (2013) published papers on a process to detect and quantify cracks by incorporating depth perception. The former study reconstructed a scene using several overlapping images of an object. Cracks were then detected and classified using machine learning techniques. The accuracy and precision of these classifiers were about 95%. The approach used by the algorithm calculates the width of cracks by first segmenting the crack and determining its centerline. Then, 35 lines oriented from zero to 175 degrees at increments of five degrees were compared to the segmented crack. In the direction of the line that is most perpendicular to the crack, the distance of the intersection between the line and the crack segment was considered the crack width (Figure 5-4). Additionally, an algorithm was developed to consider perspective errors. Figure 5-5 shows a comparison of crack detection methods and their ability to ignore non-crack elements. The method used in this study was able to quantify cracks as small as 0.1 mm from a distance of 20 m, as seen in Figure 5-6. This was achieved with a 600 mm focal length telephoto lens. The results of this study suggest that a reliable, commercially available crack detection software is feasible.

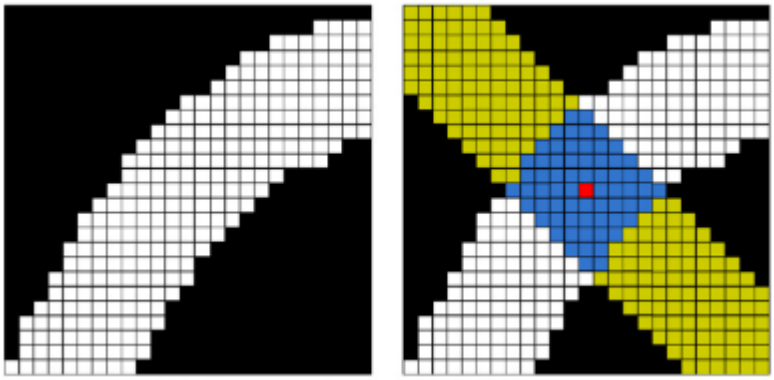
Figure 5-4. An example crack, white, is intersected by a strip, yellow, in this case, the 135˚ strip kernel. The width of the crack is estimated as the intersection area, blue, divided by the width of the strip kernel (Jahanshahi and Masri, 2013)

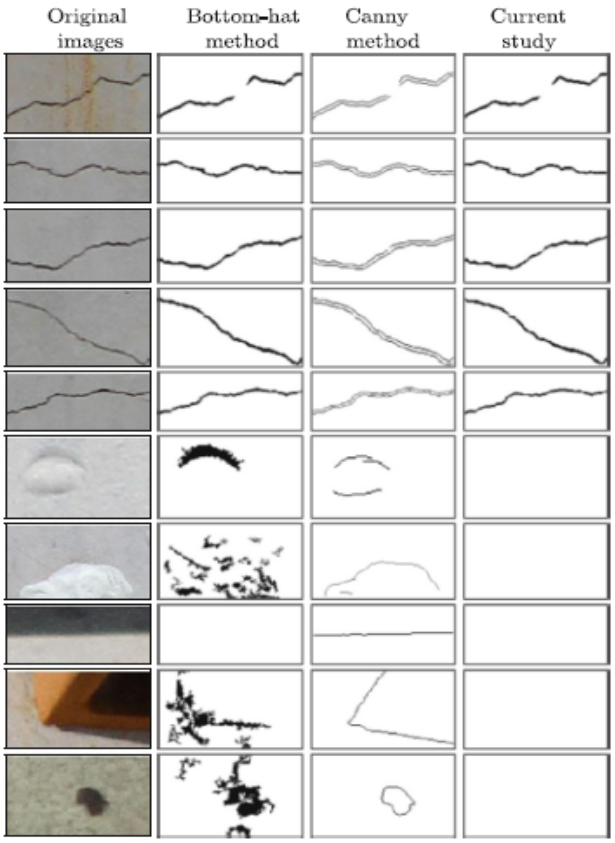

Figure 5-5. Comparison of ability to ignore non-crack features (Jahanshahi et al., 2013)

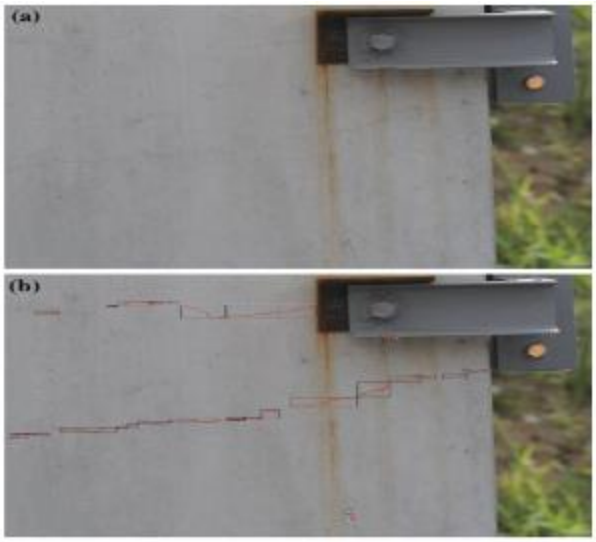

Figure 5-6. Detected cracks in image taken from 20 m (Jahanshahi et al., 2013)

Following this, Jahanshahi and Masri (2013) developed a new method that utilizes depth perception to quantify crack thickness, with the purpose of quantifying cracks in nuclear power plants. The benefit of using depth perception is that no reference points are needed in the images, meaning that a scale does not need to be attached to the structure as a reference in order to determine dimensions of the image. The crack quantification method was similar to the method used in the study by Jahanshahi et al. (2013). However, this research provided more reliable

measurements. In their conclusions, Jahanshahi and Masri (2013) state, “since the proposed approach is contactless, its incorporation with autonomous or semi-autonomous mobile systems, such as unmanned aerial vehicles (UAV), which can move close to the structure and collect images, enables the proper inspection of inaccessible regions for cracks.” It is also stated that the use of an external light source could increase the performance of the algorithm proposed in this study. These comments show that the method used in this research could be incorporated into a commercial system for crack detection.

Zhang et al. (2014) proposed a method to automatically detect and quantify cracks in subway tunnels. Images were first stitched into a mosaic, and then pre-processed to eliminate isolated dark pixels. Cracks were extracted and segmented, and then they were classified by a machine learning algorithm. The test accuracy of the classifier was 91.6%. Figure 5-7 shows an example image and the automatically detected cracks. The quantification of cracks was performed in a manner similar to methods used in other studies. The crack length was calculated from the segmented elements after classification, and the width of the crack was determined from the centerline of the crack. This study shows promise for automatic crack detection and quantification, despite its limitations. In order to quantify cracks, the start and end point of the crack must be defined, which increased the amount of user input. The working distance, focal length, and pixel size resolution for this project all remain constant in a subway tunnel because the geometry and camera used are constant. This means the algorithm could not be as flexibly applied to images with a different pixel size resolution. However, the algorithm does show promise for fully automatic deficiency image processing with further development.

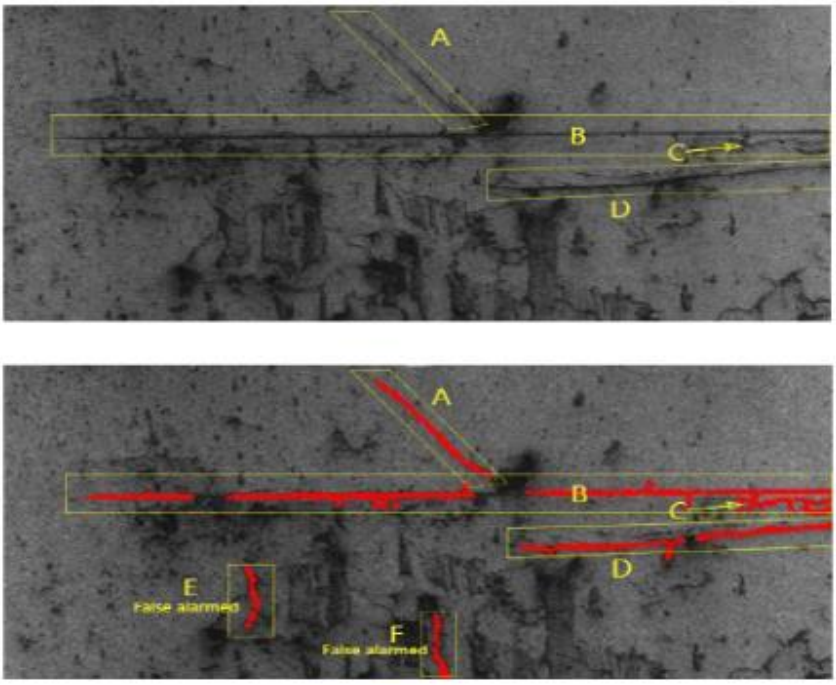

Figure 5-7. Crack detection and classification output (Zhang et al., 2014)

The research performed by Li et al. (2014) deals with the use of a stationary camera at ground level with a telephoto lens to capture images of cracks in the superstructure and substructure of a bridge. Although the algorithm developed in this research does not consider

GPS coordinates of the images, it is able to effectively capture images of cracks and extract crack widths. Image processing software was developed to quantify the minimum, maximum and average width of each crack. The average accuracy of this method of detection was 92.6%, with a maximum error for the maximum crack width of 0.05 mm. The user interface for the program is shown in Figure 5-8. This research shows promise for commercial software which, with further development, could be used to detect cracks in images.

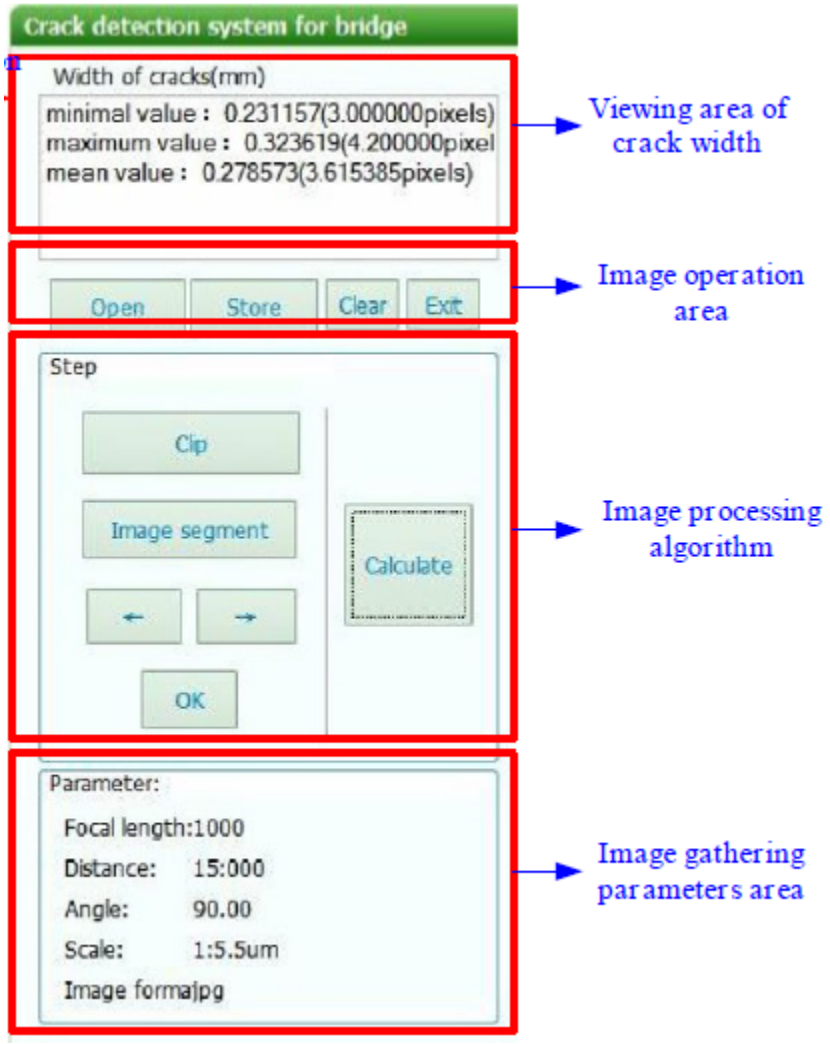

Figure 5-8. Crack detection software interface (Li et al., 2014)

The algorithm developed by Adhikari et al. (2014) detects cracks from crack branch points, rather than searching for crack and non-crack pixels. The scope of this research included crack quantification, as well as crack depth quantification from statistical data. The procedure outlined in this paper begins with pre-processing and stitching images together to encompass a whole crack, followed by the detection of cracks. After detection, the crack centerline was found, and the crack was segmented. The crack length was estimated as half the perimeter of the crack skeleton, which is reasonable because the centerline is one pixel wide. The crack width was calculated by dividing the crack length from the crack area, which only provides a value for the average width. Figure 5-9 shows outputs from a sample image. Adhikari et al. (2014) state, "[…] extensive research is required in developing several condition state rating models for each type

of defects in concrete elements." This research shows that for commercial image processing deficiency detection software to be developed, further advancements may be needed.

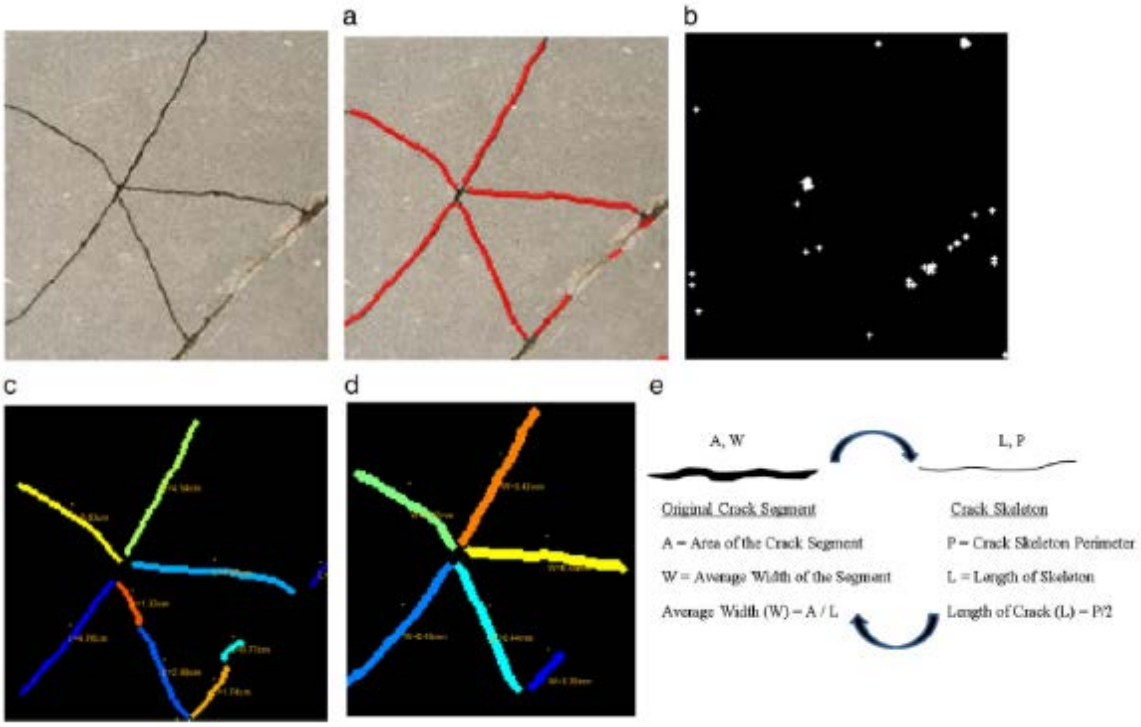

Figure 5-9. Output from sample image. (a) shows detected cracks, (b) shows the branch points of detected cracks, (c) shows crack length, (d) shows crack width, and (e) shows how the crack length and width are estimated (Adhikari et al., 2014)

In a paper published by Kim et al. (2015) the use of an sUAV to collect images of a structure and the use of image processing to detect deficiencies in the images is described. To automatically detect cracks, the study used preprocessing, pattern recognition, segmentation, feature extraction and crack classification. This study was able to extract crack properties, even from very noisy images. The program was able to measure crack widths as small as 0.1 mm, or 0.0039 inches, with less than 0.1 mm error. Figure 10 shows the steps the image processing algorithm takes to detect and quantify a crack, and Figure 11 shows the output provided by the crack detection software developed in this study. The program developed in this study shows potential for future commercially available software, with a simple user interface and reliable outputs.

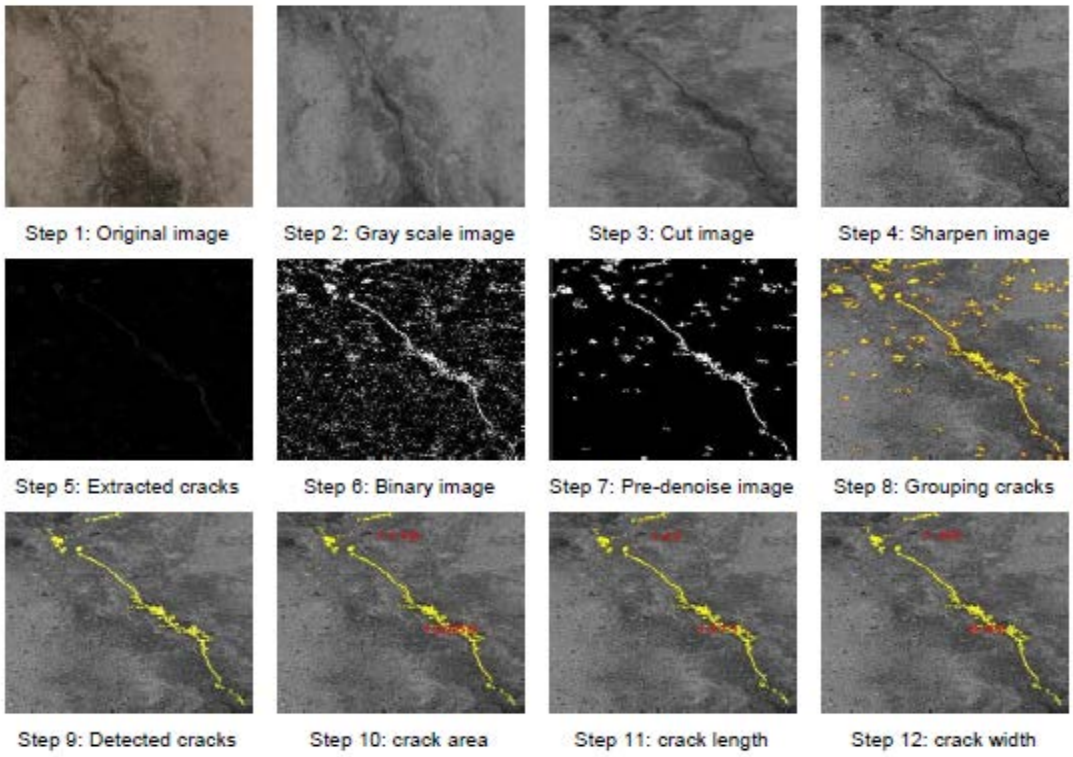

Figure 5-10. Crack estimation algorithm steps (Kim et al., 2015)

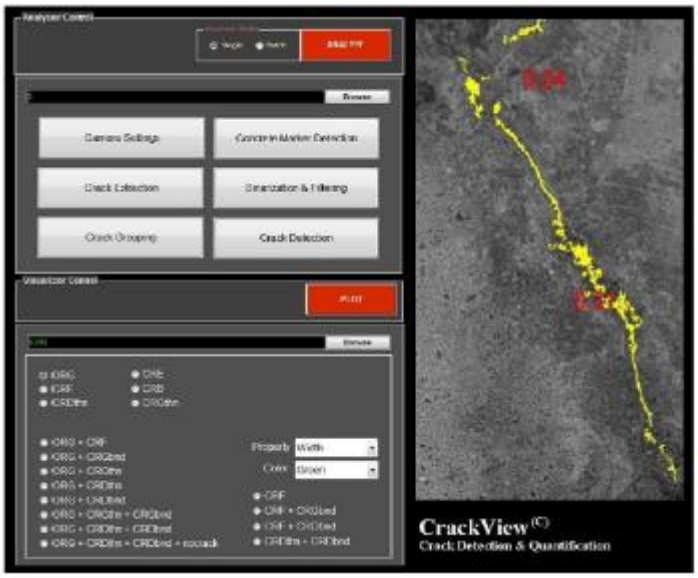

Figure 5-11. Crack detection software interface (Kim et al., 2015)

In a study by Pragalath et al. (2018), an algorithm was developed to quantify condition states from images. The researchers developed a tool with a user interface to allow inspectors to interactively quantify deficiencies in images (Figure 5-12). This tool requires images to be loaded individually, and the user must input distress levels, i.e. minimum, moderate, or extensive damage in the image). With this information, the algorithm will detect and quantify the lengths of cracks to provide a qualitative state of distress for an element in an image. The authors stated

image processing for damage quantification and condition rating is a “substantial area of research” (Pragalath et al. 2018).

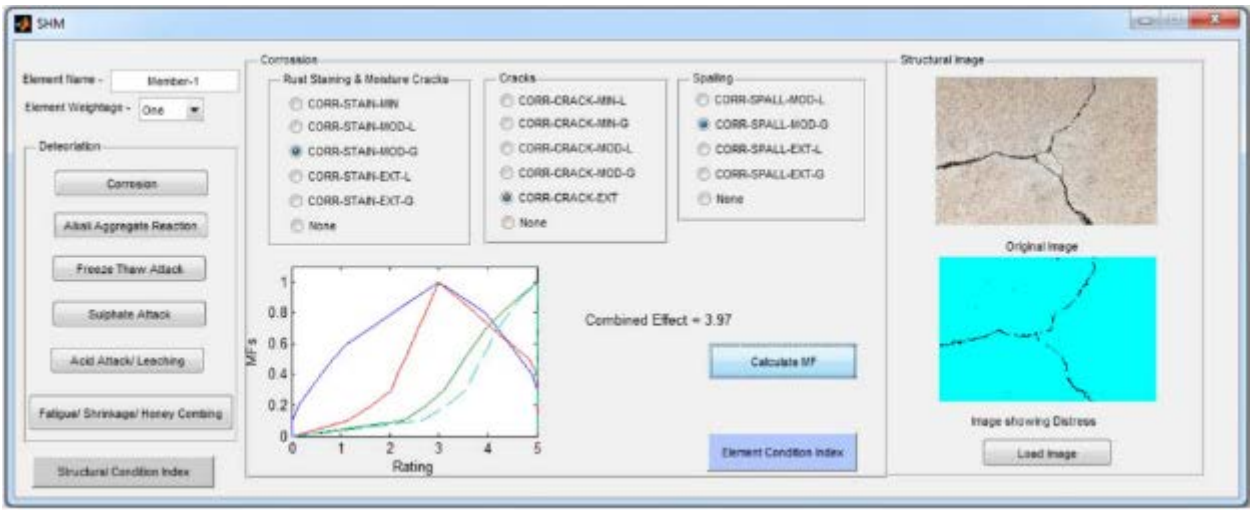

Figure 5-12. User interface to quantify deficiencies in images (Pragalath et al., 2018)

In addition to several studies on crack detection and quantification, there have been studies on corrosion detection. Lee et al. (2006) used color to detect corrosion in steel bridge girders. After performing a statistical analysis on images with and without corrosion, corrosion was determined based on variation of color in the image. Using statistical modeling, images were classified as defective (i.e. containing corrosion) or non-defective. This system was able to efficiently categorize the sample images collected in this study.

A shortcoming of this approach is that images were taken from approximately three feet away from the steel beam surfaces, and were oriented perpendicular to the surface. This is a problem because images may not be taken perpendicular to the surface during an inspection, which would cause the image to be distorted. Still, this research shows that colors in an image can be used to detect corrosion. By incorporating this information, commercially available software for corrosion detection could be feasible.

Medeiros et al. (2010) considered texture in addition to color to detect corrosion in steel. This study used hue, saturation, and intensity to detect corrosion. For the texture analysis, this study used an algorithm to consider how sharp grayscale levels transition between pixels. Sharper transitions were determined to have coarser texture. This study found that by applying both color and texture analysis to an image, corrosion defects were more reliably detected. Using the procedure outlined in this paper, more than 90% of the true corrosion was detected, and less than 4% of detected corrosion pixels were falsely identified. By considering both color and texture analysis, development of commercially available software could be more accurate.

Jahanshahi and Masri (2012) proposed an approach to automatically detect corrosion using depth perception and pattern classification algorithms. To detect corrosion texture, smoothness, coarseness and regularity were measured. Color was also considered in classifying corrosion in this research. With varying program inputs for texture and color analysis, detection accuracy ranged from approximately 70% to 90%. The area of corrosion could also be calculated

by multiplying the number of pixels detected as corrosion by the pixel size resolution. The ability to detect and quantify corrosion show promise for future development of commercially available corrosion detection software.

Most existing deficiency detection and quantification algorithms are still experimental in nature. The variety of deficiencies in structures presents a challenge, with each deficiency type requiring a different algorithm or manual processing of the images. Past research indicates that automatic deficiency detection and quantification is feasible. However, fully functional, fully autonomous programs have not been developed for commercial use. In addition, many of the programs developed in research require some level of user input or verification. As Adhikari, et al. (2014) state, "There is always human intervention at some point in automation process." Studies, such as the one by Kim et al. (2015) show potential for future commercially available deficiency detection and quantification software, with a simple user interface and reliable outputs. Still, more development is needed before deficiency detection algorithms are used commercially.

5.1.2 Commercial Image Processing Systems

In addition to the academic studies and methods presented in the previous section, there are also a limited number of commercially available systems designed to perform image processing for defect detection. Commercially available software falls into two main categories: software which provides tools to aid in the development of defect detection and quantification programs, and software which is part of a platform that is fully developed and capable of detecting cracks and corrosion within the constraints provided by the platform. This first type of software, which will be referred to as "image processing libraries" was investigated to determine its usefulness in the context of this project, with varying levels of success. The possibility of purchasing commercially available software that could be used to automatically detect any cracks or corrosion present in the images taken by the sUAV was also investigated. Some of the software options provide several capabilities in line with the needs of this project; however, none were designed with the specific purposes of sUAV inspection in mind.

There are some sUAV that are being marketed for structural inspections. While these systems do an excellent job of mapping areas and 3D modeling, they do not yet have capability to automate any of the structural inspection process. Any inspection performed with these systems requires qualified inspectors to interpret the models and images provided by the system.

5.1.2.1 Image Processing Libraries

The Image Processing Toolbox in Matlab contains many functions specifically designed for image processing. Matlab has tutorials and detailed explanations of its built-in functions, making it a good resource for understanding how an algorithm works.

During this project, an initial attempt at an autonomous crack detection and quantification algorithm was developed in Matlab. The program was successful for clean stock photos of cracks. However, creating a program that is able to process a group of real-world pictures with varying brightness and with many crack-like features (i.e. sticks, control joints, shadows) was a challenge (Figure 5-13). Additionally, retrieving area, length, and the average width of cracks was achieved, but the maximum width perpendicular to the orientation of the crack was not able

to be calculated in this attempt. As stated in previous sections, some researchers have been able to overcome these challenges; however, creating a fully functional defect detection software program is beyond the scope of this project.

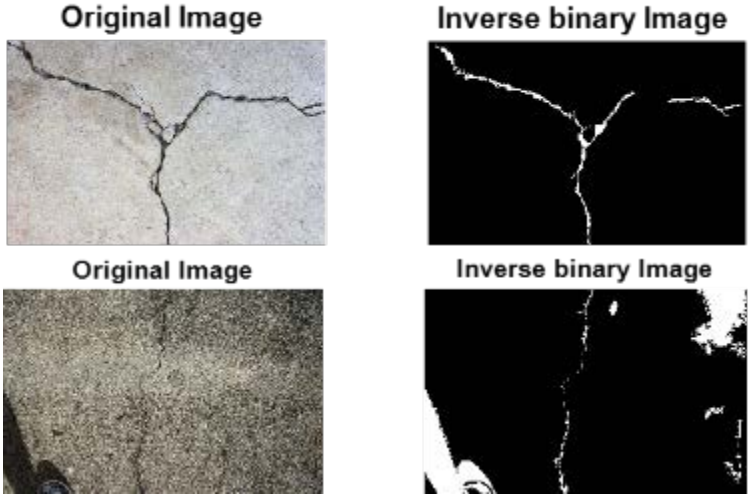

Figure 5-13. Comparison of images with low and high levels of noise processed by the Matlab program developed

OpenCV is an open source library of programming functions primarily created for real-time computer vision. OpenCV contains functions for edge detection and other image processing tasks. In order to use OpenCV on a Windows operating system, Microsoft Visual Studio is needed. The primary interface for the library is C++, and development of a functional crack detection and quantification program would require substantial coding. Dozens of image processing tutorials are on OpenCV's website.

5.1.2.2 Crack Detection and Quantification Systems

The CrackScope system is a platform designed to detect cracks on asphalt roads from a moving vehicle. It accomplishes this using a line-scan camera, which essentially scans the road surface one row of pixels at a time. To minimize erroneous measurements due to lighting conditions, the system utilizes a laser to illuminate the asphalt from the same angle as the cameras, therefore doing away with any shadows that could be perceived by the image processing software as part of a crack. The CrackScope software detects a crack by separating the pictures into small segments, and deciding whether or not that segment is part of a crack using the grayscale image information. Then, the segment is compared to its neighbors, and if they also represent part of a crack, they are connected, and if not, are disregarded as image noise. The system was found to have an accuracy of 91 to 96 percent, and can provide crack data such as length and width, as well as crack maps to the user. Though this system's capabilities mirror the needs of this project, the entire system is not something that could feasibly be mounted on an sUAV. Furthermore, it is designed to be used from a fixed distance and angle, and with its own light source; therefore, it would not be useful within the parameters of this project. Additionally, an FDOT project, Investigation of Automated and Interactive Crack Measurement Systems (Gunaratne et al., 2008) researched the use of automated crack measurement systems including CrackScope. The report says that CrackScope shows promise, but is not ready for implementation.

The Pavemetrics system is a vehicle mounted platform, similar to the CrackScope system, that is used to assess the condition of roads and is capable of detecting cracks and potholes. It does this using two cameras to take images that, with their proprietary software, can be used to produce a 3D image. The 3D image is then used to locate and quantify the crack, as to provide the user with information such as crack width and length. As with the CrackScope system, this system's capabilities mirror the needs of this project, however the entire system is not something that could feasibly be mounted on an sUAV, and due to the fact that it is meant to be used from a fixed distance and angle, and with its own light source.

5.1.2.3 Commercial sUAV Structural Inspection Systems

The senseFly Albris is marketed as a mapping and inspection sUAV, and it comes equipped with useful sensors, such as high definition and thermal images, and pilot aids, such as object detection and semi-autonomous flight. This sUAV is intended to be used in conjunction with different image processing programs capable of producing 3D surface maps and models. The senseFly Albris is intended to be used for inspections; however, it seems that this is achieved by creating 3D surface models of the subject that still need to be inspected by qualified inspectors. The senseFly Albris does not yet have crack and corrosion detection and quantification capabilities, however with new software, it may in the future.

The Cyberhawk sUAV is designed to be used for civil engineering applications. It is capable of producing digital elevation models and orthophotos, which have a uniform scale similar to a map; however, inspections performed with this system still rely on a qualified inspector to analyze images obtained and detect cracks and corrosion on the structure.

5.2 Deficiency Tracking

A large portion of current bridge inspection reports focuses on quantification of deficiencies. Specific deficiencies are mentioned in element inspection notes, and each bridge element is assigned condition states that represent the amount and severity of deficiencies on the element. As specific deficiencies are typically documented in paragraph form, depending on the wording of the element inspection notes, locating deficiencies from previous inspections may be unintuitive. Therefore, as part of this research, a supplementary method of cataloguing and displaying deficiencies was investigated to provide inspection flight planning assistance.

Figure 5-14 shows a simplified map of bridge deficiencies on a bridge deck and superstructure. This figure is based off the inspection report for bridge 720690, Atlantic Boulevard over San Pablo River. If informed by the location of the sUAV when deficiencies are identified, this map can be produced automatically. Additionally, the labeled deficiencies in Figure 5-14 are described in an automatically generated table. For example, a deficiency code EB1 would be an elastomeric bearing in the location indicated on the deficiency map. In this case, that the elastomeric bearing has cracked and torn corners. A map of significant deficiencies could decrease the time required for inspection preparation.

Code	Description
'SG1'	36 in long peeling paint
'EB1'	Corners cracked and torn in 2in long area
'PB1'	0.25inx0.5in deep gap between masonry plate and beam seat
'PB2'	0.25inx0.5in deep gap between masonry plate and beam seat

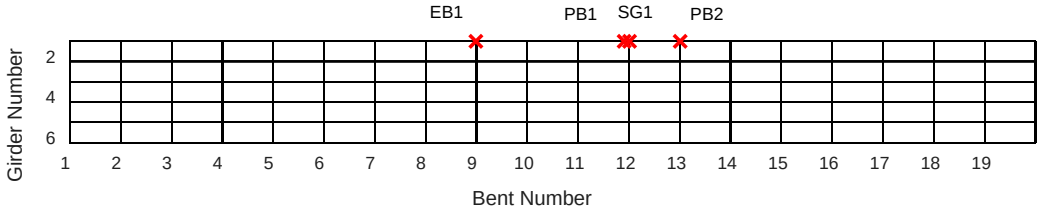

Figure 5-14. Sample bridge deficiency map and list for efficient cataloguing of deficiencies

As stated in Section 4.9, it is important to be able to quantify the size of deficiencies in images. The calculation of pixel sizes in images is straightforward if the focal length, the sensor density (pixels/length), and the stand-off distance are all known. The camera used for inspections automatically stores the focal length at which an image is taken, and the pixel density is known from the specifications of the camera. Therefore, if images are tagged with the stand-off distance, the true dimensions of objects in the image could be measured. Another method for measuring the size of deficiencies that was considered during this project would be to attach parallel laser pointers with a known spacing onto the camera. This would essentially project a scale onto the images taken. Both of these potential methods have one large flaw. If images are not taken perpendicular to the surface, objects in the image will become distorted, adding error to the measurements.

Figure 5-15 shows the pixel resolution in inches for various focal lengths and stand-off distances for the Sony α6000. The dotted lines show the pixel size in an image. Four cases are shown: 16 mm focal length images saved to SD card, 16 mm focal length images streamed to ground station, 50 mm focal length images saved to SD card, and 50 mm focal length images streamed to ground station. These focal lengths were chosen because they are the extents of the zoom lens used for inspections. Clearly, the full resolution images saved to the SD card, which are 24 Megapixels, are higher resolution than the images streamed to the ground station, which are streamed at 1080p. The bottom solid line represents the minimum threshold for Condition State 3 cracking in prestressed concrete elements, and the top solid line represents Condition State 3 cracking in reinforced concrete elements in an aggressive environment.

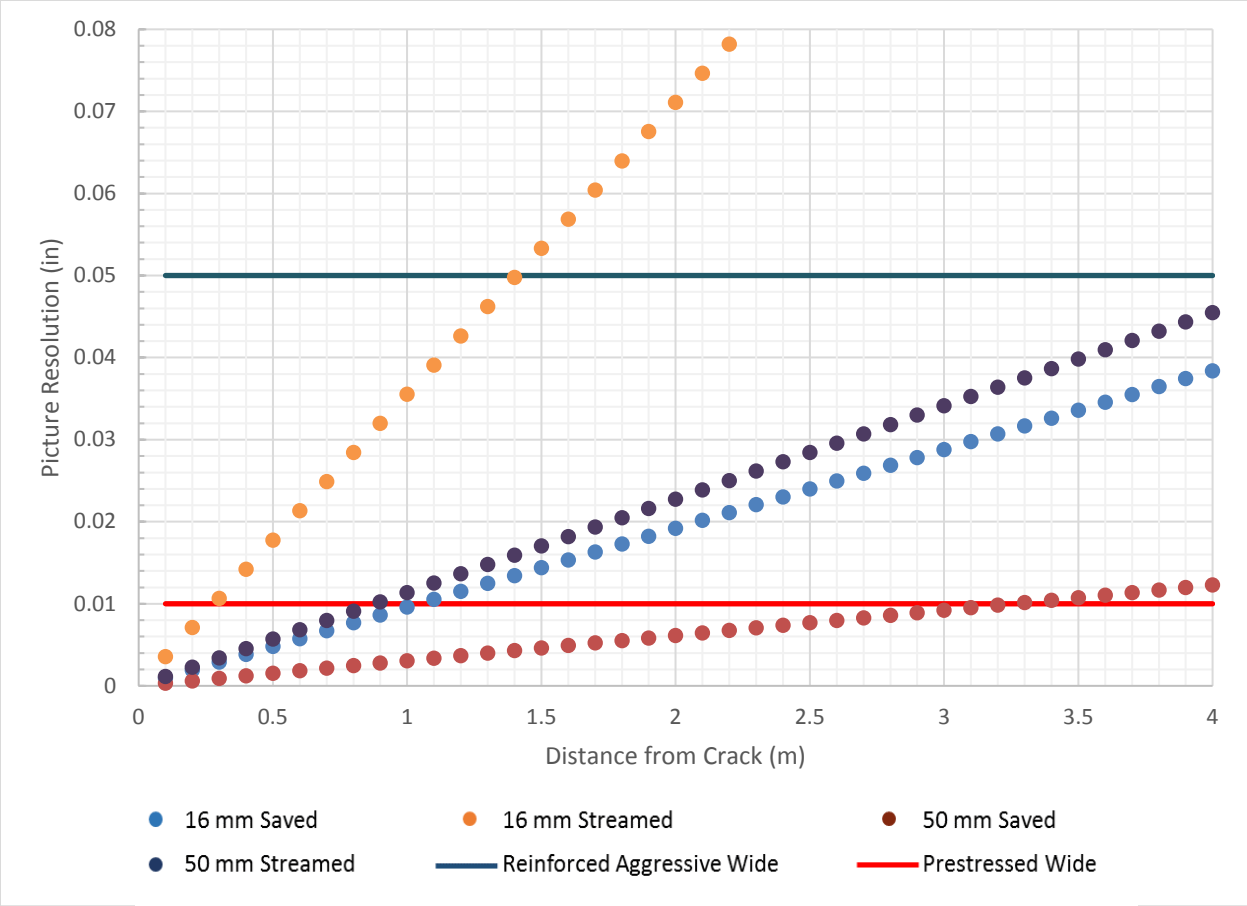

Figure 5-15. Pixel sizes for various combinations of focal lengths and stand-off distances for Sony α6000

5.3 Digital Image 3D Reconstruction

Digital image 3D reconstruction, which is the creation of three-dimensional models from a set of images, would be a robust, although computationally expensive, method of interactively determining size and location of deficiencies. For this project, Agisoft PhotoScan was used to demonstrate the use of 3D reconstruction software for inspection image processing.

The basic steps for 3D reconstruction using Agisoft are as follows: add photos, align photos, build a dense point cloud, scale the model, build a mesh, and build texture (see Figure 5-16). The last two steps can be skipped, depending on the level of detail required for the model. When aligning the photos, Agisoft estimates the position of the camera for each image. Then, using these estimated positions, the depth of objects in each image are calculated, and Agisoft makes a point cloud, similar to LiDAR. At this point, Agisoft has enough information for the user to scale the model and measure dimensions, including depth, of features. It should be noted that, in order to scale the model, some dimensions on the model must be known. Building a mesh and texture will make the model more detailed, but will not improve accuracy of measurements. Additionally, Agisoft can overlay images on top of reconstructed models, to create very realistic reconstructions.

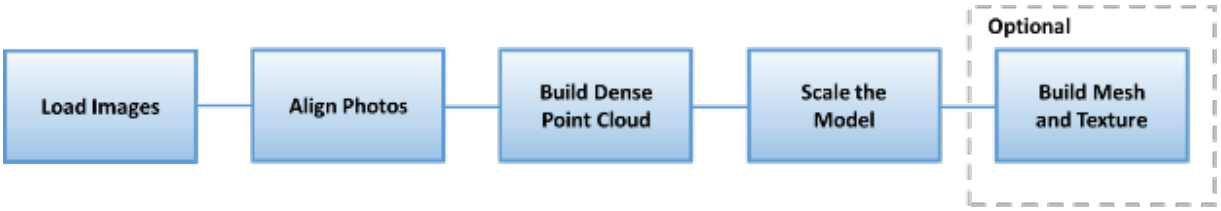

Figure 5-16. Steps to build a model in Agisoft

Use of 3D reconstruction has been considered in two cases: (1) to reconstruct specific deficiencies and compare models over time, and (2) large scale reconstruction of entire bridges or spans. As an example of reconstruction of a specific deficiency, a model was made of a known spall on 260102, US-441 over Rachel Boulevard. The yellow line in Figure 5-17(b) is a line drawn to scale the image.

(a) (b)

Figure 5-17. Spall on 260102: (a) Image of spall with ruler for scale, and (b) reconstructed spall with image laid over model

The depth of the spall was measured with a ruler in the field to be about 0.7 inches. Using Agisoft, after the reconstructed model was scaled from dimensions taken in the field, the depth of the spall was measured in the program to be about 0.9 inches. Both of these measurements have some error, but the reconstructed image provides a reasonable estimate of the true measurement. A screen capture of the graphical user interface for Agisoft is shown in Figure 5-18. The main window is the reconstructed model. The view shown is a side view of the spall, showing its depth. The model can be translated and rotated, so the deficiency can be viewed from a variety of angles, providing there are a sufficient number and arrangement of images making up the model.

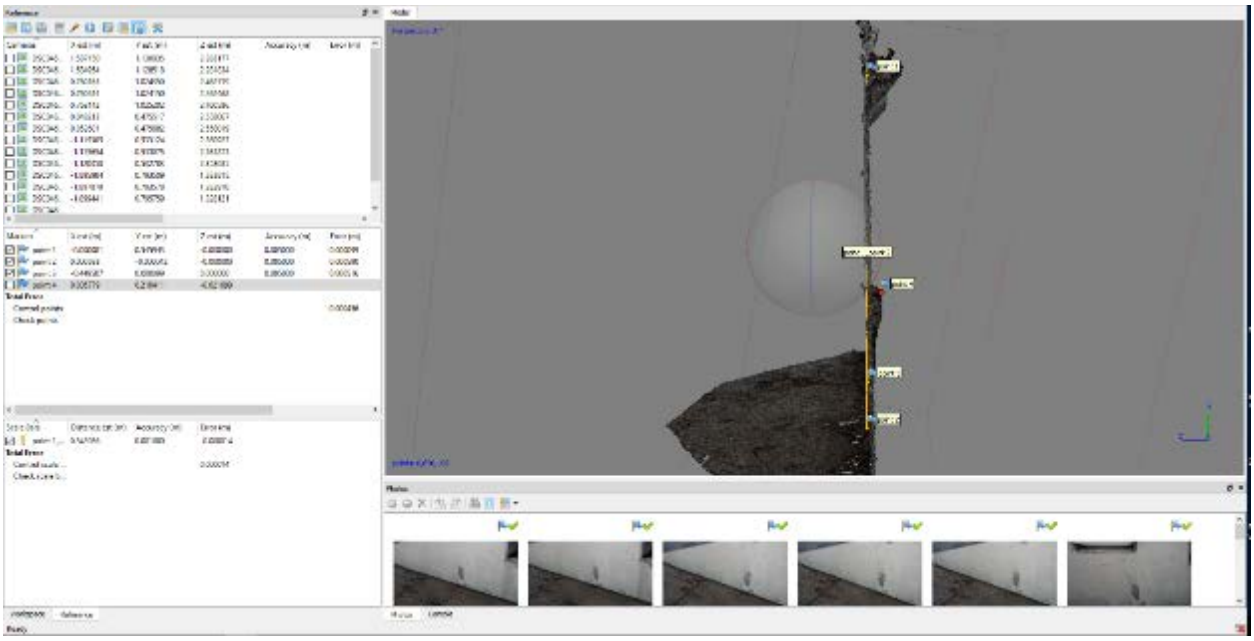

Figure 5-18. User interface in Agisoft

Because 3D reconstruction requires significant computational resources, it can take hours to complete for large models. A large scale reconstruction was created from more than 180 images of Pier Cap 34 of 720114. The reconstructed pier cap is shown in Figure 5-19. The file size of this reconstructed Pier Cap is about 0.65 GB, in addition to the 1.06 GB from the photos. A discussion of data storage options is provided in Section 6.1.

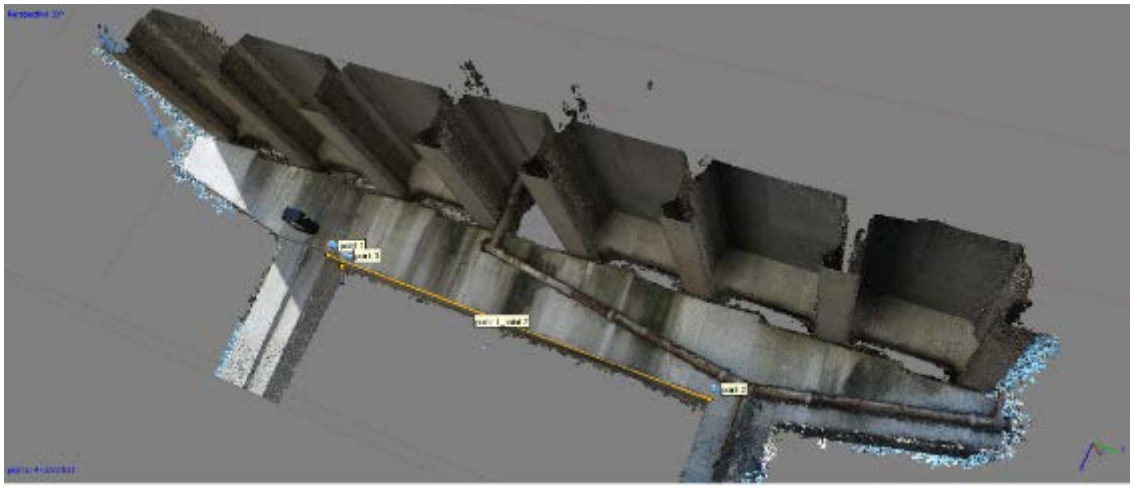

Figure 5-19. Reconstruction of Pier Cap 34 of 720114

There are some important considerations for 3D reconstruction. Both the quantity of images and the variety in position of the camera must be sufficient in order to create an accurate reconstruction. For example, if 100 images are taken from the same location, with the camera oriented in the same direction, Agisoft will have difficulty determining depth information of the scene. Also, as mentioned before, some dimensions in the reconstructed model must be known in order to scale the model to measure other objects. Often, especially for bridges, dimensions of

structural elements can be used to scale models. In order to use Agisoft or a similar program to quantify deficiencies in for inspections, the error of measurements must be further quantified.

Based on these sample reconstructed models, if 3D reconstruction methods are adopted for processing images taken during inspections, it is recommended to create 3D reconstructions of specific deficiencies, rather than large scale 3D reconstructions. Reconstructions of specific deficiencies require fewer images. They can be made with at least three images, but more still images will result in models that are more accurate. Because they require fewer images, they will require less storage than large scale reconstructions, which will be discussed in more detail in Section 6.1. Deficiency reconstructions will also require less time to create than large scale reconstructions. The model of the spall shown in Figure 5-17 and Figure 5-18 took about ten minutes to process on a typical desktop computer. If specific deficiencies are reconstructed, this would align well with recommended practices for sUAV special or damage bridge inspections given in Section 4.9, and models can be directly be compared over time.

6 Practical Considerations for sUAV Structural Inspections

Besides physically conducting structural inspections with an sUAV, two operational changes must be considered if sUAV inspections are adopted. First, depending on the type of sUAV inspection, data storage requirements could be significantly increased over traditional inspection methods. Additionally, the cost of sUAV inspections will be different than current inspection practices. This section will look into these two practical considerations in further detail.

6.1 Data Storage

FDOT stores inspection data in a centralized database for the life of the structure. Inspection data includes images of deficiencies and inspection reports. Additional data that FDOT stores includes inventory images, work orders, and field preparation requirements. Inventory and deficiency images comprise the majority of the data storage requirements for bridge inspections. The storage size for all bridge inspections on the FDOT database is about 312 GB, and there are about 180,000 bridge inspection folders. Therefore, the average storage size for a single bridge inspection folder is about 1.8 MB.

The amount of storage required for sUAV inspections depends on the type of structure, the type of inspection, and the desired form of data. For example, the data storage requirements will vary between HMLP and bridge inspections, it will vary between routine bridge inspections and special or damage inspections, and it will vary based on whether video or still images are desired. For this report, the data storage requirements will be discussed for both HMLP and bridge inspections.

For sUAV HMLP inspections, the total storage for all videos and images of a single HMLP will be quantified. For sUAV bridge inspections, the total storage will be quantified for both demonstration routine inspections and for demonstration special or damage inspections. The total storage from all videos and images of prestressed concrete girder spans will be used to provide an estimate of the amount of data created during sUAV routine inspections, and the storage from individual images of specific deficiencies will be used to estimate the amount of data created during an sUAV special or damage inspection.

6.1.1 HMLP Inspections

As discussed in Section 3, six HMLPs were inspected throughout the project. As the HMLP inspections were conducted towards the beginning of the project, only video was stored, and no still images were taken. Images collected from these inspections were all pulled from video frames. Table 6-1 shows a summary of the total data collected during these six HMLP inspections, including both video and images saved from video frames.

Table 6-1. Summary of all data collected during HMLP inspections

Inspection	Structure	Total (MB)	Video (MB)	Images (MB)
SR-6 and I-75	32P049	1376	1366	10
	32P050	1352	1342	10
	32P054	1110	1097	13
Town Center Parkway and I-295	72P740	1301	1281	20
	72P741	1185	1162	23
	72P743	1141	1117	24

As can be seen, over 1 GB of video is collected from an inspection of a single HMLP. The storage required for the images pulled from frames of the videos alone is much less than the storage required for video, but 10 to 20 MB of data is still significant. The size of a single image pulled from a frame of video is about 2 MB, and the resolution of these images is about 2 Megapixels.

Although the HMLP inspections completed for this project collected only video and pulled still images from video frames, an inspection method comparable to sUAV bridge inspections would be recommended. Instead of collecting video for the whole structure, streaming the camera viewfinder to the ground station and capturing high-resolution images of deficiencies or for inventory would decrease storage requirements and provide higher quality views of the structure.

6.1.2 Routine Bridge Inspections

Eight bridge inspections were conducted with an sUAV during this project from June 2017 to December 2017. For these inspections, three inspection types were considered: routine inspections, special inspections, and damage inspections. The most realistic application for sUAV routine inspections would be for prestressed concrete girder spans, as flying underneath steel girder spans often made flight control difficult.

During demonstration sUAV routine inspections of prestressed concrete girder spans, the sUAV was unable to view the bearings in as much detail as would typically be needed, and it would not be able to see some deficiencies (e.g. hairline cracking at mid-span) due to the proposed flight method. Still, on a prestressed concrete girder bridge in good condition, an sUAV could potentially be used to replace an under bridge inspection vehicle for some inspection cycles.

During this project, eight prestressed concrete girder spans were inspected as demonstration sUAV routine inspections. Depending on the number of girders in the span, between 27 and 43 images were taken during these inspections, and the average amount of storage for a single span was over 200 MB. Table 6-2 provides a summary of the storage size, number of images, and number of girders in the eight prestressed concrete girder spans where demonstration sUAV routine inspections were conducted.

Table 6-2. Summary of data size, number of images, and number of girders in prestressed concrete span demonstration sUAV routine bridge inspections

			Images		
	Structure	Span	Size (MB)	Number	Number of Girders
SR-40 over Ocklawaha River	360055	9	166	27	5
		10	233	37	5
		11	161	29	5
SR-228 over Washington St.	720114	33	246	43	8
		34	199	35	8
		35	195	35	8
		36	263	43	8
		37	205	37	10

No video was recorded during these inspections. Instead, the viewfinder from the camera was streamed to the crew on the ground, and still images were taken of bearings, the bay between girders, and notable deficiencies. The size of the images taken by the high-resolution camera on the sUAV is about 5.6 MB each, and the resolution is 24 Megapixels. As can be seen from the above table, the storage requirements for a single prestressed concrete girder span is large if all images are stored.

6.1.3 Special or Damage Bridge Inspections

For a special or damage inspection, only a select few still images of a specific deficiency may be required. As a result, the storage requirements for these inspections would likely not be significantly more than current special or damage inspections. The size of each still image is about 5.6 MB, although this will depend on the camera selected for the inspection.

If a 3D reconstructed model of a specific deficiency is required, the data storage requirements will be increased. Depending on the level of detail and the number of images used for the 3D reconstruction, the file size will typically be about 40 to 70 percent of the total storage of the images. For example, a reconstruction using 10 images totaling 56 MB could range from about 20 to 35 MB.

Clearly, if video is stored, or if all images are stored during an sUAV routine bridge inspection, the storage required for sUAV inspections will be dramatically more than the storage required for current inspections. However, if only specific high-resolution images of deficiencies are required, the impact of the additional storage may not be too great.

6.1.4 Options for Electronic Storage

Depending on the type of inspection and the type of data collected, data storage requirements will vary. Three options for electronic storage will be provided for HMLP inspections, routine bridge inspections, and special inspections or damage inspections. In order of highest to lowest electronic storage impact: 1) FDOT can store all data on its own servers, 2) FDOT can require sUAV contractors to store all data and provide relevant images for inspection

reports and structure inventory, or 3) FDOT can store only relevant images for inspection reports and structure inventory and delete the rest of the data.

The option with the highest impact to FDOT data storage for structural inspections would be to store all data from sUAV inspections on FDOT servers for the lifespan of the structure. With this option, data would be more accessible to FDOT, but would also require more storage on FDOT servers for each inspection. As image processing techniques improve in the future, one additional benefit to this storage method includes historical forensic analysis of images.

Another option to reduce the data storage impact to FDOT would be to require the contracting sUAV inspection company to store all data for the lifespan of the structure and send relevant images for inspection reports and inventory. Although the data would likely be less accessible to FDOT, it could still be accessed through the contracting sUAV company. With this method, the only changes to FDOT data storage would be from the file sizes of images. Requiring the contractor to store a large amount of data would likely increase the cost of service.

A third option, with the least impact to current data storage inspection practices would be to save only relevant images for inspection reports, structural inventory, and deficiency monitoring. If this option is chosen, data from inspections that is not relevant to inspection reports, structural inventory, or deficiency monitoring would be deleted. It may not be necessary to save video of every HMLP inspected, and it may not be necessary to save an image of every single bearing on a bridge. This method would rely on the ability of the CBI to parse through the images collected of a structure in the field to save relevant data. A qualitative summary of these three options for data storage is provided in Table 6-3.

Table 6-3. Summary of options for data storage

Option	Increase in Storage	Accessibility of All Data	Increase in Associated Costs	Post-Processing Requirements
Store all data on FDOT servers	High	High	High	High
Require contractor to store all data	Low	Medium	High	Medium
Store only relevant data on FDOT servers	Low	Low	Low	Low

6.2 Cost

Several factors may affect the difference in cost between sUAV inspections and current inspections requiring UBIV. These factors depend on the implementation of sUAV inspections. For each factor, potential cost differences will depend on whether FDOT owns and operates sUAVs for inspections or whether FDOT subcontracts sUAV operations. This section discusses these general factors, and the following sections will discuss how each factor affects HMLP or bridge inspection costs.

6.2.1 Equipment Costs

If the FDOT chooses to purchase their own sUAVs and train inspectors to pilot the vehicles, the purchase cost of the sUAV must be considered. The cost of purchasing an sUAV can vary significantly. The DJI Matrice 200, a commercial sUAV designed for applications similar to bridge inspections, costs about $6000 for the airframe, with at least an additional $600 for a suitable camera. Other potential sUAVs that could be used for structural applications can cost less than $1000, while specialty sUAVs can cost tens-of-thousands of dollars. The cost of the sUAV used for this project, including the airframe and sensors, was about $2500. The cost of sUAV equipment required for inspections is affected by the scope of the inspection and the quality of image data needed. Naturally, as the quality of image data needed increases, better sUAV platforms will be needed, which will increase sUAV equipment costs for inspections.

Subcontracting sUAV operations would have multiple benefits. FDOT would not have to purchase sUAVs and would also not need to purchase liability insurance. sUAV operators typically charge daily rates, including equipment and labor costs. Based on anonymous quotes from two sUAV companies, a typical daily rate for sUAV services would be in the range of $1000 to $2000.

Differences in equipment cost between conventional inspections and sUAV inspections depend on the type of inspection. For HMLP inspections, where the only equipment needed for visual inspection may be a pair of binoculars and a camera, equipment costs would increase. For bridge inspections, purchasing a sUAV would be less expensive than purchasing a UBIV.

6.2.2 Staff Costs

6.2.2.1 Training

If FDOT purchases and operates its own sUAVs for inspections, it will need to train operators to pilot the sUAV. In addition, the operators would need to be certified, which requires passing an aeronautical knowledge test. The cost to take the aeronautical knowledge test is approximately $150. If FDOT instead subcontracts out the sUAV inspection work, there will be no need to train operators.

6.2.2.2 In-Field Inspection Time and Crew Size

During the six HMLP inspections and eight bridge inspections conducted during this project, the time required for inspections was comparable to current inspection practices. Whether for HMLP inspections or bridge routine or special inspections, staff costs related to inspection time would not be significantly affected. As a result, changes in cost for in field inspection time would likely only be due to changes in crew size. As discussed in Section 2.2, the recommended crew for sUAV inspections would consist of three members: a remote pilot in command (RPIC), an inspector, and a visual observer (VO). Changes in cost from conventional structural inspections to sUAV inspections would again depend on the type of inspection. For HMLP inspections, the crew size, and so the cost, would likely increase. For bridge inspections, the crew size would likely not change.

6.2.2.3 Post-processing

An additional factor for staff costs for sUAV inspections includes post-processing of data collected during inspections. Based on the inspections conducted during this project, the recommended practice for sUAV inspections is to collect only still images, which would reduce the post-processing time of selecting images for an inspection report. If only still images are taken, post-processing time and cost for sUAV inspections would likely be similar to current practices.

6.2.3 HMLP Cost Comparison

Based on information from the six sUAV inspections of HMLPs conducted during this project, an approximate comparison between conventional HMLP inspections and sUAV HMLP inspections can be provided. The difference in cost between the two inspection methods would be primarily due to differences in equipment and a potential difference in crew size.

6.2.3.1 Qualitative Cost Comparison

Current inspection practices for HMLPs require one crew-hour, which includes both the in-field inspection and compiling the inspection report. The in-field portion of the inspection typically takes twenty minutes. As discussed in Section 1.2, two inspectors make up the crew for current HMLP inspection practices. One inspector performs the visual portion of the inspection, walking around the pole, carefully looking over its surface through a pair of binoculars, while the other physically inspects the condition of the foundation and the tightness of the bolts.

sUAV inspection practices for HMLPs would likely take the same amount of time for the in-field portion of the inspection. During the inspections conducted throughout this project, the sUAV collected video of the entire HMLP, and images desired for inventory or deficiency tracking were extracted from the video. With this method, additional time would be required for post-processing. However, after conducting all inspections, it is recommended that only relevant, high-resolution still images are taken in the field. This approach would eliminate the time required to watch the video after the inspection, it would reduce data storage requirements, and it would result in higher-resolution images needed for inventory and deficiency tracking. Therefore, there would be no change in inspection time and post-processing.

As stated in Section 6.2.2.2, sUAV inspections would require additional personnel. For sUAV operations, an RPIC, an inspector, and a VO are recommended. The physical inspector could not participate in sUAV operations while physically inspecting the structure. As a result, the crew size would likely need to be increased by two to provide a VO and a RPIC for sUAV operations.

6.2.4 Approximate Quantitative Cost Comparison

Current inspection times take one hour, including about twenty minutes for an in-field inspection and the rest of the time for report generation. If FDOT purchases sUAVs and conducts HMLP inspections, the increase in staff costs can be approximated. If two extra inspectors are sent to each HMLP inspection to be an RPIC and a VO, the in-field portion of the inspection could double in salary costs. Even if there is not a VO present, as a VO is not required, one extra crew member would be required, which would increase costs of the in-field portion of the

inspection by up to 50%. Note that if a subcontractor is hired to conduct the sUAV inspections, there will likely be a flat daily rate, and the cost per HMLP will depend on the number of inspections conducted.

Table 6-4 provides an approximate comparison of costs for a single HMLP inspection. An inspection is assumed to take one crew hour for a two-person crew. This table provides an increase in cost for one additional crew member for the duration of the in-field portion of the inspection, which is assumed to be twenty minutes. If a VO is used, another crew member would add to staff costs. The hourly rate used is from an FDOT cost estimation worksheet, and there is no multiplier for overhead or operating margin. Regardless of the actual hourly rate, assuming the additional crew members would be paid at the same rate as the inspectors, the increase in cost for a routine HMLP inspection due to additional crew members during the in-field portion of the inspection would be about 17% for one additional crew member and 33% for two additional crew members.

Table 6-4. Approximate comparison of staff costs for conventional and sUAV HMLP inspections

	Unit Cost	Current Inspection		sUAV Inspection	
	($/hr)	Time (hr)	Cost ($)	Time (hr)	Cost ($)
Visual Inspector	32	1.00	$ 32.00	1.00	$ 32.00
Physical Inspector	32	1.00	$ 32.00	1.00	$ 32.00
RPIC	32	N/A	$ -	0.33	$ 10.67
Total Cost per HMLP			$ 64.00		$ 74.67

6.2.5 Bridge Cost Comparison

Based on information from the eight sUAV inspections of bridges conducted during this project, an approximate comparison between conventional bridge inspections and sUAV bridge inspections can be provided. The difference in cost between the two inspection methods would be primarily due to differences in equipment and reduced need for MOT.

6.2.5.1 Qualitative Cost Comparison

sUAV routine inspections of bridges would be unlikely to reduce the overall time of the inspection or the number of crew members required. However, use of an sUAV would eliminate the need for MOT, which can lead to significant cost savings. Additionally, a UBIV mobilization would not be required. Depending on whether FDOT purchases sUAVs or subcontracts sUAV inspections to other companies, the change in equipment cost will vary. If FDOT purchases sUAVs for inspections, the initial cost of purchasing an sUAV would be an investment, but it would be significantly less expensive than a purchasing a UBIV. Owning sUAVs would have the benefit of reducing mobilization costs. The sUAV can be placed in a truck and transported to the site.

For a typical routine inspection, cost savings will vary based on if FDOT conducts inspections or if subcontractors are hired. The difference in cost between FDOT conducted routine sUAV inspections and FDOT conducted UBIV inspections, if FDOT owns the equipment, will primarily come from MOT. However, if a significant portion of routine

inspections can be completed by sUAVs, FDOT may be able to reduce the number of UBIVs needed in its fleet, reducing both equipment purchasing and maintenance costs.

For inspections that are conducted by consultants with rented equipment, the rental cost for sUAVs may lead to additional cost savings over UBIV rental costs. As stated above, typical daily rates for sUAV inspections would typically cost about $2000, while UBIV rental costs, based on inspection cost estimation tools, typically cost about $2500 to $3250.

6.2.5.2 Approximate Quantitative Cost Comparison

In order to compare current routine inspection costs with sUAV inspections, one bridge inspected during this project was used as a case study. The dimensions of the structure are given in Table 6-5 below.

Table 6-5. Dimensions of structure chosen for cost case study

Bridge Length (ft)	Deck Width (ft)	Minimum Clearance (ft)	Equivalent Spans	Material
815	35.43	25.919	14.394	P/S Conc. Girder

Approximate costs from the most recent routine inspection of this structure are compared to the difference in cost if an sUAV had been used instead of a UBIV in Table 6-6. As shown in this table, the cost for a routine inspection of this structure could decrease by almost 10%. There are a couple of important notes about this table. First, it is assumed that FDOT will contract the sUAV work out, resulting in a flat daily rate. Also, the structure chosen is used to quantify an approximate difference in cost between current inspection practices and sUAV inspection practices. Due to the wide variety of bridge superstructure types, and other factors including site conditions, this comparison may not be representative for all routine bridge inspections. As stated above, the the cost of UBIV rental, mobilization, and use can be approximated from $2500 and $3250. However, because FDOT conducted this inspection with a UBIV in its inventory, equipment costs per day for this routine inspection are lower. The unit cost per day of an sUAV is taken from the higher of the two quotes provided by sUAV companies. Finally, the salary cost given in Table 6-6 is not multiplied by an overhead or an operating margin, since FDOT personnel would conduct the inspection. The number of hours is not the time the inspection took, or an equivalent time in crew hours, it is the total number of hours billed by all employees.

Table 6-6. Cost of routine inspection of prestressed concrete girder bridge

Cost Item	Unit Cost	Unit	Quantity	Current Cost	sUAV Cost
Salary Costs	$ 45.00	hour	58	$ 2,610.00	$ 2,610.00
MOT	$ 2,000.00	day	1	$ 2,000.00	$ -
UBIV	$ 200.00	day	1	$ 200.00	$ -
sUAV	$ 1,800.00	day	1	$ -	$ 1,800.00
Total				$ 4,810.00	$ 4,410.00

6.2.6 Comparison of Costs

As described in this section, sUAV inspections would affect the cost of HMLP and bridge inspections. If used for HMLP inspections, the cost would likely increase due to an

increase in crew size. Additionally, the sUAV would increase the equipment cost of current HMLP inspections. However, for routine bridge inspections, sUAVs would likely decrease the overall cost due to a reduction of required MOT and UBIV use. The speed and ease with which an sUAV could be deployed could further reduce cost for special or damage inspections.

7 sUAV Structural Inspection Recommendations and Conclusion

7.1 Recommendations for sUAV Platform

Several key features needed for effective sUAV inspections can be identified. First, the sUAV should have a camera that can be mounted to either the top or bottom of the sUAV. Without this, the sUAV will likely be unable to take images of the bridge underside. Additionally, the sUAV should be equipped with sensors to assist the RPIC with flight. Especially for flight underneath bridges, where there is insufficient GPS and there are many obstructions, an obstacle avoidance system should be used. For this study, an optical flow sensor and a laser range finder primarily informed the sUAV to keep a safe distance from the bottom of the bridge. Also, a high-resolution camera with good low light performance should be used.

If improved views of the bearings or views of the top face of bottom flanges of steel girders are required, a smaller sUAV may be needed to fly in the bay between beams. However, especially with wind gusts and turbulence created from the sUAV, these confined space operations would carry considerable risk. Another limitation to using a smaller sUAV would be decreased payloads. As a result, the imaging sensors would likely need to be lower quality than the ones used for this project.

7.2 Recommendations for sUAV Structural Inspections

Utilizing an sUAV for structural inspections provides some benefits over current inspection methods, but it also has inherent limitations. Weather is a significant limiting factor for sUAV use. High winds and precipitation can prohibit safe operation of sUAVs. The sUAV cannot make contact with obstructions, such as overhanging trees, it may be affected by electrical wires, and battery life limits flight time. Also, the inspection crew must be skilled in piloting and troubleshooting the craft, and they must be familiar with and abide by regulations set by the FAA.

For HMLP inspections, an sUAV allows for a close-up look at the entire structure and therefore can provide a more thorough inspection. Conversely, sUAV inspections would require a larger crew and more equipment than current inspection practices, which would lead to an increase in cost. sUAV inspections of HMLPs can be recommended if FDOT believes the improved views of the structure would be worth the increase in inspection cost.

Specifically for bridge inspections, the primary advantages of using sUAVs for inspections include the ability to inspect structures with load restrictions, especially post impact, and removing the need for MOT, which may reduce costs. Additionally, sUAVs can be deployed rapidly if one is needed for a special inspection or a damage inspection. However, while an inspector may brush away debris and touch parts of the structure, the sUAV cannot make contact with the structure. This would prohibit the use of an sUAV for fracture critical inspections, and could reduce the quality of sUAV bridge inspections if there is debris on a pier cap. The sUAV used for these demonstrations is also not able to safely fly inside the bay between beams, so it cannot see the top of the bottom flanges of steel beams, and it cannot see bearings as well as current inspection practices. Other smaller platforms may be able to access these areas, but

would have a smaller payload. Flight control in low light and GPS denied areas underneath bridges must also be improved.

The use of sUAV technology to assist in bridge inspections is feasible, but it is difficult to capture all of the same information as current inspection practice. This study has provided a step towards sUAV structural inspection implementation by performing six inspections of HMLPs and eight GPS-free inspections underneath bridges. Future improvements to sUAVs could make them more suitable to structural inspections. Some advancements that should be considered include improved and more stable GPS free flight in low light areas, improved accessibility of the sUAV, automatically tagging the location of images taken during an inspection, development of more robust automatic deficiency detection programs, and error quantification of deficiency measurements from 3D reconstructed models.

Recommended applications for sUAV bridge inspections include periodically replacing the use of UBIVs on bridges in good condition (e.g. every other or every third inspection cycle). The most immediate and significant impact an sUAVs could make on current inspection practices would be for special and damage inspections. If a single specific deficiency must be monitored, mobilizing an sUAV could be more efficient than mobilizing a UBIV, and no MOT would be required. For a damage inspection, the use of UBIVs may be impossible, making an sUAV a realistic alternative.

7.3 Recommendations for Image Processing

Although state of the art image processing algorithms show promise, commercial programs for deficiency detection and quantification are still some time away. If creating a program to automatically detect deficiencies is of interest, considerable development costs would be required. Therefore, it is recommended to process images interactively. Inspectors can determine which images are useful while in the field, similar to how inspectors would currently select images. If further processing is needed to quantify a deficiency, inspectors can create a scaled 3D reconstructed model from multiple images. Other options for determining the size of objects in an image include attaching a laser range finder to the camera or attaching two parallel laser range finders to the camera to project a scale. It is also recommended to create a local coordinate system for the sUAV and tag images with the location. This could make locating deficiencies more straightforward for future inspections.

7.4 Recommendations for Data Storage and Cost Considerations

Based on the amount of data that can be generated from sUAV inspections and the options for data storage, storing only relevant images on FDOT servers is recommended. It is recommended to collect still images instead of videos, as image qualities are much higher and they require less storage than video. By allowing certified inspectors to decide which images are relevant, and deleting other images, the increase in storage requirements would be minimized. Some data collected during inspections would not increase the quality of the inspection, but would only add to the data storage requirements. For example, some images will be out of focus, and many images will be taken of elements in good condition. Additionally, if video is collected instead of still images, not only will the data storage requirements be high, but the time required

to watch the video after the inspection and pull video frames for the inspection report would not provide as high quality data as identifying relevant deficiencies in the field and capturing high-resolution images.

Based on estimations of inspection costs, HMLP inspection staff costs would be likely to increase. Additionally, more equipment would be needed for each HMLP inspection. Conversely, sUAV bridge inspection costs would likely decrease. For routine inspections, the reduction may not be too significant, but the speed and ease with which an sUAV could be deployed could further reduce cost for special or damage inspections. The reduction in cost would be due primarily to the elimination of the need for MOT and for UBIV mobilization.

References

Adhikari, R., Moselhi, O., and Bagchi, A. (2014). “Image-based retrieval of concrete crack properties for bridge inspection.” *Automation in Construction*, 39, 180-194.

Brooks, C., Dobson, R., Banach, D., Dean, D., Oommen, T., Wolf, R., Havens, T., Ahlborn, T. and Hart, B. (2015). *Evaluating the Use of Unmanned Aerial Vehicles for Transportation Purposes* (MTRI-MDOTUAV-FR-2014). Michigan Department of Transportation, Houghton, MI.

Chan, B., Guan, H., Jo, J., and Blumenstein, M. (2015). "Towards UAV-based bridge inspection systems: A review and an application perspective." *Structural Monitoring and Maintenance* 2(3), 283-300.

Federal Highway Administration (FHWA). (2012). Bridge Inspector's Reference Manual. Federal Highway Administration, Arlington, VA.

Florida Department of Transportation (FDOT). (2016). Bridge and Other Structures Inspection and Reporting. Florida Department of Transportation, Tallahassee, FL.

Florida Department of Transportation (FDOT) District 6. (2018). Traffic Signal Mast Arms and High Mast Light Poles Inspections. Contract 19609. Florida Department of Transportation, Miami, FL.

Fujita, Y., Mitani, Y., and Hamamoto, Y. (2006). A method for crack detection on a concrete structure. *Proc. 18th International Conference on Pattern Recognition*, pp. 901-904, Hong Kong.

Gillins, M., Gillins, D., and Parrish, C,. (2016). "Cost-Effective Bridge Safety Inspections Using Unmanned Aircraft Systems (SUAV)." *Proc. Geotechnical and Structural Engineering Congress*, pp. 1931-1940, Phoenix, AZ, 2016.

Gunaratne, M., Amarasiri, S., and Nasseri, S. (2008) *Investigation of Automated and Interactive Crack Measurement Systems* (FDOT Research Report No. BD544-36), University of South Florida, Tampa, FL.

Hallermann, N., and Morgenthal, G. (2014). "Visual inspection strategies for large bridges using Unmanned Aerial Vehicles (UAV)." *Proc. 7th International Conference on Bridge Maintenance, Safety and Management*, pp. 661-667, Shanghai, China.

Irizarry, J., Gheisari, M., and Walker, B. (2012). "Usability assessment of drone technology as safety inspection tools." *Journal of Information Technology in Construction* 17(12), 194-212.

Irizarry, J., Kim, S., Johnson, E., and Lee, K. (2017). “Potential Unmanned Aircraft Systems Based Operations within a Department of Transportation: Findings from a Focus Group Study” *International Conference of the Associated Schools of Construction (ASC)*, Seattle, Washington.

Jahanshahi, M.R., and Masri, S.F. (2012). “Parametric performance evaluation of wavelet-based corrosion detection algorithms for condition assessment of civil infrastructure systems.” *Journal of Computing in Civil Engineering*, 27(4), 345-357.

Jahanshahi, M.R. and Masri, S.F. (2013). “A new methodology for non-contact accurate crack width measurement through photogrammetry for automated structural safety evaluation. *Smart Materials and Structures*,” 22(3), 035019.

Jahanshahi, M.R., Masri, S.F., Padgett, C.W., and Sukhatme, G.S. (2013). “An innovative methodology for detection and quantification of cracks through incorporation of depth perception.” *Machine Vision and Applications,* 24(2), 227-241.

Khan, F., Ellenberg, A., Mazzotti, M., Kontsos, A., Moon, F., Pradhan, A., and Bartoli, I. (2015). "Investigation on bridge assessment using unmanned aerial systems." *Proc. Structures Congress*, pp. 404-413, Portland, OR.

Kim, J., Kim, S., Park, J., and Nam, J. (2015). “Development of crack detection system with unmanned aerial vehicles and digital image processing.” *Proc. 2015 World Congress on Advances in Structural Engineering and Mechanics*. Incheon, Korea

Lee, S., Chang, L., and Skibniewski, M. (2006). “Automated recognition of surface defects using digital color image processing.” *Automation in Construction*, 15(4), 540-549.

Li, G., He, S., Ju, Y., and Du, K. (2014). “Long-distance precision inspection method for bridge cracks with image processing.” *Automation in Construction*, 41, 83-95.

Medeiros, F.N., Ramalho, G.L., Bento, M.P., and Medeiros, L.C. (2010). “On the evaluation of texture and color features for nondestructive corrosion detection.” *EURASIP Journal on Advances in Signal Processing*, 2010(1), 1.

Moller, P. (2008). *Caltrans Bridge Inspection Aerial Robot* (CALSTRANS Report No. CA08-0182). California Department of Transportation, Division of Research and Innovation, Sacramento, CA.

National Bridge Inspection Standards. 23 CFR Part 650 Subpart C (2004), Federal Highway Administration, Washington, D.C.

Otero, L., Gagliardo, N., Dalli, D., Huang, W.H., and Cosentino, P. (2015). *Proof of Concept for Using Unmanned Aerial Vehicles for High Mast Pole and Bridge Inspections* (Florida Department of Transportation Research Report No. BDV28 TWO 977-02). Florida Institute of Technology, Melbourne, FL.

Pragalath, H., Seshathiri, S., Rathod, H., Esakki, B., and Gupta, R. (2018). “Deterioration Assessment of Infrastructure Using Fuzzy Logic and Image Processing Algorithm.” *Journal of Performance of Constructed Facilities*, 32(2), 04018009.

Small Unmanned Aircraft Systems. 14 CFR Part 107 (2016). Department of Transportation Federal Aviation Administration, Washington, D.C.

Yamaguchi, T. and Hashimoto, S. (2010). “Fast crack detection method for large-size concrete surface images using percolation-based image processing.” *Machine Vision and Applications*, 21(5), 797-809.

Zhang, W., Zhang, Z., Qi, D., and Liu, Y. (2014). “Automatic crack detection and classification method for subway tunnel safety monitoring.” *Sensors*, 14(10), 19307-19328.

Zhu, Z., German, S., and Brilakis, I. (2011). “Visual retrieval of concrete crack properties for automated post-earthquake structural safety evaluation.” *Automation in Construction*, 20(7), 874-883.

Zink, J. and Lovelace, B. (2015). *Unmanned aerial vehicle bridge inspection demonstration project* (Report No. MN/RC 2015-40). Minnesota Department of Transportation, St. Paul, MN.

Appendix

This appendix provides response data from inspection surveys and additional image data from sUAV inspections. This data provides more information on inspector evaluations of inspections and the quality of images obtained during inspections.

A1 Raw Survey Data

The feedback from surveys are presented in this section. First, qualitative feedback from HMLP inspection surveys are provided, followed by quantitative feedback from bridge inspections.

A1.1 Raw Survey Response Data from HMLP Inspections

UNIVERSITY OF FLORIDA
sUAV FOR STRUCTURAL INSPECTION
---------- POST-INSPECTION INTERVIEW ----------

Inspector: _[redacted] Date: __Nov. 4, 2016___

Location: ___Tampa, Florida_

Inspection Day Questions

1. What is your overall opinion of the sUAV inspection system?

   The sUAV appeared to be built well and appears that it would be durable.

2. With respect to setup time, mobility, flight/inspection time, and safety, what are some advantages and disadvantages of this system compared to the current inspection method?

Advantages: Drone can obviously reach areas close up that an inspector could not or only could with the aid of magnification devices. Also, in this test application with the HMLP, the drone could provide views of the top of the luminaire device. An area that could not be viewed from the ground, even with binoculars. The ability to stop at any height and remain stable during flight. The ability to pan the camera as needed during flight.

Disadvantages: Set up time was a bit long relative to the inspection of a HMLP. What I mean is if it takes 20 minutes to set up for a HMLP that takes 60 minutes to completely inspect, than 20 minutes is long. If it takes 20 minutes to set up for a Bridge Inspection that takes 5 hours to completely inspect, than 20 minutes is not too long. Mobility during this test was restricted to straight vertical lifts. With that in mind, I would still like to the device operate more freely and dynamic. Sun location during certain times could restrict the ability to see an area as well as would be desired (causing a "white out"/ blinding affect).

3. After seeing some of the streaming video from the sUAV, what benefit do you think these views of the structure will provide? Would video or still images be more useful?

I did have the chance to work the camera gimbal during one of the flights which allowed me to view the monitors during the flight. Even in the outside light, on a monitor I found the quality to be very good. I believe both streaming videos and stills have their advantages. The raw video can be very useful in being able to review a structure again without having to return to the site

to do so. Still images is what would be needed for the comprehensive write up of our inspection reporting on the structure.

4. What impacts would this method have on the time and cost of the in-field portion of inspections compared to the current method?
   The impact for a HMLP inspection would be considerable. This mainly due to the short time it normally takes to accomplish a HMLP inspection in general. Also, there is no specialized access equipment needed to typically accomplish a HMLP inspection.

5. Can you think of any improvements that would make the system more useful for inspectors?

Reduced set up times and more compact ancillary equipment needed to accomplish the sUAV inspection.

6. Do you have any additional thoughts, comments or concerns about this system?

Overall I like the system and welcome the advancement of this technology in our industry. It is in my opinion the true value of this unit will be in bridge inspections more so than HMLP inspections. I feel the system should be more mobile and compact. I do realize that the size of the unit may be due to the camera size and the heavy unit may be better suited for windy conditions.

UNIVERSITY OF FLORIDA
sUAV FOR STRUCTURAL INSPECTION
---------- POST-INSPECTION INTERVIEW ----------

Inspector: [redacted] Date:

11/3/2016

Location: I-75 at SR-6 HMLP Inspection

Inspection Day Questions

7. What is your overall opinion of the sUAV inspection system?

   I think it will be a good tool to supplement our current inspections. With a few tweaks I think it could benefit the HMLP inspections.

8. With respect to setup time, mobility, flight/inspection time, and safety, what are some advantages and disadvantages of this system compared to the current inspection method?

   Disadvantages are that it requires set up time whereas current process does not require much set up time and you also have to someone skilled in flying the aircraft. Advantages are that you can see the entire pole from about an arm length. If the camera was equipped with a zoom it would make this even better.

9. After seeing some of the streaming video from the sUAV, what benefit do you think these views of the structure will provide? Would video or still images be more useful?

   The videos are nice but for our reporting structure the still images would be the most useful. The videos are good to but the stills are easier to incorporate into a report.

10. What impacts would this method have on the time and cost of the in-field portion of inspections compared to the current method?

    I think this overall method would add additional time to each inspection which in turn adds additional costs. However, the potential benefits may out weigh the additional time and costs.

11. Can you think of any improvements that would make the system more useful for inspectors?

    I think a camera zoom would be a big improvement and also the ability to fly around the HMLP at each seam instead of having to land and fly up each side.

12. Do you have any additional thoughts, comments or concerns about this system?

    None at this time.

A1.2 Survey Data from Bridge Inspections

Cumulative responses:

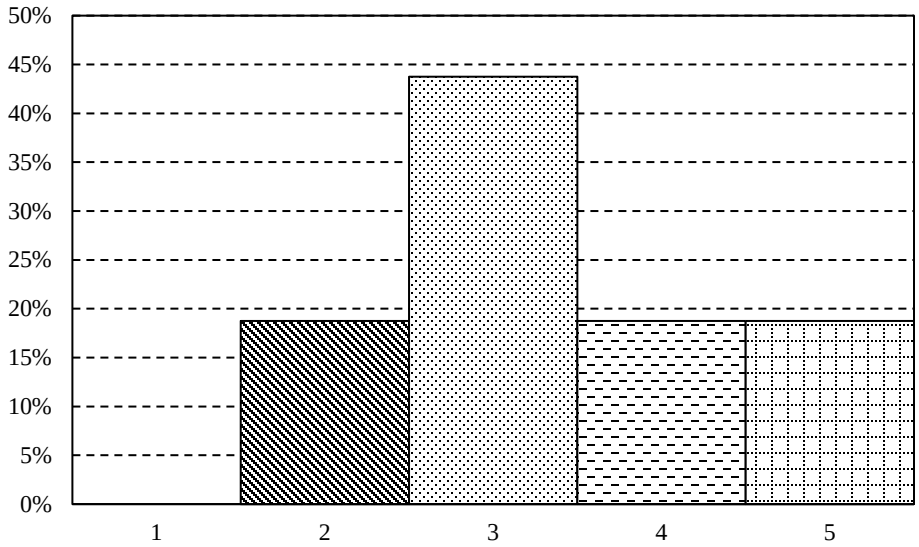

Figure A1-0-1. Overall rating of the sUAV inspections

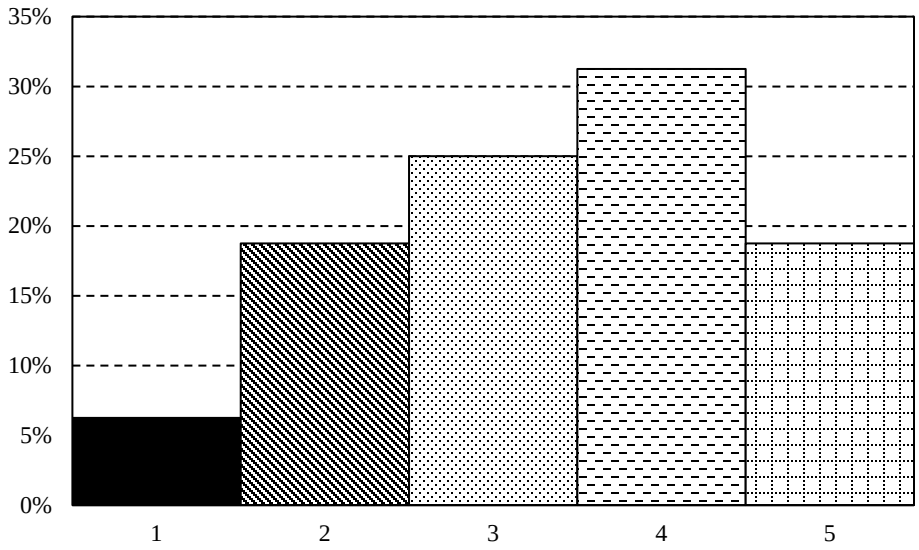

Figure A1-0-2. Safety rating of the sUAV inspections

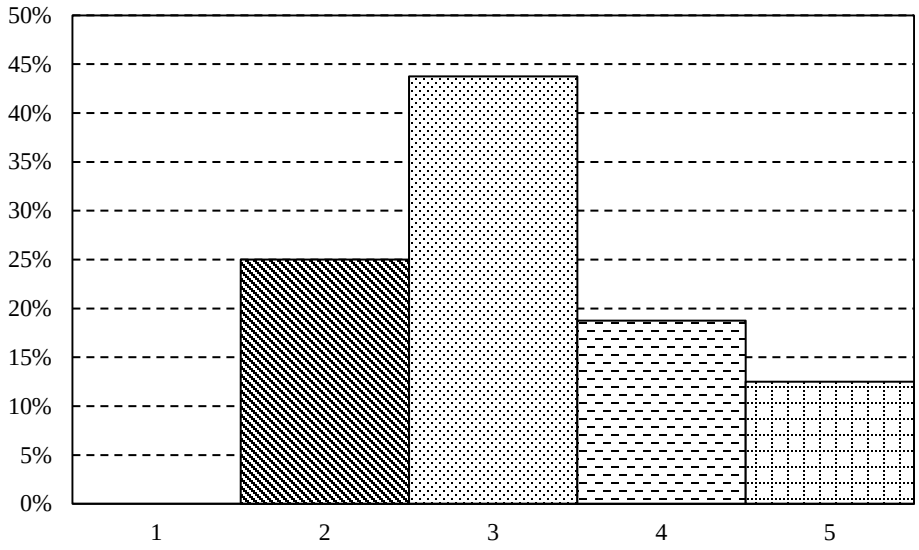

Figure A1-0-3. Rating of setup time and effort for the sUAV inspections

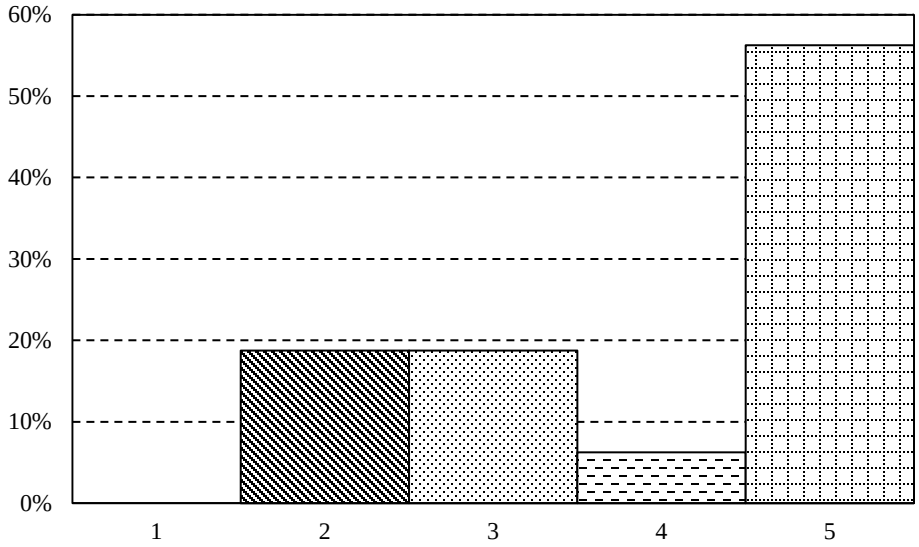

Figure A1-0-4. Rating of inspection time for the sUAV inspections

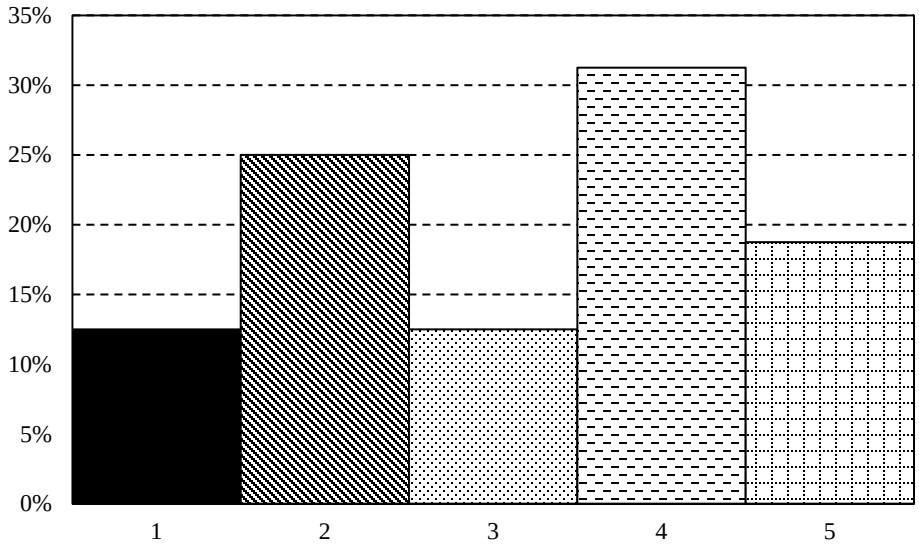

Figure A1-0-5. Rating of ability of sUAV to access restrictive areas

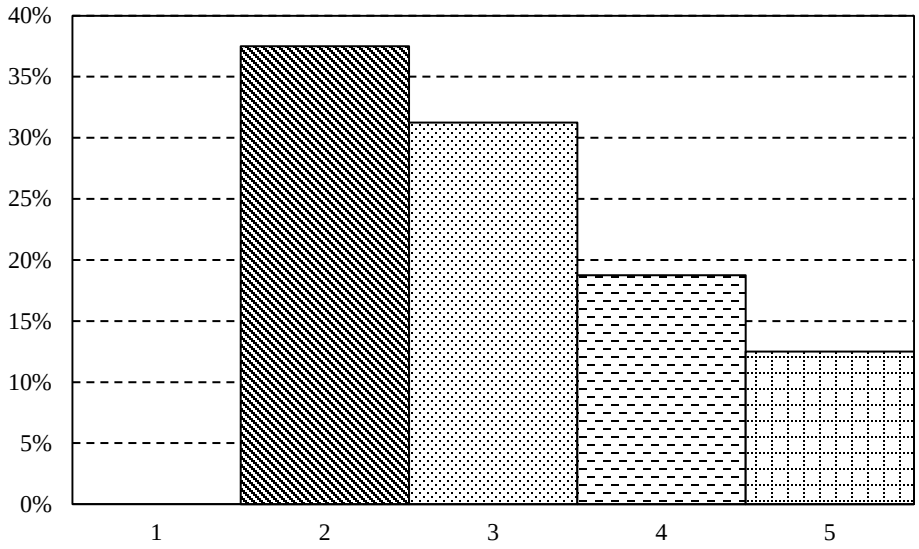

Figure A1-0-6. Rating of amount of equipment and crew size for the sUAV inspections

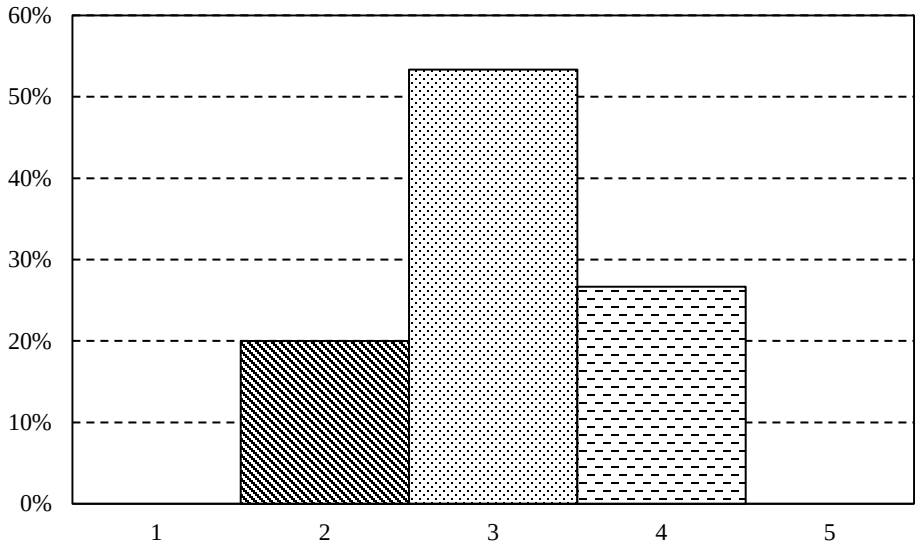

Figure A1-0-7. Rating flight control of sUAV

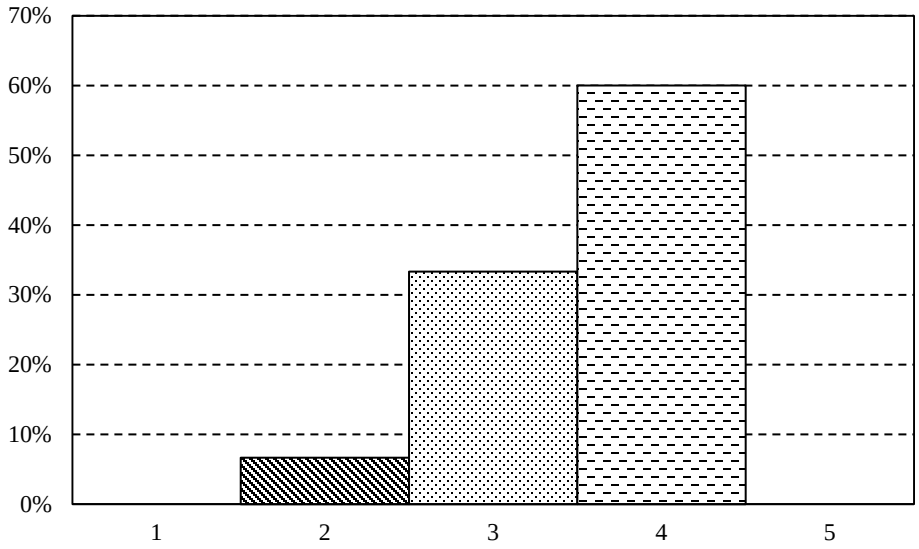

Figure A1-0-8. Rating of camera control

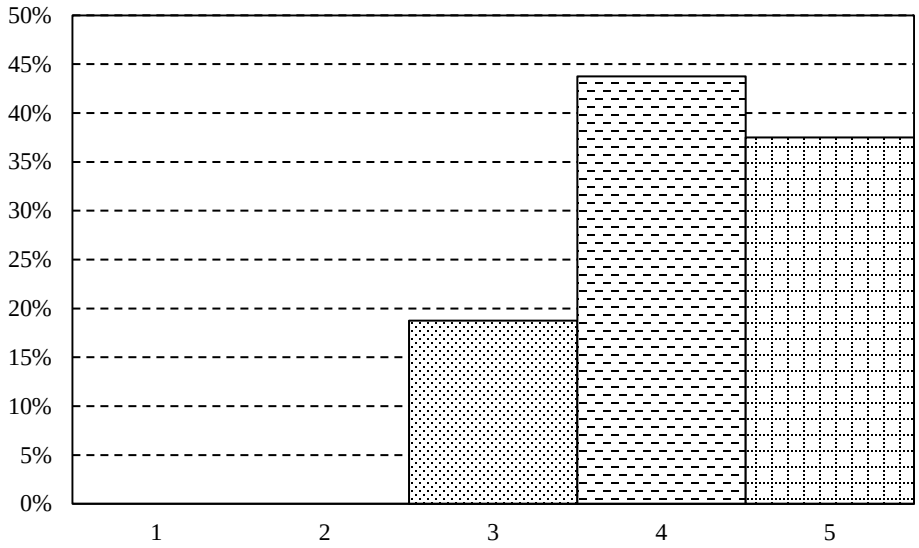

Figure A1-0-9. Video quality rating

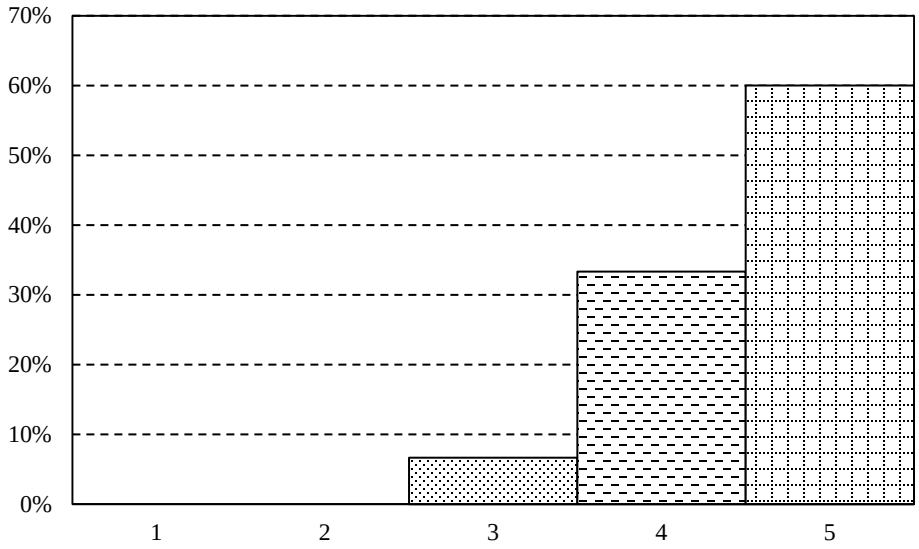

Figure A1-0-10. Image quality rating

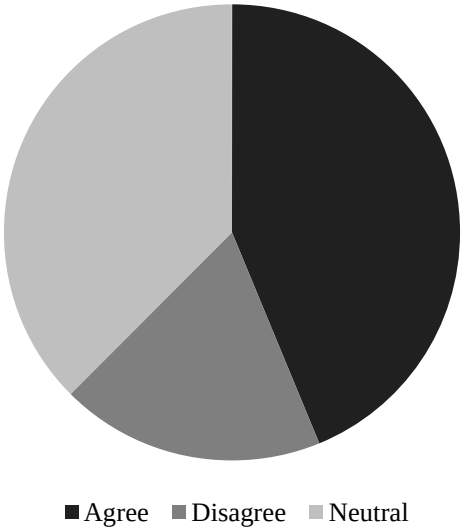

Figure A1-0-11. Opinion on whether sUAV system could improve the quality of bridge inspections

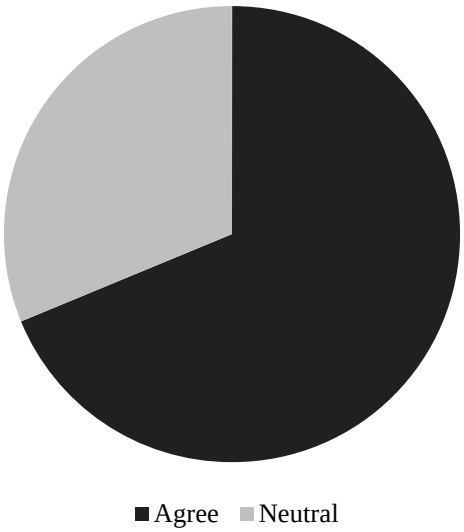

Figure A1-0-12. Opinion on whether sUAV system could improve the safety of bridge inspections

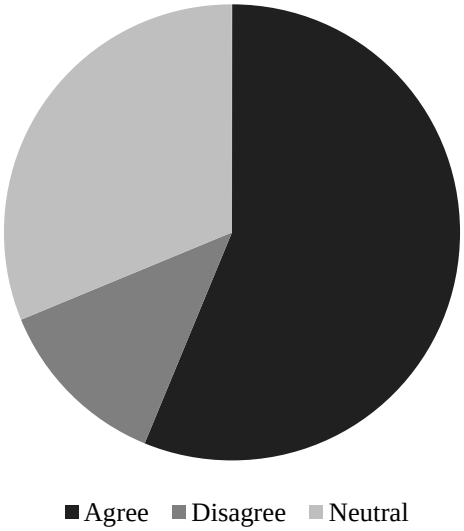

Figure A1-0-13. Opinion on whether sUAV system should be adopted

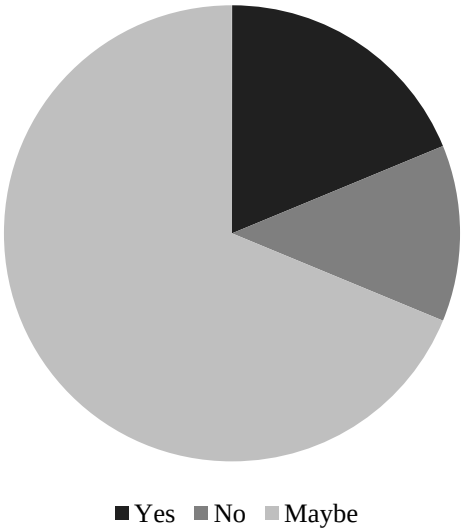

Figure A1.2-0-14. Opinion on whether sUAV system could improve the speed of an inspection

Individual responses over time:

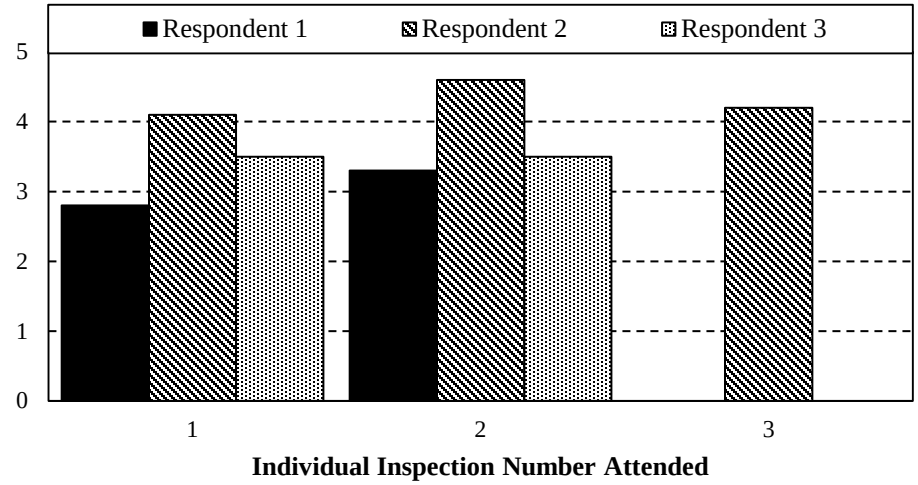

Figure A1-0-15. Average of all quantitative feedback responses per inspection over time for repeat respondents

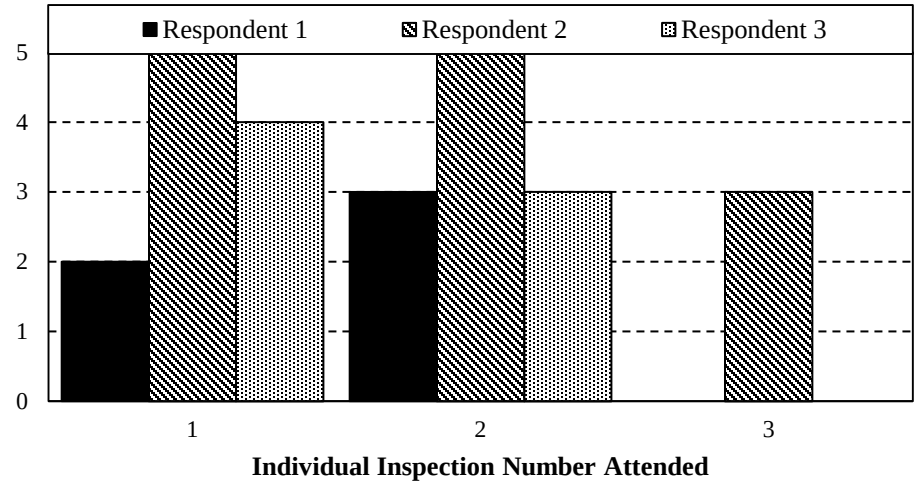

Figure A1-0-16. Overall rating of sUAV system per inspection over time for repeat respondents

A2 Representative Images from Inspections

Additional images from inspections are presented in this section. Thousands of images were taken throughout this project, so a sample of six to ten images from each structure will be provided in this appendix to give a more representative overview of the quality of images obtained during sUAV inspections. First, images pulled from video frames of HMLP inspection are provided, followed by images taken during bridge inspections.

A2.1 Representative Images from HMLP Inspections

32P049

Figure A2-0-1. 32P049 - View of Lower Slip Joint from Southeast

Figure A2-0-2. 32P049 - View of Lower Slip Joint from Northwest

Figure A2-0-3. 32P049 - View of Second Slip Joint from Southeast

Figure A2-4. 32P049 - View of Second Slip Joint from Northwest

Figure A2-5. 32P049 - View of Lights from Southeast

Figure A2-6. 32P049 - View of Lights from Northwest

32P050

Figure A2-7. 32P050 - View of Lower Slip Joint from Southeast

Figure A2-8. 32P050 - View of Lower Slip Joint from Northwest

Figure A2-9. 32P050 - View of Second Slip Joint from Southeast

Figure A2-10. 32P050 - View of Second Slip Joint from Northwest

Figure A2-11. 32P050 - View of Lights from Southeast

Figure A2-12. 32P050 - View of Lights from Northwest

32P054

Figure A2-13. 32P054 - View of Lower Slip Joint from Northeast

Figure A2-14. 32P054 - View of Lower Slip Joint from Southeast

Figure A2-15. 32P054 - View of Lower Slip Joint from Southwest

Figure A2-16. 32P054 - View of Lower Slip Joint from Northwest

Figure A2-17. 32P054 - View of Second Slip Joint from Northeast

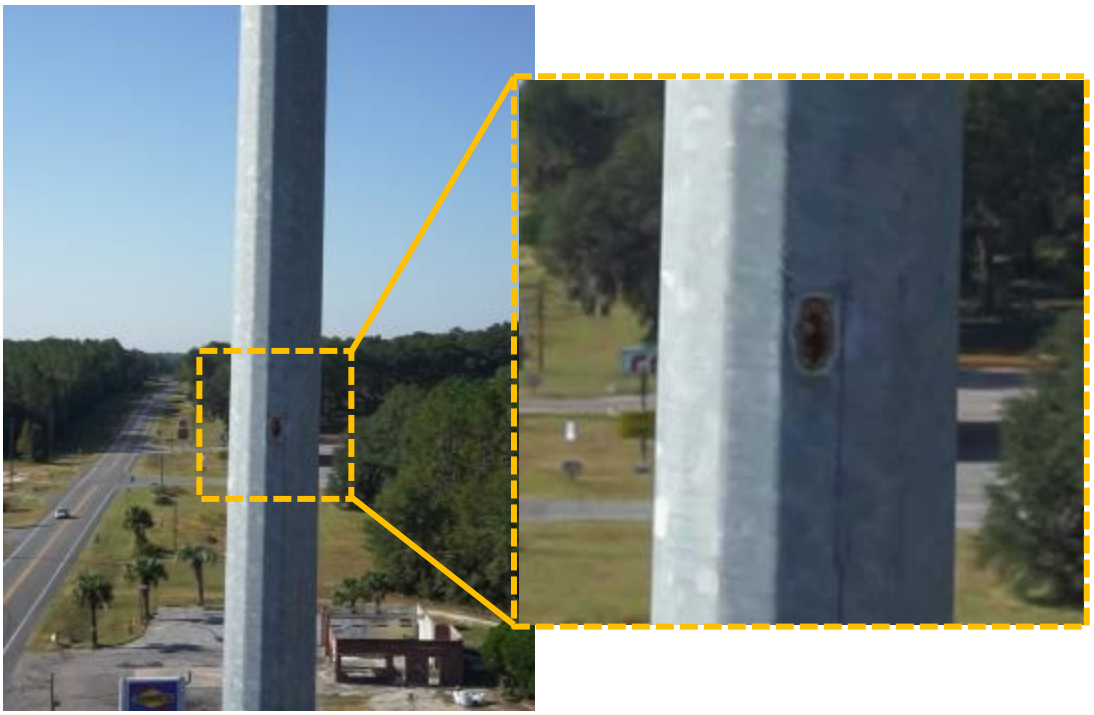

Figure A2-18. 32P054 - View of Corrosion above Second Slip Joint from Northeast

Figure A2-19. 32P054 - View of Lights from Northeast

72P740

Figure A2-20. 72P740 - View of Lower Slip Joint from North

Figure A2-21. 72P740 - View of Lower Slip Joint from East

Figure A2-22. 72P740 - View of Lower Slip Joint from South

Figure A2-23. 72P740 - View of Lower Slip Joint from West

Figure A2-24. 72P740 - View of Second Slip Joint from North

Figure A2-25. 72P740 - View of Second Slip Joint from East

Figure A2-26. 72P740 - View of Second Slip Joint from South

Figure A2-27. 72P740 - View of Second Slip Joint from West

Figure A2-28. 72P740 - View of Lights from East

Figure A2-29. 72P740 - View of Lights from West

72P741

Figure A2-30. 72P741 - View of Lower Slip Joint from North

Figure A2-31. 72P741 - View of Lower Slip Joint from East

Figure A2-32. 72P741 - View of Lower Slip Joint from South

Figure A2-33. 72P741 - View of Lower Slip Joint from West

Figure A2-34. 72P741 - View of Second Slip Joint from North

Figure A2-35. 72P741 - View of Second Slip Joint from East

Figure A2-36. 72P741 - View of Second Slip Joint from South

Figure A2-37. 72P741 - View of Second Slip Joint from West

Figure A2-38. 72P741 - View of Lights from East

Figure A2-39. 72P741 - View of Lights from West

72P743

Figure A2-40. 72P743 - View of Lower Slip Joint from North

Figure A2-41. 72P743 - View of Lower Slip Joint from East

Figure A2-42. 72P743 - View of Lower Slip Joint from South

Figure A2-43. 72P743 - View of Lower Slip Joint from West

Figure A2-44. 72P743 - View of Second Slip Joint from North

Figure A2-45. 72P743 - View of Second Slip Joint from East

Figure A2-46. 72P743 - View of Second Slip Joint from South

Figure A2-47. 72P743 - View of Second Slip Joint from West

Figure A2-48. 72P743 - View of Lights from North

Figure A2-49. 72P743 - View of Lights from Southeast

A2.2 Representative Images from Bridge Inspections

Atlantic Boulevard over the San Pablo River

Figure A2-50. 720690 – Typical view of diaphragm between steel girders

Figure A2-51. 720690 – Typical view of bearing under steel girder

Figure A2-52. 720690 – Typical view down steel girders span

Figure A2-53. 720690 – Typical view of diaphragm connection to steel girder

Figure A2-54. 720690 – Exterior view of prestressed concrete girders over a pier cap

Figure A2-55. 720044 – Typical view of bearing under prestressed concrete girders

Figure A2-56. 720690 – Exterior view of steel and prestressed concrete girders over a pier cap

SR-A1A over the Halifax River

Figure A2-57. 790148 – Typical view of conduit with broken straps

Figure A2-58. 790148 – Typical view of pier cap

Figure A2-59. 790148 – Typical view of conduit

Figure A2-60. 790148 –View of cracking with efflorescence in pier cap

Figure A2-61. 790148 – Close up view of cracking with efflorescence in pier cap

Figure A2-62. 790148 – Typical view of cracking with efflorescence in deck underside

Figure A2-63. 790148 – Typical view of bearing under steel girder

Figure A2-64. 790148 – Typical view of diaphragm connection to steel girder at beam end

Figure A2-65. 790148 – Typical view of conduit with broken straps

SR-44 over the Indian River

Figure A2-66. 790152 – Typical view of bearing under prestressed concrete girders

Figure A2-67. 790152 – Typical view of bearing under prestressed concrete girders

Figure A2-68. 790152 – Typical view of cracking with efflorescence in deck underside

Figure A2-69. 790152 – Typical view of cracking with efflorescence in deck underside

Figure A2-70. 790152 – View of debris on pier cap

Figure A2-71. 790152 – Typical view of pipe above pier cap

Figure A2-72. 790152 – Typical view of pipe above pier cap

Figure A2-73. 790152 – View of spall in deck underside

US-19 over the Suwannee River

Figure A2-74. 300031 – Typical view of debris on top of pier cap

Figure A2-75. 300031 – Typical view of exterior bearings above pier cap

Figure A2-76. 300031 – Typical view of pier cap taken from outside of bridge

Figure A2-77. 300031 – Typical view of pier cap taken from outside of bridge

Figure A2-78. 300061 – Typical view of vegetation growth and debris on top of pier cap

Figure A2-79. 300031 – Typical view of debris growth on pier cap

SR-6 over the Withlacoochee River

Figure A2-80. 320061 – Typical view of floorbeam connection to girder

Figure A2-81. 320061 – Typical view of floorbeam connection to girder

Figure A2-82. 320061 – Typical view of cracking in deck underside

Figure A2-83. 320061 – Typical view of girder splice connection

Figure A2-84. 320061 – Typical view of exterior of girder

Figure A2-85. 320061 – Typical exterior view of bearing under girder

SR-40 over the Ocklawaha River

Figure A2-86. 360055 – Typical view of bearing under prestressed concrete girder

Figure A2-87. 320055 – Typical view down bay between prestressed concrete girders

Figure A2-88. 360055 – Typical view of bearing under prestressed concrete girder

Figure A2-89. 360055 – View of spall in pier cap

Figure A2-90. 360055 – Typical view of bearing under prestressed concrete girder

Figure A2-91. 360055 – Typical view of bearing under steel girder

Figure A2-92. 360055 – View of rocker bearing near maximum range of movement

US-41 over CSXRR

Figure A2-93. 290032 – Typical view of steel beam end

Figure A2-94. 290032 – Typical view of steel beam ends

Figure A2-95. 290032 – Typical view of bearing under steel beam and steel beam ends

Figure A2-96. 290032 – Typical view of diaphragm between steel beams

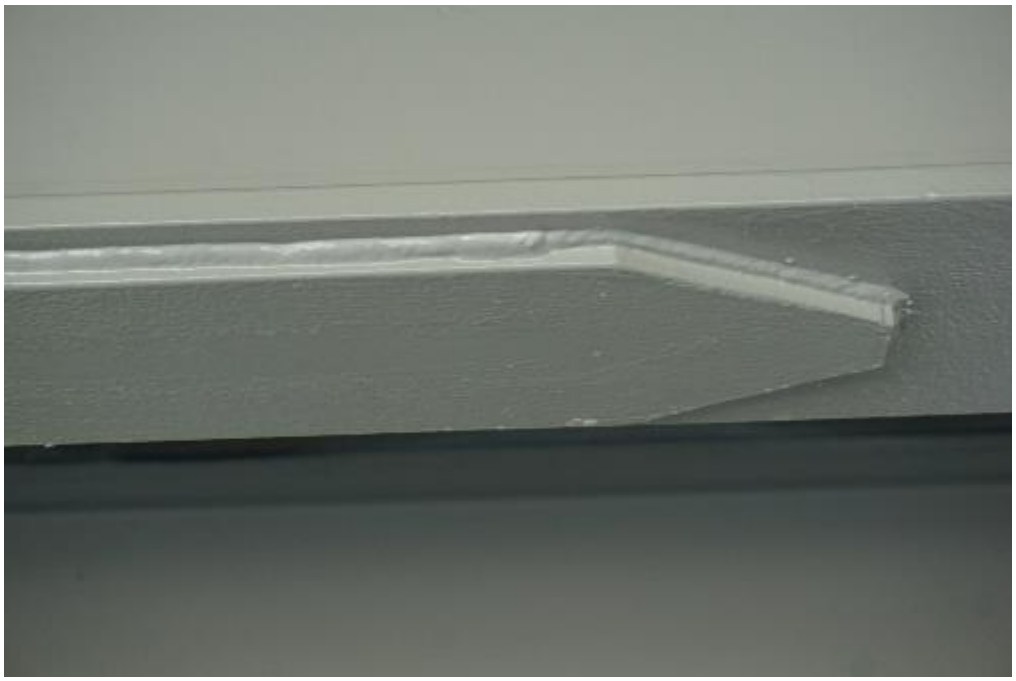

Figure A2-97. 290032 – Typical view of terminal of cover plate

Figure A2-98. 290032 – Typical view of terminal of cover plate

SR-228 over Washington Street

Figure A2-99. 720114 – Typical view of diaphragm between steel girders

Figure A2-100. 720114 – Typical view of spall in deck underside

Figure A2-101. 720114 – Typical view of spall in pier cap underneath steel beam

Figure A2-102. 720114 – Typical view down bay between prestressed concrete girders

Figure A2-103. 720114 – Typical view of bearing under prestressed concrete girder

Figure A2-104. 720114 – Typical view of bearing under prestressed concrete girder